PHOSPHOMETHYLETHANOLAMINE *N*-METHYLTRANSFERASE FROM SPINACH

CHARACTERIZATION OF *S*-ADENOSYL-L-METHIONINE: PHOSPHOMETHYLETHANOLAMINE *N*-METHYLTRANSFERASE FROM SPINACH

By

SHARONPAL KAUR DHADIALLA, B.Sc. HON.

A Thesis

Submitted to the School of Graduate Studies

in Partial Fulfilment of the Requirements

for the Degree

Masters in Science

McMaster University

MASTERS IN SCIENCE (1999) McMaster University
(Biology) Hamilton, Ontario

TITLE: Characterization of *S*-adenosyl-L-methionine: Phosphomethylethanolamine *N*-methyltransferase From Spinach.

AUTHOR: Sharonpal Kaur Dhadialla, B.Sc. Hon. (Bishops University)

SUPERVISOR: Dr. Elizabeth A. Weretilnyk

NUMBER OF PAGES: xv, 124

ABSTRACT

In response to salinity and drought, some higher plants accumulate the secondary metabolite glycinebetaine which functions as a compatible osmolyte (Rhodes and Hanson, 1993). Choline, a precursor of glycinebetaine (Rhodes and Hanson, 1993), is also a component of a primary metabolite phosphatidylcholine, an ubiquitous membrane phospholipid (Moore, 1982). In leaves of the glycinebetaine accumulator spinach, choline is synthesized as phosphocholine (PCho) and PCho is synthesized by three sequential *N*-methylations of phosphoethanolamine (PEA) → phosphomethyl-EA (PMEA) → phosphodimethyl-EA (PDEA) → PCho. The methyl group donor is *S*-adenosyl-L-methionine, SAM (Summers and Weretilnyk, 1993). The enzyme SAM: PMEA *N*-methyltransferase (PMEAMeT) is suggested to *N*-methylate PMEA → PDEA → PCho (Weretilnyk and Summers, 1992).

A four-step strategy was developed for the partial purification of PMEAMeT on the basis of PMEA-dependent methylations (PMEAMeT activity) that involved the extraction of soluble leaf protein, ammonium sulfate precipitation, and column chromatography on DEAE Sepharose, Phenyl Sepharose and High Q Anion matrices. PDEA-dependent methylating activity co-purified with PMEAMeT activity which suggested PMEAMeT may *N*-methylate PMEA → PDEA → PCho. PMEAMeT was purified 43-fold and has specific activities of 14.7 and 18.0 $nmol \bullet min^{-1} \bullet mg^{-1}$ protein with PMEA and PDEA as substrates, respectively. Thin layer chromatography was used to identify the reaction products formed during the 30 minute assay incubation: with PMEA as the substrate, PDEA and PCho were detected in a ratio of 9: 1 as products; and with PDEA as the substrate, PCho was detected as the only product.

PMEAMeT was estimated to have a native molecular mass of 76 kDa by HPLC gel filtration chromatography. Both PMEA and PDEA *N*-methylating activities have an alkaline pH optimum between 8.5 and 9.0 in 0.1 M Tris-HCl buffer. Neither activity was

affected by the omission of Na_2-EDTA from the assay. The addition of 10 mM Mg^{2+} to the assay inhibited PMEA and PDEA-dependent methylation by approximately 49% and 32%, respectively; whereas, the addition of 1 and 10 mM Mn^{2+} to the assay completely inhibited both activities.

Both activities were inhibited by the reaction products *S*-adenosyl-L-homocysteine by over 90% at 0.2 mM and PCho by approximately 80% at 10 mM. Of the products of PCho hydrolysis, choline inhibited PMEA-dependent methylation by 10% at 10 mM; whereas, P_i inhibited PMEA and PDEA-dependent methylation by 38 and 19%, respectively at 10 mM. The compatible osmolyte glycinebetaine inhibited PMEA and PDEA-dependent methylation by between 20 and 30% at 140 mM; however, the inibition of PMEA-dependent methylation can be partly accounted for by the presence of Cl^- ions in the assay. If present at these concentrations in the same subcellular compartment, these metabolites could serve as regulators of PMEAMeT activities *in vivo*.

Study of PMEAMeT contributed to identifying the number of enzymes that *N*-methylate PEA → PMEA → PDEA → PCho and possible regulatory metabolites for choline biosynthesis *in vivo*. These data are pertinent to basic research and also to genetic-engineering studies aimed at introducing the glycinebetaine-accumulating trait into crop plants as an approach to enhancing osmotic-stress resistance.

ACKNOWLEDGEMENTS

I wish to thank McMaster University for the opportunity to do graduate studies. Special thanks go to Dr. Elizabeth. A. Weretilnyk for the guidance and assistance offered throughout this project. I would also like to thank my committee members: Dr. Bradley N. White, Dr. Turlough M. Finan, and Dr. George J. Sorger. I would also like to thank the following people that assisted me in the research: Dr. Peter S. Summers, David D. Smith, Tom Burian and Dr. Tarlochan S. Dhadialla. I am greatly indebted to my family Joginder S., Harpal K., Ashminder K., Kiran K. Dhadialla and to the Dhadialla family at large and great thanks to my friends at large for their support.

This is in dedication to Rejdip S. Dhadialla and to a lasting peace in Kenya.

TABLE OF CONTENTS

LIST OF FIGURES

LIST OF TABLES

LIST OF ABBREVIATIONS

ATP	Adenosine triphosphate
BADH	Betaine aldehyde dehydrogenase
BSA	Bovine serum albumin
cDNA	Complementary deoxyribonucleic acid
CDP-Cho	Cytidine diphosphate choline
CDP-DEA	Cytidine diphosphate dimethylethanolamine
CDP-EA	Cytidine diphosphate ethanolamine
CDP-MEA	Cytidine diphosphate methylethanolamine
CMO	Choline monoxygenase
cpm	Counts per minute
DEAE	Diethylaminoethyl
DMSP	Dimethylsulphoniopropionate
DTT	Dithiothreitol
EDTA	Ethylenediaminetetraacetic acid
HEPES	*N*-(2-hydroxyethyl)piperazine-*N*'-(2-ethanosulfonic acid)
HPLC	High performance liquid chromatography
kDa	Kilodaltons
MGDG	Monogalactosyldiacylglycerol
mRNA	Messenger ribonucleic acid
NAD	Nicotinamide adenine dinucleotide
NADP	Nicotinamide adenine dinucleotide phosphate
OD	Optical density
P_i	Inorganic phosphate
PP_i	Pyrophosphate

PAR	Photosynthetically active radiation
PCho	Phosphocholine
PDEA	Phosphodimethylethanolamine
PDEAMeT	Phosphodimethylethanolamine *N*-methyltransferase
PEA	Phosphoethanolamine
PEAMeT	Phosphoethanolamine *N*-methyltransferase
PMEA	Phosphomethylethanolamine
PMEAMeT	Phosphomethylethanolamine *N*-methyltransferase
PtdCho	Phosphatidylcholine
PtdDEA	Phosphatidyldimethylethanolamine
PtdEA	Phosphatidylethanolamine
PtdEAMeT	Phosphatidylethanolamine *N*-methyltransferase
PtdMEA	Phosphatidylmethylethanolamine
QAC	Quaternary ammonium compounds
SAH	*S*-adenosyl-L-homocysteine
SAM	*S*-adenosyl-L-methionine
SDS-PAGE	Sodium dodecyl sulphate-polyacrylamide gel electrophoresis
SMM	*S*-methylmethionine
TCA	Trichloroacetic acid
TLC	Thin layer chromatography
Tris	Tris(hydroxymethyl)aminomethane
UV	Ultraviolet
VIS	Visible light

LITERATURE REVIEW

Salinity and drought are interrelated, abiotic (osmotic) stresses that represent two of the major constraints to plant and crop distribution and productivity world wide (Boyer, 1982; Le Rudulier et al., 1984). Understanding the mechanisms that confer adaptation to saline and dry environments holds much theoretical and practical value (Hanson and Hitz, 1982; Boyer, 1982; Flowers et al., 1977; Greenway and Munns, 1980). Adaptive mechanisms to these osmotic stresses can be expressed at four levels: (1) developmental, (2) morphological, (3) physiological, and (4) metabolic (Deluaney and Verma, 1993). Complex adaptive mechanisms, such as those expressed at levels (1), (2) and (3), involve the interplay of numerous gene products, many of which remain largely uncharacterized (McCue and Hanson, 1990; Deluaney and Verma, 1993). However, present technology can be applied to understand and manipulate less complex mechanisms, namely cell-level metabolic adaptations which may involve only single or few gene products (McCue and Hanson, 1990).

Osmotic adjustment, or the accumulation of solutes by cells, is based upon a number of cellular metabolic responses that result in the lowering of the water potential (Ψ_w) of a cell which then helps plants take up and retain water under conditions of osmotic stress (Hanson and Hitz, 1982; Rhodes, 1987; Taiz and Zeiger, 1994). One of the metabolic responses is the accumulation of small, low molecular weight organic solutes called compatible osmolytes that are believed to contribute substantially in establishing a low cellular Ψ_w (Yancey et al., 1982; Rhodes, 1987). Recently, there has been an interest in introducing compatible osmolyte biosynthesis in crop plants as an approach to improving osmotic stress resistance (Le Rudulier et al., 1984; McCue and Hanson, 1994).

The relatively simple biosynthetic pathway of the compatible osmolyte glycinebetaine has been targeted for metabolic engineering in crops (Holmstrom et al.,

1994; Rathinasabapathi et al., 1994; Lilius et al., 1996) since the enzymes and the corresponding genes responsible for the two step synthesis of glycinebetaine from its precursor choline are available (Rhodes and Hanson, 1993; Burnet et al., 1995; Rathinasabapathi et al., 1997). However, introducing the glycinebetaine biosynthetic pathway in crops likely requires the up-regulation of the choline biosynthetic pathway (Nuccio et al., 1998). Choline is also required ubiquitously for phosphatidylcholine (PtdCho) biosynthesis, a dominant membrane phospholipid (Moore, 1982). Therefore, understanding how choline biosynthesis is regulated for both glycinebetaine and PtdCho production in glycinebetaine accumulating plants is pertinent to genetic engineering studies. Interestingly for a primary metabolic pathway, little is known about the enzymes or the corresponding genes involved in choline biosynthesis.

The first few sections of the literature review describe the process of osmotic adjustment and sections that follow focus on the compatible osmolyte glycinebetaine. Then, choline and glycinebetaine biosynthetic pathways and their regulation is discussed. In the section on choline biosynthetic pathways, the focus is on the *N*-methylation reaction sequence and, finally, the results of metabolically-engineering the glycinebetaine biosynthetic pathway are presented. For comparison, information on choline and glycinebetaine biosynthetic pathways in other organisms, namely microorganisms, yeast and mammals, is also presented.

METABOLIC ADAPTATION: OSMOTIC ADJUSTMENT.

Cells must maintain a lower Ψ_w than the external media, so that a Ψ_w gradient ($\Delta\Psi_{w(cell\text{-}external)}$) is established with a net flux of water into cells. The accumulation of solutes within a cell creates an intracellular osmotic potential (Ψ_s), which usually exceeds the external Ψ_s which causes the net flux of water into a cell (Wyn Jones and Gorham, 1983). In the presence of a relatively rigid plant cell wall, the net influx of water generates an intracellular turgor potential, Ψ_p (Wyn Jones and Gorham, 1983; Wyn Jones et al., 1977). Thus, at equilibrium the Ψ_w balance can be expressed as $\Psi_{w(external)} = \Psi_{w(cell)} = \Psi_p + \Psi_s$ (Wyn Jones et al., 1979).

Under conditions of drought and salinity, there is a decrease in the external Ψ_w which can cause a decrease in the cellular Ψ_p if water is lost from cells. However, maintaining sufficient Ψ_p is critical in growth and expansion of plant cells and other aspects of plant structure and metabolism (Wyn Jones and Gorham, 1983). In plant cells, there is probably a threshold Ψ_p ($\Psi_{p,\,th}$) below which growth cannot occur and so growth ceases before $\Psi_p = 0$ (Wyn Jones et al., 1979). Short-term responses to decreases in the external Ψ_w, which maintain sufficient cellular Ψ_p, are largely determined by physical parameters such as cell wall elasticity and hydraulic conductivity (Wyn Jones and Gorham, 1983; Rhodes, 1987). However, longer-term responses to decreases in the external Ψ_w require lowering the cellular Ψ_s through osmotic adjustment (Hanson and Hitz, 1982; Wyn Jones and Gorham, 1983; Rhodes, 1987). Therefore, there is an active net accumulation of solutes by the cell which leads to a partial re-establishment of the Ψ_s difference between cell and external media ($\Delta\Psi_{s(cell\text{-}external)}$) and that of cellular Ψ_p (Wyn Jones and Gorham, 1983; Rhodes, 1987). The ability - or lack thereof - to maintain a sufficient cellular Ψ_w gradient between plant and soil through osmotic adjustment is clearly capable of affecting metabolic function (Hanson and Hitz, 1982). Thus, osmotic adjustment is an important metabolic adaptation to drought (Morgan, 1984) and salinity (Wyn Jones et al., 1977) and a desirable trait of importance to agriculture (Le Rudulier et al., 1984).

Osmotic adjustment must be based upon cellular metabolic responses associated with: (1) the accumulation of organic solutes and (2) with increases in, and maintenance of, cellular ion gradients as well as with (3) cellular solute compartmentation and (4) solute translocation within a plant (Hanson and Hitz, 1982). Solutes that are accumulated may either be synthesized within the cell, generally the case with organic solutes, or transported into the cell, the case with ions (Borowitzka, 1981). Both synthesis and transport processes require metabolic energy, complex controls and retention of solutes against considerable concentration gradients (Borowitzka, 1981).

Model for osmotic adjustment of the cytoplasm.

A model, especially applicable to salinity, has been proposed for the types of solutes that are accumulated in the cytoplasm to lower the Ψ_s (Wyn Jones et al., 1977). For clarity, the term cytoplasm does not include the vacuole but includes the cytosol and other cytoplasmic organelles (Wyn Jones et al., 1977). The model suggests the total ionic strength of the cytoplasm does not not exceed 200 to 250 mM with K^+ as the dominant cation and where a lower Ψ_s is required, organic solutes are accumulated in preference to readily available inorganic ions, such as NaCl (Wyn Jones et al., 1977; Yancey et al., 1982). It is noteworthy that NaCl is sequestered in the vacuole, contributing to the lowering of Ψ_s of that compartment. The above model for the accumulation of organic solutes for cytoplasmic osmotic adjustment is also recognized in eubacteria, cyanobacteria, fungi, algae, fish and mammals (Somero, 1992).

Why are inorganic ions not accumulated?

In the cytoplasm of plants and other eukaryotes, the concentration of free K^+ is maintained between 100 to 150 mM and those of other free major ions are: Na^+, <20 mM; Cl^-, 20-30 mM; Mg^{2+}, 1-4 mM; and Ca^{2+}, <0.1 mM (Wyn Jones et al., 1979). It is found that concentrations of inorganic ions higher than *in vivo* perturb metabolic function by interfering at the level of macromolecular activity and/ or structure. For example, (1) enzyme activity is typically inhibited by 100 mM monovalent inorganic ions, such as NaCl; (2) ribosome activity is inhibited by greater than 110 mM K^+ and 5 mM Mg^{2+}; (3) ribosome structure dissociates into protein subunits in 500 mM Na^+, Cl^-, K^+ and NH_4^+; and (4) membrane structure, including binding of extrinsic proteins, dissociates in greater than 200 mM monovalent inorganic ion concentrations (Wyn Jones et al., 1979; Pollard and Wyn Jones, 1979). Interestingly, ribosome activity seems to be the most sensitive metabolic function with specific requirements for K^+ and Mg^{2+} and a sensitivity to free Na^+, Cl^- and Ca^+ (Wyn Jones et al., 1979). Thus, ribosome activity may be a major determinant for the concentrations of free inorganic ions that can be tolerated in the cytoplasm (Wyn Jones et al., 1979). Thus, accumulating high concentrations of readily available salts, such as NaCl,

to lower the Ψ_s during osmotic stress would seriously impair metabolic function (Yancey et al., 1982).

Interestingly, a single group of organisms, halophillic archaebacteria actually have extremely high concentrations of Na^+ and K^+ of up to 7 M in the cytoplasm to maintain a low Ψ_s needed to survive in their highly saline environments (Somero, 1992). However, these obligate halophiles have evolved highly unusual proteins and membranes to retain metabolic function at the above inorganic ion concentrations (Yancey et al., 1982; Somero, 1992). The proteins are highly enriched in acidic residues and depleted in basic ones, and thus carry a net negative charge. Therefore, a high concentration of a counterion, like K^+, is required to allow proteins to fold and maintain their native structures. Similarly, membranes have very acidic compounds containing hydrocarbons ether-linked to glycerol.

Organic solute accumulation, Compatible osmolytes.

The organic solutes that are accumulated in the cytoplasm are often termed "compatible osmolytes" because, unlike inorganic ions, these solutes necessarily do not perturb metabolic function, ie they are compatible (Brown and Simpson, 1972). Compatible osmolytes have low molecular weights, are highly water-soluble, and are either uncharged molecules or zwitterions at physiological pH (Yancey et al., 1982). Interestingly, compatible osmolytes are found to fall within a few classes of organic compounds, namely, polyols, amino acids and their derivatives, tertiary sulphonium compounds (TSC) and quarternary ammonium compounds (QAC; Yancey et al., 1982; Somero, 1992; Samaras et al. 1995; Hanson et al., 1995; Popp and Smirnoff, 1995). In addition to lowering the Ψ_s, some compatible osmolytes may counteract the damaging effects on enzymes and other proteins and membranes of high salt concentrations and high temperatures (Somero, 1992; Smirnoff, 1995; Papgeorgiou and Murata, 1995).

What is the common property of the various compatible osmolytes that allows their accumulation in the cytoplasm? Compatibility with metabolic function is proposed to result from the preferential exclusion of these solutes from the surface and immediate hydration sphere of proteins, and presumably of other macromolecules (Somero, 1992;

Timasheff, 1992). This situation favours minimization of macromolecule surface area and thereby, retention of the native macromolecular structure in the presence of high concentrations of compatible osmolytes (Somero, 1992; Timasheff, 1992). In contrast, a reason for the perturbing effects of high concentrations of inorganic ions (for example) is that they readily enter the hydration sphere of proteins and bind to the macromolecule, thereby favouring denaturation since this maximizes the number of ion binding sites (Somero, 1992; Timasheff, 1992).

Most compatible osmolytes are not products of primary metabolic pathways, but rather are synthesized at the ends of short, secondary pathways (Borowitzka, 1981). Biochemical proximity to a primary pathway is probably necessary for a rapid supply of primary metabolite precursor that may be required for compatible osmolyte synthesis during osmotic adjustment (Borowitzka, 1981). Although, it is proposed that a compatible osmolyte should be separated by several enzyme steps from its primary metabolite precusor to allow for fine control over the pool size of the former (Borowitzka, 1981).

Organisms that accumulate compatible osmolytes have, thus, evolved a rather simple strategy at the metabolic level allowing them to adapt to a broad range of external Ψ_w (Yancey et al., 1982; Somero, 1992). These organisms need only alter the regulation of relatively few enzyme activities that are involved in increasing the pool size of the compatible osmolyte. Furthermore, additional alterations at the metabolic level do not have to be specifically invoked to accommodate increasing concentrations of these compatible osmolytes.

Compatible osmolytes in higher plants.

Compatible osmolytes identified in higher plants are: (1) the amino acid proline; (2) acyclic polyols mannitol and sorbitol; (3) the cyclic polyol pinitol; (4) the TSC dimethylsulphoniopropionate; and (5) QAC's glycinebetaine, β-alanine betaine, choline-O-sulfate, proline betaine and pipetocholate (Figure 1; reviewed in Rhodes and Hanson; 1993; Samaras et al., 1995; Popp and Smirnoff, 1995; Hanson et al., 1995). QAC's are

FIGURE 1: Structural formulae of some quarternary ammonium compounds of higher plants (Figure modified from Rhodes and Hanson [1993]).

The quarternary ammonium compounds (QACs) are: (a) glycinebetaine; (b) β-alanine betaine; (c) choline-O-sulfate; (d) prolinebetaine; and (e) pipetocholate. These QAC are likely to act as compatible osmolytes in higher plants, facilitating adaptation to saline and/ or dry environments (Rhodes and Hanson, 1993).

a) 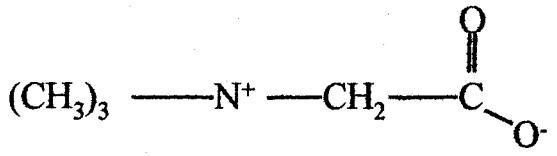

c) 

b) 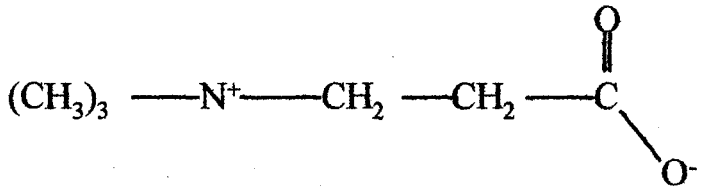

d) 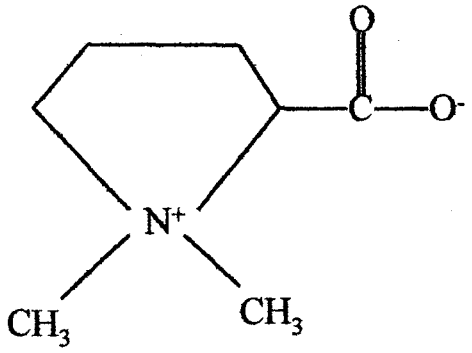

e) 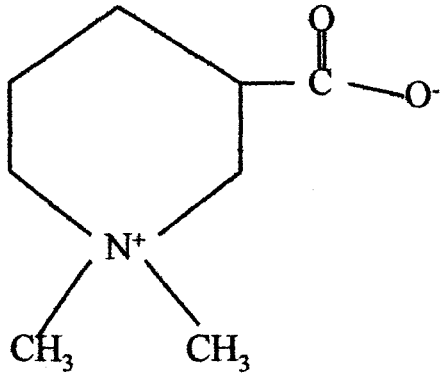

suggested to be amongst the most effective compatible osmolytes (reviewed in Rhodes and Hanson, 1993).

Early work that suggested the above QAC's could function as compatible osmolytes is: 1. the solutes are found at relatively high concentrations of greater than 5 $\mu mole \bullet g^{-1}$ dry weight in plants from saline and dry habitats; 2. glycinebetaine, β-alanine betaine and choline-O-sulfate are shown to accumulate in certain higher plants in response to osmotic stress; and 3. there is a near linear relationship between the accumulation of the three QACs above and the lowering of the leaf Ψ_s in response to osmotic stress (reviewed in Rhodes and Hanson, 1993). Glycinebetaine is the best studied compatible osmolyte in terms of: taxonomic, tissue and sub cellular distribution; osmolyte compatibility; and its metabolism and that of its primary metabolic precursor choline (Rhodes and Hanson, 1993; Weretilnyk and Summers, 1992; Summers and Weretilnyk, 1993; Weretilnyk et al., 1995).

GLYCINEBETAINE.

Taxonomic, tissue and sub cellular distribution of glycinebetaine.

Glycinebetaine accumulation is suggested to be associated with plants adapted to saline and dry conditions (Wyn Jones and Storey, 1981) and it accumulates in some genera of the following angiosperm (flower-producing) families: Amaranthaceae, Avicenniaceae, Chenopodiaceae, Compositiae, Convolvulceae, Gramineae, Leguminoseae, Plumbaginaceae and Solanceaea (reviewed in Rhodes and Hanson, 1993). There is between 5 to 10 $\mu mole \bullet g^{-1}$ dry weight of glycinebetaine under nonstress conditions and between 40 to 100 $\mu mole \bullet g^{-1}$ dry weight under osmotic stress conditions found in glycinebetaine accumulating genera. Interestingly, low levels of glycinebetaine (100 to 1000-fold less) are detected in non-glycinebetaine accumulating genera found in the families listed above, such in Lactuca from Compositiae. Low levels of glycinebetaine are also detected in non-glycinebetaine accumulating genera from families in which no glycinebetaine accumulating genera have been found, such as Magnolia from Magnoliaceae. These observations suggest the ability to accumulate glycinebetaine is a

novel recruitment of the even more widespread ability to synthesize the QAC (Weretilnyk et al., 1989). Thus, glycinebetaine synthesis may be an archetypal characteristic that is strongly expressed in living plants (Rhodes and Hanson, 1993) and data points to a single evolutionary origin for glycinebetaine synthesis in dicotyledons (Weretilnyk et al., 1989).

In mature plants, shoots normally contain more glycinebetaine than the roots (Storey and Wyn Jones, 1979) and it is presumably synthesized in both young and mature leaves and transported to young tissue (including young leaves) and roots (Hanson and Wyse, 1982; McDonnell and Wyn Jones, 1988). Seeds, which are exposed to severe dessication stress, also accumulate large amounts of glycinebetaine (Wyn Jones et al., 1977; Wyn Jones and Storey, 1981).

Glycinebetaine is shown to be preferentially located in the cytoplasm as opposed to the vacuole in leaf cells of chenopods (see references in McCue and Hanson, 1990 and Rhodes and Hanson, 1993). Within the cytoplasm, glycinebetaine has been found in chloroplasts of salinized chenopod leaf cells (Robinson and Jones, 1986; Gerard et al., 1991). In leaves of spinach plants salinized with up to 300 mM NaCl, up to 300 mM glycinebetaine would accumulate in the cytoplasm with 20 to 40% in chloroplasts and glycinebetaine accumulation would make a significant contribution of up to 60% of the cytoplasmic leaf Ψ_s (Hanson, 1992). Glycinebetaine accumulation would contribute up to 50% of the cytoplasmic Ψ_s of leaves of drought-stressed barley, if also located in the cytoplasm (Hitz et al., 1981).

Compatibility of glycinebetaine with metabolic function.

Several properties make glycinebetaine compatible with metabolic function at the high concentrations (up to 300 mM) it can accumulate to in the cytoplasm of plants under osmotic stress (Hanson, 1992). Glycinebetaine is highly water-soluble, has a low molecular weight, and is a zwitterion at physiological pH and therefore would not affect the charge balance of the cytoplasm nor bind directly to charged protein groups (Wyn Jones and Storey, 1981; Borowitzka, 1981). Numerous studies support the compatibility

of glycinebetaine with metabolic function and these include: (1) the activity of enzymes is not inhibited by up to 1 M; (2) ribosome activity is not inhibited by 250 mM over a basal concentration of 120 mM K^+; and (3) ribosome structure does not dissociate in 500 mM (Pollard and Wyn Jones, 1979; Brady et al., 1984; Gibson et al., 1984). Glycinebetaine may also stabilize macromolecules under stress conditions (Csonka, 1989; Papageorgiou and Murata, 1995). The QAC partially counteracts the NaCl- and KCl-inhibition of enzyme activity; counteracts the metal chlorides-induced dissociation and inactivation of the oxygen-evolving photosystem II complex; elevates the denaturation temperature of globular proteins and promotes subunit interactions; and can be used as an osmoticum to isolate active, intact mitochondria (Pollard and Wyn Jones, 1979; Papageorgiou and Murata, 1995; Rhodes, 1987; Wyn Jones et al., 1977).

A number of eubacteria also use glycinebetaine as a compatible osmolyte during osmotic adjustment (Csonka and Hanson, 1991). In the mammalian kidney, glycinebetaine functions as a renal compatible osmolyte used to maintain the osmotic (Ψ_s) balance of kidney cells (Chambers and Kunin, 1987; Garcia-Perez and Burg, 1990).

Origin of glycinebetaine.

Glycinebetaine is a product of secondary metabolism in higher plants and is synthesized from choline via a short, two-step pathway (Hanson and Hitz, 1982). In bacteria, glycinebetaine can be taken up directly from the environment and accumulated in response to a low external Ψ_w (Csonka and Hanson, 1991). Alternatively, a number of gram-positive and -negative bacteria can take up choline from the environment and convert the choline to glycinebetaine via a two-step glycinebetaine pathway (Boch et al., 1994). The pro U operon system specifies a high affinity uptake system for glycinebetaine in *Escherichia coli* and *Salmonella typhimurium* (Csonka, 1989) and the OpuA operon specifies an uptake system for glycinebetaine in *Bacillus subtilis* (Kempf and Bremer, 1995). While, the *betT* gene specifies a choline uptake system in *E. coli* (Csonka, 1989). In mammalian liver and kidney, glycinebetaine is synthesized from choline via a two-step glycinebetaine pathway (Zeisel and Blusztajn, 1994).

CHOLINE BIOSYNTHETIC PATHWAYS

As stated earlier, choline has a role in osmotic stress adaptation in glycinebetaine accumulating plants and is also required in all higher plants as a component of PtdCho (Rhodes and Hanson, 1993; Moore, 1982). Interestingly, choline biosynthesis displays an unusual diversity in higher plants for a primary metabolic pathway (Mudd and Datko, 1988a) and a composite representation of the different choline biosynthetic pathways from the precursor ethanolamine found in various plants examined is shown in Figure 2. The origin of ethanolamine and the three *N*-methylation reactions of ethanolamine (derivatized) that form choline (derivatized) are discussed below. It will be interesting to determine if the same pathway is used for both PtdCho and glycinebetaine synthesis in glycinebetaine accumulating plants (Weretilnyk and Summers, 1992). Also, information on choline biosynthesis in other organisms is presented.

Origin of ethanolamine

Studies confirm that ethanolamine is derived from the amino acid serine in higher plants (reviewed in Rhodes and Hanson, 1993). The direct decarboxylation of serine → ethanolamine is supported by radiotracer and enzyme data in the most recent complete study using fronds of duckweed (*Lemna paucicostata*; Mudd and Datko, 1989c), although the serine decarboxylase catalyzing the reaction is yet to be purified. Whether this simple reaction or a more complex series of reactions involving derivatives of serine and ethanolamine occurs in other higher plants is not known. A more complex route of serine → phosphatidylserine → phosphatidylethanolamine → ethanolamine could not be precluded in fronds of duckweed (Mudd and Datko, 1989c) and a phosphatidylserine decarboxylase activity has been detected in spinach and tomato (reviewed in Rhodes and Hanson, 1993).

FIGURE 2: Choline and glycinebetaine biosynthetic pathways of higher plants (Figure modified from Rhodes and Hanson [1993] and Smith [1995]).

Schematic representation of the various choline biosynthetic pathways, from ethanolamine, in glycinebetaine and non-glycinebetaine accumulating plants. Also shown is the schematic for the glycinebetaine biosynthetic pathway, from choline, found in glycinebetaine accumulating plants. The heavy arrows denote steps for which there is evidence for *in vivo* radiotracer and the corresponding *in vitro* enzyme activity. Light arrows denote steps for which there is only *in vivo* radiotracer evidence. The unidirection of steps is for simplicity and does not imply that the reverse step does not occur. The star above the PEA to PMEA step denotes a proposed common (or conserved) and committing first step in choline biosynthesis in all higher plants examined (Mudd and Datko, 1989ab). The origin of choline for oxidation to glycinebetaine is PCho in members of the Chenopodiaceae and PtdCho (semi-circular arrow) in members of the Graminiaceae (Rhodes and Hanson, 1993).

Abbreviations: MEA, methylethanolamine; DEA, dimethylethanolamine; PEA, phosphoethanolamine; PMEA, phosphomethylethanolamine; PDEA, phosphodimethylethanolamine; PCho, phosphocholine; CDP-EA, cytidine diphosphate ethanolamine; CDP-MEA, cytidine diphosphate methylethanolamine; CDP-DEA, cytidine diphosphate dimethylethanolamine; CDP-Cho, cytidine diphosphate choline; PtdEA, phosphatidylethanolamine; PtdMEA; phosphatidylmethylethanolamine; PtdDEA, phosphatidyldimethylethanolamine; PtdCho, phosphatidylcholine.

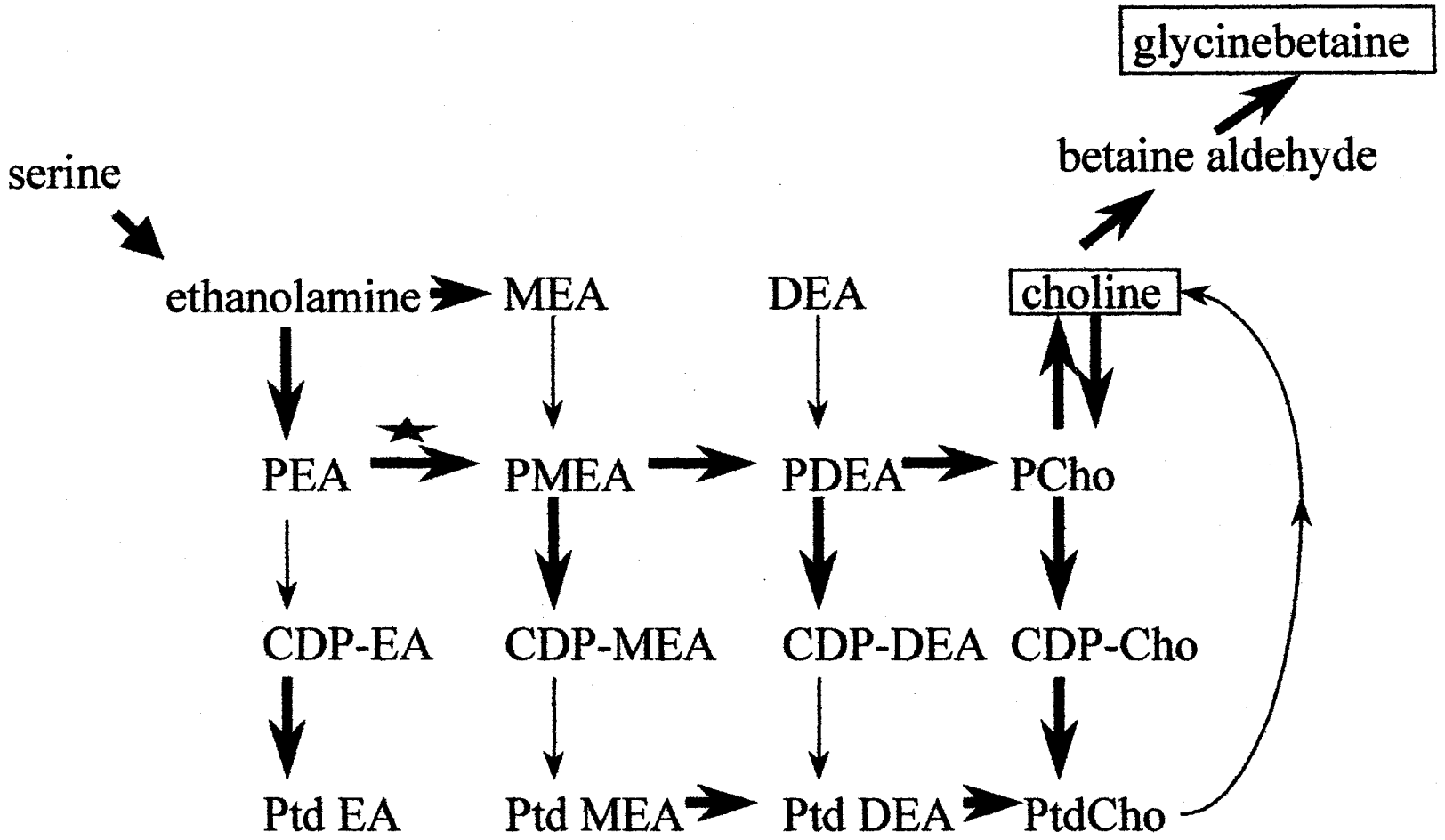
glycinebetaine
betaine aldehyde
serine
ethanolamine
MEA
DEA
choline
PEA
PMEA
PDEA
PCho
CDP-EA
CDP-MEA
CDP-DEA
CDP-Cho
Ptd EA
Ptd MEA
Ptd DEA
PtdCho

_N_-methylation reaction sequences.

The first *N*-methylation reaction is PEA → PMEA in all plants examined (see star in Figure 2), with the single exception of ethanolamine → MEA for endosperm tissue of the plant castor bean. The subsequent two *N*-methylations are of PMEA → PDEA → PCho and/ or PtdMEA → PtdDEA → PtdCho, and the methyl group donor for all *N*-methylation reactions is SAM. Thus, *N*-methylations occur via the freebase, phosphobase and phosphatidylbase levels in choline biosynthesis in higher plants and the exact reaction sequence for each plant examined is detailed below (reviewed in Rhodes and Hanson, 1993). The differing *N*-methylation sequences may reflect developmental, physiological, genetic and/ or environmental differences between higher plants (Weretilnyk et al., 1995).

GLYCINEBETAINE ACCUMULATING PLANTS. In drought-stressed barley leaves, the first reaction is of PEA → PMEA with the subsequent two *N*-methylations at the phosphobase and phosphatidylbase routes to form PCho and PtdCho, respectively (Hitz et al., 1981). In salt-stressed and non salt-stressed spinach leaves, the first reaction is of PEA → PMEA with the two subsequent *N*-methylations at the phosphobase level to form PCho (Summers and Weretilnyk, 1993). Consistent with the above *in vivo* work, *in vitro* phosphobase (PEA, PMEA, PDEA) *N*-methylating activities are detected in leaves of salt-stressed and non salt-stressed spinach (Weretilnyk and Summers, 1992; Summers and Weretilnyk, 1993). Furthermore, the enzyme ethanolamine kinase (E.C. 2.7.1.82) that phosphorylates ethanolamine → PEA has been partially purified from spinach leaves (Mercer, 1994).

NON-GLYCINEBETAINE ACCUMULATING PLANTS. In duckweed fronds, the first reaction is of PEA → PMEA with the subsequent two *N*-methylations also at the phosphobase level to form PCho (Datko and Mudd, 1986). In soybean (*Glycine max*) suspension cultures and leaves, the first reaction is of PEA → PMEA with the subsequent two *N*-methylations at the phosphatidylbase level to form PtdCho (Mudd and Datko,

1988a). In carrot (*Daucus carrota*) suspension cultures, the first reaction is of PEA → PMEA with the two subsequent *N*-methylations at the phosphobase and phosphatidylbase levels to form PCho and PtdCho, respectively (Mudd and Datko, 1988a). Consistent with the *in vivo* work, the respective phosphobase (PEA, PMEA, PDEA) *N*-methylating activities and phosphatidylbase (PtdMEA, PtdDEA) *N*-methylating activities are detected in extracts from the above three plants.

Work on seed material using castor bean endosperm provides the only exception of the first reaction being of ethanolamine → MEA and not of PEA → PMEA (Prud'homme and Moore, 1992a). The subsequent two *N*-methylations occur at both the phosphobase and phosphatidylbase levels to form PCho and PtdCho, respectively (Prud'homme and Moore, 1992). Consistent with the *in vivo* work, the ethanolamine *N*-methylating activity is detected in extracts from the seed endosperm supporting the existence of this novel reaction (Prud'homme and Moore, 1992b). The *N*-methylation of ethanolamine in this plant as opposed to PEA in the other plants was proposed to reflect a tissue-difference and not a species-difference, since data from the other plants is from non-storage tissue (Rhodes and Hanson, 1993).

_N_-methyltransferases in higher plants.

N-methyltransferases catalyse the transfer of an intact methyl group from the donor molecule SAM to the nitrogen atom of an acceptor molecule (Poulton, 1981). In *N*-methylation reactions, the positive charge on the sulphur atom of SAM draws electrons away from the adjacent carbon of the methyl group, promoting attack by a nitrogen atom of the attacking nucleophile (Poulton, 1981). To date, no plant *N*-methyltransferase from choline biosynthetic pathways has been purified or the corresponding gene(s) isolated and neither is the number of *N*-methyltransferases responsible for the three *N*-methylation reactions (*N*-methylation sequence) known conclusively for any higher plant. Probably the most information available is on the phosphobase *N*-methyltransferases of the glycinebetaine accumulator spinach (Weretilnyk and Summers, 1992; Summers and Weretilnyk, 1993; Weretilnyk et al., 1995; Smith, 1995; Smith et al., *submitted*).

SPINACH: GLYCINEBETAINE ACCUMULATING PLANT. At least two cytosolic phosphobase *N*-methyltransferases are suggested to be responsible for the conversion of PEA → PMEA → PDEA → PCho in spinach leaves (Figure 3). A PEA *N*-methyltransferase (PEAMeT) is capable of catalysing all three *N*-methylations of PEA to form PCho in leaves (Smith, 1995). A second distinct enzyme PMEA *N*-methyltransferase (PMEAMeT) is suggested to be responsible for catalyzing two *N*-methylations of PMEA → PDEA → PCho in leaves and roots (Weretilnyk and Summers, 1992; Weretilnyk et al., 1995; Smith, 1995). PEAMeT is light-regulated (Weretilnyk et al., 1995) and PMEAMeT is apparently not light-regulated. Evidence for the existence of at least two enzymes comes from *in vitro* biochemical studies of the differential distribution of the activities in leaves and roots and the differential response of the activities in leaves to ambient light conditions (Weretilnyk and Summers, 1992; Weretilnyk et al., 1995). PEAMeT has been partially purified (5301-fold) from spinach leaves and preliminarily characterized (Smith, 1995; Smith et al., *in press*). The enzyme has a native molecular mass of 77 kDa as estimated by gel filtration, an estimated molecular mass of 54 kDa by SDS-PAGE and a 5301-fold pure sample is capable of catalysing the synthesis of PCho from PEA with PEA as the sole substrate. In contrast, the second enzyme PMEAMeT has not been purified or characterized. The function of the partly overlapping activities of the two enzymes is not known and whether the existence of these two enzymes provides support for the same or distinct choline biosynthetic pathways for PtdCho and glycinebetaine synthesis in glycinebetaine accumulating plants is yet to be determined (Smith, 1995).

NON-GLYCINEBETAINE ACCUMULATING PLANTS. The ethanolamine *N*-methyltransferase activity of castor bean endosperm is cytosolic and the enzyme has been preliminary biochemically characterised in crude extracts (Prud'homme and Moore, 1992b). The phosphobase *N*-methyltransferase activities of duckweed, carrot and soybean are

FIGURE 3: Choline and glycinebetaine biosynthetic pathways in leaves of the glycinebetaine accumulating plant, *Spinacia oleraceae* (Figure modified from Hanson et al [1995]).

Choline biosynthesis as PCho from the precusor ethanolamine occurs mainly in the cytosol and that of glycinebetaine from choline in chloroplasts (Weretilnyk et al., 1995; Hanson et al., 1995). The enzymes involved are: step 1, ethanolamine kinase; steps 2, 3 and 4, PEA *N*-methyltransferase (PEAMeT); steps 3 and 4, PMEA *N*-methyltransferase (PMEAMeT); step 5, PCho phosphatase; step 6, choline monoxygenase (CMO); and step 7, betaine aldehyde dehydrogenase (BADH).

Abbreviations: PEA, phosphoethanolamine; PMEA, phosphomethylethanolamine; PDEA, phosphodimethylethanolamine; PCho, phosphocholine; SAM, *S*-adenosyl-L-methionine; SAH, *S*-adenosyl-L-homocysteine; P_i, inorganic orthophosphate; Fd, ferredoxin; NAD^+, nicotinamide adenine dinucleotide (oxidized form); NADH; nicotinamide adenine dinucleotide (reduced form).

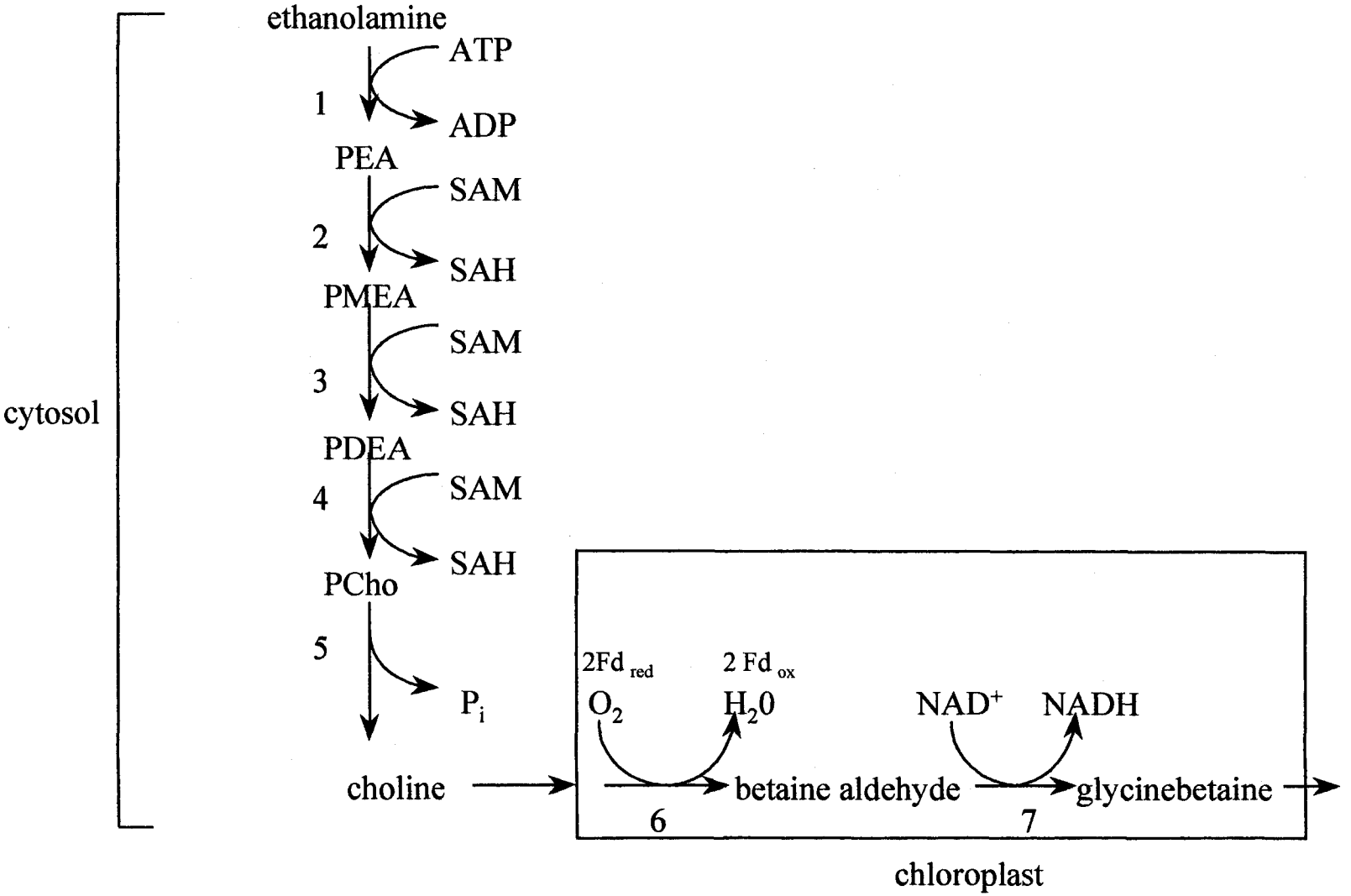
cytosol
ethanolamine
ATP
1
ADP
PEA
SAM
2
SAH
PMEA
SAM
3
SAH
PDEA
SAM
4
SAH
PCho
5
P_i
choline
$2Fd_{red}$
$2\ Fd_{ox}$
O_2
H_2O
NAD^+
NADH
6
betaine aldehyde
7
glycinebetaine
chloroplast

soluble, but have not been localized, and the phosphatidylbase *N*-methyltransferase activities of carrot, soybean and castorbean endosperm are predominantly microsomal (Datko and Mudd, 1988b).

_N_-methyltransferases in yeast and mammalian liver and brain.

YEAST. Two microsome-associated enzymes are responsible for the three *N*-methylations of PtdEA to form PtdCho in *Saccharomyces cerevisiae* (Yamashita et al., 1982; Kodaki and Yamashita, 1987). A PtdEA *N*-methyltransferase (designated as PtdEAMeT), encoded by *PEM2*, catalyzes all three *N*-methylations of PtdEA → PtdMEA → PtdDEA → PtdCho. However, the enzyme *N*-methylates PtdEA at a much lower rate than PtdMEA and PtdDEA. The second PtdEA *N*-methyltransferase enzyme (designated as PtdEAMeT II) encoded by *PEM1*, catalyzes only the first step of PtdEA → PtdMEA. Evidence for the existence of two *N*-methyltransferases comes from screening for *S.cerevisiae* mutants that were auxotrophic for choline synthesis (Yamashita and Oshima, 1980): mutant *pem 2* was deficient in synthesising PtdCho from PtdMEA and mutant *pem 1* was deficient in synthesising PtdMEA from PtdEA (Kodaki and Yamashita, 1987). The structural genes *PEM2* and *PEM1* were cloned by genetic complementation of *pem* mutants and nucleotide analysis of gene coding frames provides a molecular mass of 23 kDa for PtdEAMeT and 101 kDa for PtdEAMeT II (Kodaki and Yamashita, 1987). The *N*-methyltransferases may have evolved through a gene duplication event since the larger PtdEAMeT II exhibits internal sequence homology and homology with the smaller PtdEAMeT (Kodaki and Yamashita, 1987). The introduction of the structural genes into choline mutants showed that both genes are required to maintain PtdCho at wild type levels, although *PEM2* gene (PtdEAMeT) transformants do produce some PtdCho (Kodaki and Yamashita, 1987).

MAMMALIAN. *De novo* choline synthesis is only quantitatively significant in liver (Vance, 1990) and is found at much lower levels in other tissues (Andriamampandry et al., 1982, 1983). In liver, a single integral membrane-bound PtdEA *N*-methyltransferase

(designated as PtdEAMeT) catalyses the three *N*-methylations of PtdEA to form PtdCho (Vance, 1990). Like the yeast PtdEAMeT enzyme, liver PtdEAMeT also catalyzes PtdEA at a much lower rate than PtdMEA and PtdDEA (Ridgeway and Vance, 1987). However, there is no evidence for an enzyme that can only catalyze PtdEA to PtdMEA which would be comparable to the yeast PtdEAMeT II enzyme (Vance, 1990). The enzyme is purified from rat liver microsome with the highest specific activity in the endoplasmic reticulum fraction, it has four transmembrane segments and a remarkably small molecular mass of 18.3 kDa for an enzyme catalyzing such complex reactions (Ridgeway and Vance, 1987; Cui et al., 1993).

In rat brain cells, distinct phosphobase *N*-methyltransferases are reported to be responsible for each of the three *N*-methylations of PEA that form PCho (Andriamampandry et al., 1992; Mukherjee et al., 1995). A PEA *N*-methyltransferase (designated as PEAMeT) catalyzing the PEA → PMEA step and a PDEA *N*-methyltransferase (designated as PDEAMeT) catalyzing the PDEA → PCho step have both been partially purified from rat brain. Thus, different mammalian tissues (liver compared to brain) may synthesise choline through different routes (Andriamampandry et al., 1990) as has been proposed for higher plants (Rhodes and Hanson, 1993).

GLYCINEBETAINE BIOSYNTHETIC PATHWAY.

Glycinebetaine biosynthesis from choline has mainly been studied in leaves of Chenopodiaceae and Gramineae (Figure 2; Figure 3; Hitz et al., 1981; Hanson and Rhodes, 1983; Weretilnyk et al., 1989; McDonnell and Wyn Jones, 1988; Lerma et al., 1988; Lerma et al., 1991). The two-step oxidation of choline → betaine aldehyde → glycinebetaine occurs in the chloroplast stroma in leaf cells of chenopods (Figure 3; Hanson et al., 1985) and perhaps also in those of Gramineae, although this has yet to be demonstrated (McDonnell and Wyn Jones, 1988). There seems to be only one pathway for glycinebetaine biosynthesis, in contrast to those for choline (Hanson and Rhodes, 1993) and since glycinebetaine catabolism is not detected (Hanson and Wyse, 1982), the

pool size is principally controlled by the flux through the biosynthetic pathway (Hanson et al., 1985).

Origin of choline.

The formation of choline may be considered a committing step in glycinebetaine biosynthesis since choline presumably has no intrinsic value, at least in leaves of chenopods (Hanson and Rhodes, 1983). The origin of choline differs between chenopods and Gramineae (Figure 2). Experimental data suggests in chenopods PCho is hydrolyzed by a presumably specific PCho phosphatase to release choline (Hanson and Rhodes, 1983). The formation of PCho from ethanolamine occurs mainly in the cytosol via the choline biosynthetic pathway in chenopods (Figure 3; Weretilnyk et al., 1995), but the subcellular location of PCho hydrolysis is not known ie is PCho or choline is transported into chloroplasts in chenopods?

In Gramineae, the origin of choline is PtdCho (Figure 2; Hitz et al., 1981; McDonnell and Wyn Jones, 1988). As PtdCho synthesis takes place principally in the endoplasmic reticulum (Moore, 1982), PtdCho is suggested to be transported to chloroplasts (putative site) via membrane flow or specific phospholipid transfer proteins (McDonnell and Wyn Jones, 1988; Giddings and Hanson, 1982). Computer modelling data suggest a distinct pool comprising 20% of total leaf PtdCho is the origin of choline in wilting barley leaves (Hitz et al., 1981) and the pool of PtdCho does not appear to be class-specific (Giddings and Hanson, 1982). PtdCho is presumably hydrolyzed by a phospholipase D-like activity to release the choline (Hitz et al., 1981), but the subcellular location (chloroplastic or otherwise) is not known. The transportation of PtdCho to chloroplasts is required for the synthesis of monogalactosyldiacylglycerol (MGDG), a major chloroplast membrane phospholipid (McDonnel and Wyn Jones, 1988). The conversion of PtdCho $\rightarrow$ MGDG results in the release of choline which would possibly be available for glycinebetaine synthesis. Thus, glycinebetaine synthesis in gramineae may be a consequence of another metabolic pathway rather an end unto itself. The greater tolerance of chenopods to osmotic-stress conditions relative to Graminae has suggested to be linked to their capacity to

synthesize glycinebetaine without any recourse to PtdCho, an ubiquitous membrane phospholipid.

Enzymes and genes of the pathway.

More information is available on the glycinebetaine biosynthetic enzymes than those of choline biosynthesis. The enzymes catalyzing the two steps are known for the chenopod spinach and are localized to the chloroplast stroma (Figure 3; Brousquisse et al., 1989; Weigel et al., 1986). The first step of choline → betaine aldehyde is catalyzed by choline monoxygenase, CMO (Brousquisse et al., 1989). CMO is a soluble, ferrodoxin (Fd)-dependant enzyme, it is strongly promoted by light and requires reducing power from photosystem I, ie Fd (Weigel et al., 1986; Brousquisse et al., 1989). The enzyme has been purified from leaves of spinach plants, is a homodimer with a subunit molecular mass of 45 kDa and has a native molecular mass of 98 kDa (Brousquisse et al., 1989; Burnet et al., 1995). Also, a full-length CMO cDNA (1,662 bp) has been cloned from spinach leaves (Rathinasabapathi et al., 1997). CMO is found to be an unusual iron-sulfur protein with little similarity to other plant oxygenases, but it does appear to be distantly related to bacterial oxygenases which require Fd or have an Fd-like domain (Rathinasabapathi et al., 1997).

The second, essentially irreversible, step of betaine aldehyde → glycinebetaine is catalysed by a pyridine nucleotide-dependant betaine aldehyde dehydrogenase, BADH (Weigel et al., 1986). BADH has been purified from spinach leaves (Weretilnyk and Hanson, 1989; Arakawa et al., 1987) and from leaves of *Amarathus hypochondriacus* L. (Valuenzuela-Soto and Munoz-Clares, 1994). The enzyme is a homodimer with a subunit molecular mass of 63 kDa and a native molecular mass of 125 kDa (Weretilnyk and Hanson, 1989; Valuenzuela-Soto and Munoz-Clares, 1994). Although the majority (90%) of spinach BADH activity is localized to the chloroplast stroma, there is a minor cytosolic isozyme (Weigel et al., 1986) which could play a role in scavenging betaine aldehyde, which is toxic to plant cells, that may leak from the chloroplast (Weretilnyk and Summers, 1992). The cDNA of stromal BADH cloned from spinach leaves has been used to isolate

other BADH cDNA clones from sugar beet, barley and sorghum and this revealed the cDNA clones exhibit high homology (Weretilnyk and Hanson, 1990; McCue and Hanson, 1992; Ishitani et al., 1995; Wood et al., 1996). Interestingly, plant BADHs seem to lack or have an atypically short transit peptide sequence for targeting to chloroplasts and the mechanism by which the enzyme enters the chloroplast is not known (Weretilnyk and Hanson, 1990; McCue and Hanson, 1992; Ishitani et al., 1995; Wood et al., 1996).

Recent evidence shows the role of BADH may not be limited to glycinebetaine synthesis. The enzyme is inferred to catalyze the last step in the synthesis of another compatible osmolyte 3-dimethylsulfoniopropionate, DMSP (Trossat et al., 1996), where DMSP-aldehyde is oxidized → DMSP in chloroplast stroma (Trossat et al., 1997). Also, *in vitro* the enzyme catalyzes the oxidation of intermediates in the breakdown of putrescine and polyamine, 3-aminopropionaldehyde and 4-aminobutyraldehyde, respectively (Trossat et al., 1997). Thus, BADH is no longer considered highly substrate-specific for betaine aldehyde and it appears that plants have a family of aldehyde dehydrogenases with distinct but overlapping substrate specificities (Trossat et al., 1997).

Glycinebetaine pathway in other organisms.

Glycinebetaine is also synthesized by the two-step oxidation of choline, via the intermediate betaine aldehyde, in some bacteria and mammalian liver (Csonka and Hanson, 1991; Zeisel and Blusztajn, 1994). In *Arthobacter globiformis* and *A. pascens*, both steps can be catalyzed by a single choline oxidase (Rozwadowski et al., 1991; Deshnium et al., 1995). Alternatively, the reactions are catalyzed by two enzymes in other bacteria: a membrane-bound choline dehydrogenase (which can also catalyze the second step) and a soluble BADH (Boch et al., 1994). The genes involved in the pathway have been isolated from *E. coli* and consist of *betA* (choline dehydrogenase), *betB* (BADH), *betI* (a putative regulatory protein) and *betT* (choline transport system; Csonka, 1989).

In mammalian liver, the pathway is localised in an organelle as in higher plants: a flavoprotein choline dehydrogenase is bound to the inner mitochondrial membrane and an NAD^+-linked BADH is found in the mitochondrial membrane (for references see Hanson

and Hitz, 1982 and Weigel et al., 1986). Like the cytosolic BADH in higher plants, a NAD^+-linked BADH is also present in the cytosol of the hepatocytes (for references see Hanson and Hitz, 1982), and may serve to scavenge any betaine aldehyde that leaks from mitochondria. Glycinebetaine also serves as a source of methyl groups in mammalian liver (Zeisel and Blusztajn, 1994), unlike in higher plants where it is a metabolic end-product (Hanson and Wyse, 1982).

REGULATION OF CHOLINE BIOSYNTHETIC PATHWAYS IN PLANTS.

Substantially more choline is synthesized in leaves of glycinebetaine accumulating plants in comparison to non-glycinebetaine accumulating plants and, therefore, the regulation of choline biosynthesis may be specialized to accommodate the high flux rates through the pathway in glycinebetaine accumulating plants (Rhodes and Hanson, 1993). Although, how the pathway would be regulated in order to meet the requirements of both PtdCho and glycinebetaine synthesis has not yet been examined (Weretilnyk et al., 1995). Choline biosynthesis is under feedback regulation in higher plants that have been examined (Figure 2; Hanson and Rhodes, 1983; Mudd and Datko, 1989ab). The synthesis and addition of the three methyl groups require the input of metabolic energy and were proposed to likely regulate the flux through the pathway (Hitz et al; 1981). Then, the common or conserved first *N*-methyltransfer of PEA → PMEA was identified as a likely committing and key regulatory step (see star in Figure 2; Mudd and Datko, 1988ab). Indeed, regulation of the first *N*-methyltransfer would most efficiently limit the use of metabolically expensive methyl groups in choline biosynthesis (Weretilnyk et al., 1995). Presented below is the evidence that the *N*-methylation sequence in choline pathways is regulated in higher plants and that the first *N*-methyltransfer of PEA → PMEA seems a key regulatory step. Information on the regulation of serine, ethanolamine and SAM metabolism in relation to changes in the flux through the choline pathway is also discussed (also see Figure 3 for SAM metabolism).

Regulation of *N*-methylation sequence in non-glycinebetaine accumulating plants.

The PEA → PMEA step has been proposed to be a committing and key regulatory step in choline biosynthesis pathways in duckweed, soybean and carrot (Mudd and Datko, 1989ab). *In vivo* data showed that the flux through the *N*-methylation sequence is down-regulated in response to an exogenous supply of choline in plant culture media (Mudd and Datko, 1989ab) and the *in vivo* block is found at the PEA → PMEA step (Mudd and Datko, 1989a). There is indirect evidence that PCho, and maybe choline, effect this down-regulation process since both PCho and choline pool sizes increase in choline-grown plants (Mudd and Datko, 1989ab). Consistent with the *in vivo* data, *in vitro* PEA, PMEA and PDEA *N*-methylating activities are also reduced in these choline-grown plants (Mudd and Datko, 1989ab). The reason for the decrease in the phosphobase *N*-methylating activities is not known since the enzymes have not been purified nor their gene(s) cloned. However, *in vitro* PCho inhibits the PEA *N*-methylating activity in duckweed (Mudd and Datko, 1989a), with the *in vitro* effect of PCho on the PMEA and PDEA *N*-methylating activities not yet determined (Mudd and Datko, 1989ab).

Regulation of *N*-methylation sequence in glycinebetaine accumulating plants.

Studies to define a key regulatory locus in choline biosynthesis have not been as extensive in glycinebetaine accumulating plants. However, they clearly show the *N*-methylation reaction sequence participates in regulating the flux as in non-glycinebetaine accumulators. The proposal that the common or conserved *N*-methyltransfer of PEA → PMEA is a committing and key regulatory step in higher plants (see star in Figure 2; Mudd and Datko, 1989ab) is consistent with the data collected from glycinebetaine accumulating plants.

(1) The PEA → PMEA step could be a key regulatory step in the choline pathway in leaves of salinized sugar beet (Hanson and Rhodes, 1983). There is a reduction in the flux through the phosphobase *N*-methylation sequence when a PCho trap is introduced into salinized sugar beet leaves, the flux is measured using [^{14}C]-formate as a radiotracer. Experimental and computer modelling data suggest that PCho effects the down-regulation of its own

synthesis by feedback inhibiting the flux-generating step. *In vitro*, PCho has been shown to inhibit PEA *N*-methylating activity catalyzed by PEAMeT from leaves of another glycinebetaine accumulating chenopod, spinach (Figure 3; Smith, 1995). PCho is also suggested to be an *in vivo* regulatory effector of choline pathways in non-glycinebetaine accumulating plants and shown to be an *in vitro* inhibitor of PEA *N*-methylating activity in the non-glycinebetaine accumulator duckweed (Mudd and Datko, 1989ab).

(2) There is indirect evidence that the PEA → PMEA step (catalysed by PEAMeT) is a key regulatory step which down-regulates the flux through the choline pathway in the dark in leaves of spinach plants (Figure 3; Weretilnyk et al., 1995). PEA *N*-methylating activity decreases in darkness and increases in response to light. It is proposed that the glycinebetaine pathway may not operate in the dark, since the first step is light-promoted, and therefore less choline would be required resulting in the down-regulation of the choline pathway. Interestingly, in leaves PMEA → PDEA and PDEA → PCho steps are not as inhibited in the dark. An effector for the specific down-regulation of the PEA → PMEA step has not been proposed.

(3) The flux through the *N*-methylation sequence is presumably also down-regulated in leaves of glycinebetaine-deficient maize (*Zea mays* L.) plants in comparison to near-isogenic lines containing glycinebetaine (Yang et al., 1995). Glycinebetaine deficiency is attributed to a lesion in the first step of the glycinebetaine pathway and hence presumably less choline is required in these maize plants (Lerma et al., 1991). The choline pool size does not expand in glycinebetaine-deficient lines commensurate with the difference in the glycinebetaine pool size between the two lines and choline (or some other product of choline metabolism other than glycinebetaine) is suggested to down-regulate choline biosynthesis in the glycinebetaine-deficient lines (Yang et al., 1995).

Serine and ethanolamine metabolism.

Serine synthesis may not be coordinately regulated with changes in flux through choline biosynthetic pathways, at least in glycinebetaine accumulating plants. In glycinebetaine-deficient maize, serine pool size was expanded when choline synthesis from

ethanolamine was down-regulated (Yang et al., 1995). In contrast, ethanolamine synthesis seems to be coordinately regulated with flux changes in choline pathways, at least in non-glycinebetaine accumulating plants. When the flux through the choline pathway is down-regulated by the PEA → PMEA step, *in vivo* data suggests ethanolamine synthesis is also down-regulated to compensate for the decreased use of PEA in duckweed fronds (Mudd and Datko, 1989c). Thus, 'excess' PEA is not accumulated when the number of *N*-methylations is reduced (Mudd and Datko, 1989a). Further evidence that ethanolamine synthesis is regulated is shown by the down-regulation of ethanolamine synthesis when duckweed are grown in the culture media containing ethanolamine (Mudd and Datko, 1989c). The site of ethanolamine synthesis regulation is presumably the decarboxylation of serine → ethanolamine, but there is no evidence to date (Figure 2; Kinney, 1993). The mechanism for such a co-ordinated regulation between ethanolamine synthesis and the flux through the choline pathways from ethanolamine is not known.

_S_-adenosyl-L-methionine metabolism.

SAM is the methyl group donor for the *N*-methylation reactions in the choline pathway in higher plants (Figure 3) and its synthesis may also be coordinately regulated with changes in the flux through the choline pathway, at least in non-glycinebetaine accumulating plants (Mudd and Datko, 1989a). When the flux through the choline pathway is down-regulated by the PEA → PMEA step, the number of *N*-methylations in the pathway is reduced by 95% in duckweed fronds. However, SAM synthesis is also down-regulated preventing an accumulation of 'excess' SAM in duckweed and to fine-tune the concentration of SAM, the presence of a *S*-methylmethionine (SMM) cycle is suggested. In this cycle, the 'excess' SAM can be converted back to methionine and adenosine without any net consumption of methyl groups (Mudd and Datko, 1989a; Mudd and Datko, 1990):
(1) SAM + methionine → SMM + *S*-adenosyl-L-homocysteine (SAH) by SAM: methionine *S*-methyltransferase; (2) SAH + H_2O → adenosine + L-homocysteine by SAH hydrolase; and (3) SMM + L-homocysteine → 2 methionine + H^+ by SMM: homocysteine *S*-methyltransferase.

The reaction product formed by the demethylation of SAM is SAH and the majority of SAM-dependent methyltransferases are strongly inhibited by SAH, with the inhibition being generally competitive (Poulton, 1981). Thus, the tissue ratio of SAM: SAH may regulate the rate of SAM-dependent methylation reactions (Poulton, 1981). *In vitro*, SAH inhibits PEA *N*-methylating activity of PEAMeT in partially purified extracts from spinach leaves (Figure 3; Smith, 1995). SAH also inhibits, *in vitro*, the PEA and PDEA *N*-methyltransferase activities from mammalian brain (Andriamampandry et al., 1992; Mukherjee et al., 1995) and competitively inhibits the phosphatidylbase *N*-methyltransferase activities from yeast and mammalian liver (Gaynor and Carmen, 1990; Vance, 1990).

ENVIRONMENTAL REGULATION OF CHOLINE AND GLYCINEBETAINE BIOSYNTHETIC PATHWAYS.

Under conditions of drought and/ or salt-stress, *in vivo* radio tracer studies show that the accumulation of glycinebetaine is a result of increased flux through the choline and glycinebetaine pathways (Hitz et al., 1981; Hanson and Nelsen, 1978; Hanson and Scott, 1980; Hanson and Rhodes, 1983). Thus, there is an increase in *de novo* synthesis of choline to accommodate the increased need for choline required in glycinebetaine production during cellular osmotic adjustment. In chenopods, where PCho is the origin of choline, the metabolically available pools of PCho and choline are too small to accommodate the increased requirement for choline under salt-stress (Figure 3; Hanson and Rhodes, 1983). Likewise in Gramineae, where PtdCho is the origin of choline, relying on the metabolically available pool of PtdCho to supply the increased requirement of choline under drought would be detrimental to the leaf (Figure 2; Hanson and Nelsen, 1978).

Consistent with the *in vivo* work, *in vitro* activities of enzymes in choline and glycinebetaine pathways also increase in response to salt-stress in the chenopod spinach (Figure 3; Weigel et al., 1986; Summers and Weretilnyk, 1993; Rathinasabapathi et al., 1997). *In vitro* ethanolamine kinase, PEA, PMEA and PDEA *N*-methylating activities increase 2 to 3-fold (Summers and Weretilnyk, 1993) as do the activities of CMO (Rathinasabapathi et al., 1997) and both isozymes of BADH (Weigel et al., 1986) in leaf

extracts from salt-stressed spinach plants (Figure 3). Although *in vitro* PCho phosphatase activity does not increase under salt-stress, the capacity of this step is high enough to accommodate the flux through the pathway under both osmotic stress and non-stress conditions (Summers and Weretilnyk, 1993). The reason for the increase in activities of the choline biosynthetic enzymes awaits antibody production and/ or cloning of cDNA encoding these enzymes. However, antibody and cDNA probes are available for the glycinebetaine biosynthetic enzymes. For both CMO and BADH, the increase in activities is a result of increases in protein levels and an accumulation of mRNA (Weretilnyk and Hanson, 1990; Rathinasabapathi et al., 1997). The accumulation of mRNA could reflect increased stability of transcripts and/ or increased rate of gene transcription (Weretilnyk and Hanson, 1990).

The effect of drought has only been examined *in vitro* for BADH activity, the last step of the glycinebetaine pathway. Drought results in an increase in BADH activity in leaves of *A. hypochondriacus* L. (Valenzuela-Soto and Clares-Munoz, 1994) and results in an accumulation of BADH protein from leaves of barley and sorghum (Ishitani et al., 1995; Wood et al., 1996).

Co-ordinate regulation of the pathways.

Weretilnyk and Summers (1992) postulated that a mechanism exists to co-ordinate the flux through the choline and glycinebetaine pathways and such a mechanism may prevent the accumulation of 'excess' metabolically expensive choline (free or derivatized). The authors noted that ethanolamine kinase and phosphobase *N*-methylating activities (choline pathway) increase by a similar amount to CMO and BADH activities (glycinebetaine pathway) in leaves of salt-stressed spinach plants (Figure 3). Thus, when more choline is required, the flux through the choline pathway is up-regulated. Likewise, the flux through the choline pathway is down-regulated under conditions where less choline is required (Yang et al., 1995; Weretilnyk et al., 1995). Glycinebetaine-deficient lines of maize have a lesion in the first step of the glycinebetaine pathway of choline → betaine aldehyde and these lines have a smaller choline pool size in comparison to glycinebetaine-

containing maize lines (Yang et al., 1995). Darkness may also result in an *in vivo* block in the first step of the glycinebetaine pathway, which is light-promoted, so less choline is probably required and there is *in vitro* evidence that choline synthesis is down-regulated (Figure 3; Weigel et al., 1986; Weretilnyk et al., 1995). However, a co-ordinating mechanism between choline and glycinebetaine biosynthesis in glycinebetaine accumulating plants is not yet known (Weretilnyk et al., 1995).

GENETIC ENGINEERING OF GLYCINEBETAINE BIOSYNTHETIC PATHWAY

Conventional practice of breeding for more drought and/ or salt-tolerant crop varieties has had some success, although overall progress has been slow (Boyer, 1982). McCue and Hanson (1990) state that an approach of genetically engineering metabolically-adaptive traits to enhance osmotic stress-resistance is justified since many gene products have been identified and some genes have been cloned. Many higher plant-genera, including commercially important crops, do not accumulate any compatible osmolytes and this has led to an interest in metabolically-engineering compatible osmolyte pathways into plants as an approach to osmotic stress-resistance (Le Rudulier et al., 1984; McCue and Hanson, 1990).

QACs are very effective compatible osmolytes and occur in several diverse taxa of flowering plants (reviewed in Rhodes and Hanson, 1993). From an analysis of QACs in the family Plumbaginaceae, it may be reasonable to consider crop environment-specific engineering of compatible solutes (Hanson et al., 1994). In Plumbaginaceae, accumulation of glycinebetaine is the basal condition (as in other flowering plants) with the additional acquisition of different QACs in members growing in different types of habitats. So, crops may be engineered with: (1) choline O-sulfate for growth in saline soils; (2) β-alanine betaine for growth in soil that is dry and saline; and (3) the conversion of proline to proline-derived betaines to enhance proline effectiveness for growth under severe stress. To date, the two-step glycinebetaine pathway is the only QAC pathway targeted for metabolic engineering since the genes encoding the enzymes have been isolated from both microorganisms and higher plants (Hanson et al., 1994).

Microorganisms.

The two-step glycinebetaine pathway has been introduced into the cyanobacterium *Synechococcus* sp PCC7942 (which completely lacks the pathway) using microbial genes from *E.coli* (Nomura et al., 1995) and *A. globiformis* (Deshium et al., 1995). From *E.coli*, the *bet* gene cluster consisting of *betA*, *betB*, *betT* and *betI* was used for transformations and from *A. globiformis*, a single *codA* gene encoding choline oxidase which catalyzes both steps of the pathway was used. *Synechococcus* transformants could convert exogenously supplied choline (microorganisms do not synthesize choline) → betaine aldehyde → glycinebetaine and had acquired salt-tolerance. That is, transformants accumulate glycinebetaine, have higher chlorophyll and phycobilisome contents, more stable photosystems and are able to grow better than control under salt-stress.

Higher plants.

The pathway has been introduced into plants using single microbial genes that convert choline → betaine aldehyde → glycinebetaine. Tobacco was transformed with the *E.coli* choline dehydrogenase gene and leaf extracts from transformants could convert choline → betaine aldehyde → glycinebetaine (Lilius et al., 1996). Also, leaves from transformants have a higher dry weight in comparison to controls when the plants are salt-stressed. Transgenic *A. thaliana*, transformed with the *A. globiformis* choline oxidase gene, accumulate up to 1 $\mu mol \bullet g^{-1}$ fresh weight of glycinebetaine, have higher photosynthetic activity and grow better in response to salt stress (Hayashi et al., 1997).

The pathway has also been introduced into tobacco using only the gene encoding for the enzyme CMO from spinach leaves that catalyses the first step of choline → betaine aldehyde (Figure 3; Nuccio et al., 1998). BADH, which catalyzes the second step of betaine aldehyde → glycinebetaine is not required because it appears to be identical to a house-keeping enzyme of polyamine metabolism (Trossat et al., 1997). The CMO protein is correctly targeted to chloroplasts, leaf discs from transgenic plants convert choline → betaine aldehyde → glycinebetaine and the transgenics have 3-fold more glycinebetaine

than control plants. Salinization of transgenic plants show that CMO protein level increases 3 to 5-fold suggesting it would be possible to engineer a stress-modulated glycinebetaine pathway without using stress-induced promoters. Interestingly, glycinebetaine levels do not increase in salinized transgenic plants and the reason is shown to be a limited supply of endogenous choline. One point of metabolic control is the limited capacity at the first *N*-methylation step of PEA → PMEA, a common step in leaves of glycinebetaine accumulating and non-accumulating plants (Figure 2; Figure 3). That is, the addition of ethanolamine to the media did not increase glycinebetaine levels; whereas, the addition of MEA and DEA causes a 5-fold increase and the addition of PCho and choline causes a 30-fold increase. The lesser fold increase caused by MEA and DEA is believed to be a result of DEA inhibition of CMO activity. Also, the *N*-methylation of PEA → PMEA in transgenic and control plants is less than 3% that found in the glycinebetaine accumulating plant spinach. So, as a next step, the supply of choline needs to be increased, possibly through over-expressing the spinach enzyme PEAMeT that converts PEA → PMEA in plants (Figure 3) engineered with glycinebetaine pathway genes (Smith, 1995; Nuccio et al., 1998). Therefore, an understanding of the enzymes and genes involved in choline synthesis in glycinebetaine accumulating plants, such as spinach, is extremely relevant both for agricultural and basic research.

INTRODUCTION

Most of the work on choline and glycinebetaine biosynthesis and regulation of their synthesis in response to salt-stress has centred on the chenopod *Spinacia oleracea*, commonly known as spinach. In leaves, glycinebetaine biosynthesis from choline is chloroplastic (Weigel et al., 1986) and the choline is synthesized as PCho from ethanolamine in the cytosol (Figure 3; Summers and Weretilnyk, 1993; Weretilnyk et al., 1995). Glycinebetaine accumulation in response to salinity is a result of an increase in flux from ethanolamine (step 1 in Figure 3) through to glycinebetaine (Summers and Weretilnyk, 1993). Corresponding with the *in vivo* work, *in vitro* enzyme activities associated with the steps from ethanolamine to phosphocholine and from choline to glycinebetaine are higher in leaf extracts from salinized that non-salinized plants (Brousquisse et al., 1989; Weigel et al., 1986; Summers and Weretilnyk, 1993). Although the step involving the hydrolysis of phosphocholine is not higher in leaf extracts from salinized plants, the specific activity is high enough in leaf extracts from non-salinized plants to support the increased flux through the pathway under saline conditions (Summers and Weretilnyk, 1993).

Of the enzymes, ethanolamine kinase (step 1) has been purified to apparent homogeneity (Mercer, 1994) as have CMO (step 6; Burnet et al., 1995) and BADH (step 7; Weretilnyk and Hanson, 1989). Furthermore, the genes encoding CMO and BADH have been cloned from spinach leaves (Rathinasabapathi et al. 1997; Weretilnyk and Hanson, 1989). In response to salinity, the increase in CMO and BADH activities is associated with an increase in amount of enzyme protein and an accumulation of mRNA (Rathinasabapathi et al., 1997; Weretilnyk and Hanson, 1989).

The number of enzymes involved with the three *N*-methylations of PEA that form PCho (steps 2 to 4), with SAM as the methyl group donor, is uncertain which complicates the purification of these phosphobase *N*-methyltransferases. There are at least two phosphobase *N*-methyltransferases with different tissue distribution, different regulatory

properties and two overlapping activities: (1) a PEA *N*-methyltransferase (PEAMeT) that is light-regulated, can convert PEA → PMEA → PDEA → PCho in leaves (steps 2 to 4) and has been substantially purified (Smith, 1995); and (2) a PMEA *N*-methyltransferase (PMEAMeT) that is not light-regulated, can convert possibly PMEA → PDEA → PCho in leaves (steps 3 and 4) and roots and has not been purified (Weretilnyk and Summers, 1992; Weretilnyk et al., 1995).

Evidence for the existence of at least two enzymes comes from *in vitro* biochemical studies of PEA, PMEA and PDEA *N*-methylations in relation to their differential tissue distribution and differential response to light/ dark conditions:

(1) Work by Weretilnyk and Summers (1992) with different tissues shows PEA, PMEA and PDEA *N*-methylations are found in leaves; whereas only PMEA and PDEA *N*-methylations are found in roots. Furthermore, the ratio of PMEA: PDEA *N*-methylations in leaves and roots is similar, both activities being 2 to 3-fold higher in leaves. These observations suggest the enzyme that *N*-methylates PEA (PEAMeT) is distinct from the presumably single enzyme (PMEAMeT) that *N*-methylates both PMEA and PDEA (Weretilnyk and Summers, 1992).

(2) Later work reported by Weretilnyk et al (1995) with leaves shows PEA *N*-methylations are light-regulated, increasing in light and decreasing in dark; whereas PMEA and PDEA *N*-methylations are not similarly light-regulated (Figures 4A and C). Furthermore, the pattern of only PMEA and PDEA *N*-methylations in roots can be mimicked in leaves by exposing plants to prolonged periods of darkness (over 48 h) which substantially reduces PEA *N*-methylations by over 90% (Figure 4B). In contrast, PMEA and PDEA *N*-methylations are not affected by exposing plants to prolonged periods of darkness (Figure 4D). These observations suggest the enzyme that *N*-methylates PEA (PEAMeT) is light-regulated and distinct from the presumably single enzyme that *N*-methylates both PMEA and PDEA (PMEAMeT) which is not light-regulated (Weretilnyk et al., 1995).

Evidence for two overlapping enzyme activities comes from the characterization of a substantially purified PEAMeT by Smith (1995):

FIGURE 4: Phosphobase *N*-methylations in leaves of plants growing under varying light/ dark conditions (Figure modified from Weretilnyk et al [1995]).

Panels A and B, PEA *N*-methylations (open and closed circles). Panels C and D, PMEA *N*-methylations (open and closed upward triangles) and PDEA *N*-methylations (open and closed downward triangles). Open symbols, leaves from plants in light. Closed symbols, leaves from plants in dark. Panels A and C show PEA *N*-methylations in leaves increase in light and decrease in dark; whereas, PMEA and PDEA *N*-methylations are not similarly affected (Weretilnyk et al., 1995). Panel B shows PEA *N*-methylations can be substantially reduced in leaves of plants exposed to prolonged periods of darkness of 48 h (Weretilnyk et al., 1995). Panel D shows PMEA and PDEA *N*-methylations are not similarly affected in leaves of plants exposed to prolonged periods of darkness (Weretilnyk et al., 1995).

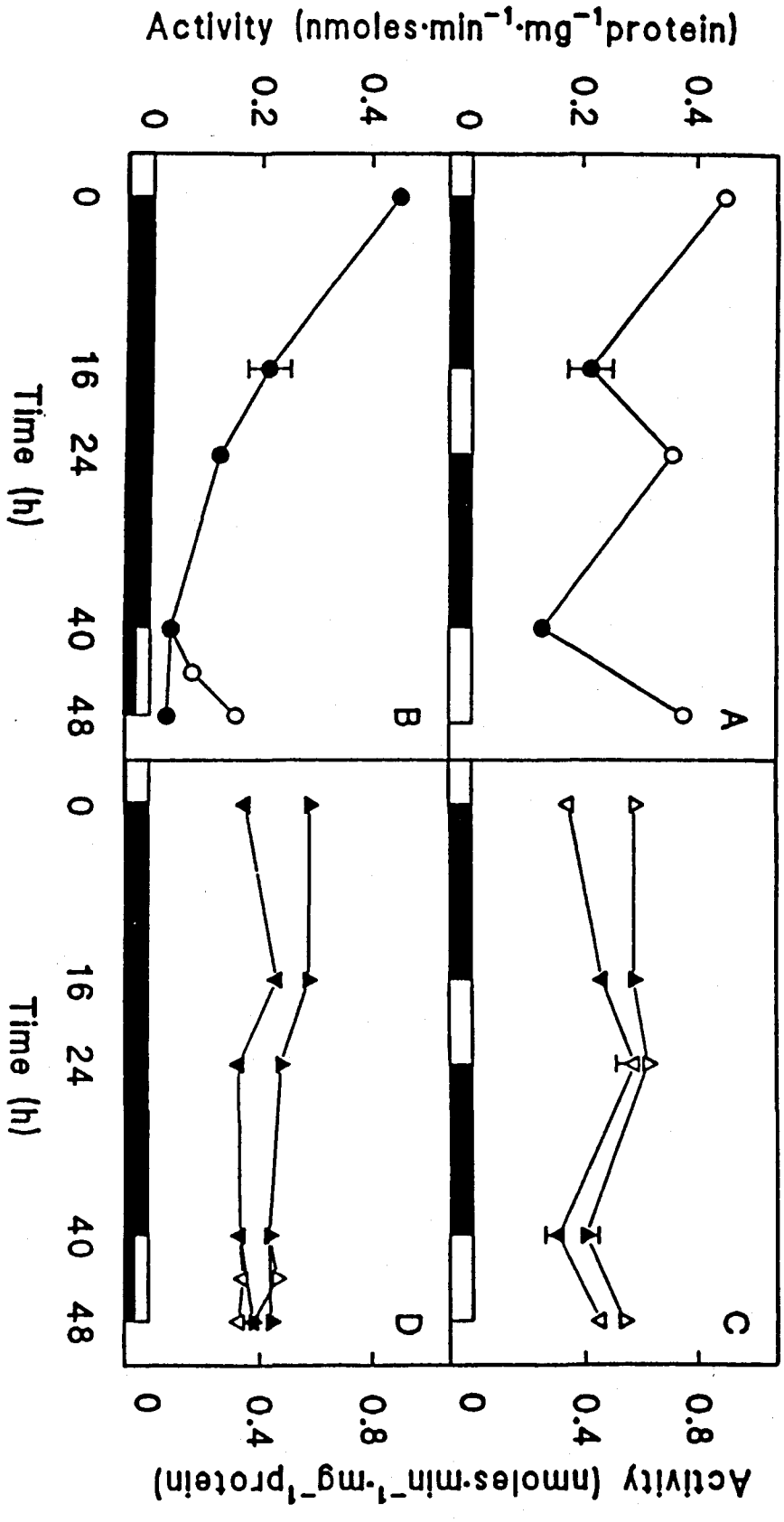
Activity (nmoles·min⁻¹·mg⁻¹protein)
0
0.2
0.4
A
B
C
D
0
0.4
0.8
Activity (nmoles·min⁻¹·mg⁻¹protein)
0
16
24
40
48
Time (h)

(3) With PEA as a sole substrate, substantially pure PEAMeT (over 5,000-fold) can synthesize PCho and, therefore, has three associated activities of PEA, PMEA and PDEA *N*-methylations *in vitro* (Smith, 1995). This observation suggests PEAMeT can synthesise PCho from PEA in leaves and, therefore, has two overlapping activities of PMEA and PDEA *N*-methylations (steps 3 and 4 in Figure 3) with PMEAMeT (Smith, 1995).

The aim of this thesis was the purification and characterization of PMEAMeT, the enzyme that is not light-regulated and possibly converts PMEA → PDEA → PCho in leaves (Weretilnyk et al., 1995) and roots (Weretilnyk and Summers, 1992) of spinach plants. A biochemical approach was required because enzymes with the same substrate specificity or genes encoding such enzymes from other plants or other organisms are not available.

PMEAMeT was partially purified from leaves on the basis of PMEA *N*-methylations (referred to as PMEAMeT activity) and the possibility that PMEAMeT has a second associated activity that *N*-methylates PDEA → PCho was also investigated. For this study, plants were exposed to prolonged periods (over 48 h) of darkness to substantially deplete leaves of PEA *N*-methylations (by over 90%) catalyzed by the light-regulated enzyme PEAMeT (Figure 4B; Weretilnyk et al., 1995) and presumably also any PMEA and PDEA *N*-methylations associated with this enzyme (Smith, 1995). Alternatively, leaves of plants purchased in markets with already low levels of PEA *N*-methylations (Weretilnyk, *unpublished*) were used as a suitable source of the enzyme. PMEAMeT was also characterized in terms of pH optimum for enzyme activities, molecular weight, verification of reaction products, inhibitory effects of divalent cations, and possible inhibitory effects of reaction products and other metabolites of the choline and glycinebetaine biosynthetic pathways. Purification of PMEAMeT provided insight into the number of enzymes, and their associated activities, that convert PEA → PMEA → PDEA → PCho in leaves (steps 2 to 4 in Figure 3); while, identification of metabolites that regulated the enzyme activities *in vitro* provided insight into *in vivo* regulation of the enzyme.

In the future, the availability of antibody and cDNA probes for PMEAMeT can be used to determine if PMEAMeT activities contribute to the salinity-induced increase observed in PMEA and PDEA *N*-methylations (steps 3 and 4; Summers and Weretilnyk,

1993). Alternatively, PMEAMeT may not play a role in osmotic stress adaptation (Weretilnyk et al., 1995) and may play a role only in PCho production for PtdCho biosynthesis. In either case, understanding choline biosynthesis and its regulation for glycinebetaine and PtdCho production is very pertinent to introducing or enhancing glycinebetaine biosynthesis in crop plants as an approach to improving osmotic stress resistance (Weretilnyk and Summers, 1992; McCue and Hanson, 1990).

MATERIALS AND METHODS

Radioisotopes and Chemicals

S-[*methyl*-^{3}H]adenosyl-L-methionine ([*methyl*-^{3}H]SAM) was purchased from New England Nuclear. The specific activity of [*methyl*-^{3}H]SAM ranged from 55.1 to 85.0 Ci•mmol^{-1} (0.55 mCi•mL^{-1}) and the concentration of SAM ranged from 6.5 to 9.9 nmol•mL^{-1}. Upon receipt, the [*methyl*-^{3}H]SAM was divided into 10 µL (0.55 µCi•µL^{-1}) aliquots and stored at -20°C.

SAM was purchased from Boehringer Mannheim, Canada. SAM was dissolved in 0.01 N H_2SO_4: ethanol (9: 1, by vol) and then quantified using the molar extinction coefficient of 15 M^{-1}•cm^{-1} at 257 nm (Eloranta et al., 1976). SAM was diluted to 12 mM, divided into 25 µL aliquots and then stored at -20°C.

Dowex-50W (H^+) X8-200 resin (Sigma) was regenerated prior to use. The resin was suspended in distilled H_2O. It was then protonated with 1.0 N HCl (20 washes) and then rinsed (20 rinses) with distilled H_2O until the pH of the resin was between 5 and 7. Unless otherwise stated, all reference to distilled H_2O refer to water purified by a Barnsted NanoPure Water Filtration System.

Preparation of phosphobases

PEA (Sigma, P-0503) was dissolved in 0.1 N HCl to a concentration of 7.5 mM and the solution was stored at -20°C.

PMEA and PDEA were synthesized by hydrolysis of phosphatidyl-PMEA (Sigma P-3274) and phosphatidyl-PDEA (Sigma P-0339) with phospholipase C using the method of Datko and Mudd (1988b). The phosphatidylbases were suspended, at 5 to 17 mg•mL^{-1}, in 5% (v/v) Triton X-100 by end-over-end rotation overnight. Phospholipase C (Sigma P-7147; Type XI *B. cereus* 1,860 units•mL^{-1} or BMH; Grade I *B. cereus* 4,000 units•mL^{-1}) was first diluted to 745 units•mL^{-1} (Sigma) or 1,580 units•mL^{-1} (BMC) with 0.042 M

dimethylglutarate-NaOH (pH 7.5, 22°C). Next, diluted phospholipase C was desalted by centrifugation through 1.2 mL Sephadex G-25 (Medium) microfuge columns, pre-equilibrated with 0.042 M dimethylglutarate-NaOH buffer (a maximum of 200 µL of enzyme suspension was desalted per column). 149 units (Sigma) or 128 units (BMC) of desalted phospholipase C was added to a suspension of phosphatidylbase and the mixture was incubated at 37°C for 90 min or until it was turbid (up to 7 h). The mixture was then phase partitioned by the addition of 3.2 mL methanol: chloroform (2:1, by vol); followed after 2 min by the addition of 2.06 mL H_2O: chloroform (0.43:1, by vol). The mixture was centrifuged for 1 min at maximum speed in an IEC Clinical Centrifuge (IEC, rotor 809 12-No 302). If the phase partition was incomplete, 4 to 5 drops of MeOH were added and the centrifugation step was repeated. The upper methanol-water phase containing the phosphobase was removed and evaporated to dryness under N_2 gas in a Meyer N-Evap Analytical Evaporator (Organomation). The resultant white pellet was dissolved in 150 µL 0.1 N HCl and the phosphobase stock solution was stored at -20°C.

Quantification of PMEA and PDEA

Concentrations of PMEA and PDEA stock solutions were determined by hydrolysis of the phosphobases with alkaline phosphatase (BMC, EC 3.1.3.1, 20,000 units•mL^{-1}) and then quantification of the released inorganic phosphate (P_i) using the method of Martin and Tolbert (1983).

A sample of the phosphobase was first diluted 10 to 15-fold with 0.1 N HCl. The phosphatase-digestion assay contained: 5 µL of diluted phosphobase, 20 units (1 µL) of alkaline phosphatase and 0.225 mL of buffer containing 50 mM $NaHCO_3$ (pH 10.4, 22°C), 1 mM $MgCl_2$ and 0.1 mM $ZnSO_4$. For controls, 5 µL of 0.1 N HCl replaced the 5 µL of phosphobase. The assays were then incubated at 30°C for 20 to 24 h and reactions were stopped by the addition of 250 µL 10% (w/v) trichloroacetic acid. To determine the amount of P_i contamination in phosphobase samples, 5 µL of diluted phosphobase was added to 226 µL of H_2O. The P_i-contamination assays were placed at -20°C for 20 to 24 h while the phosphatase-digestion assays were being carried out and then thawed and diluted 2-fold

with the addition of 250 µL of H_2O. Phosphatase-digestion and P_i-contamination assays were centrifuged at 14,000 rpm for 2 min at room temperature in an Eppendorf 5415C microcentrifuge. Next, 250 µL of the supernatant was removed and diluted with 250 µL of H_2O. To determine the amount of P_i released from phosphatase-digestion assays and present in Pi-contamination assays, a range of P_i standards from 0 to 25 nmol P_i was prepared in 500 µL volumes from a 1 mM KH_2PO_4 stock solution. 500 µL of freshly made ammonium molybdate solution was added to the assays and P_i standards. The ammonium molybdate solution contained 42 mM $(NH_4)_6MO_7O_{24}$, 0.06% (v/v) sulphuric acid and 114 mM L-ascorbic acid. The colour was developed at 37°C for 90 min and then the absorbance was read at 820 nm using a UVIKON 930 spectrophotometer. A P_i standard curve of OD_{820} versus nmoles of P_i was generated. On average, the extent of P_i contamination in PMEA and PDEA samples was 2.58% and 3.32%, respectively, of the total amount of P_i released during the corresponding phosphatase-digestion assay. The concentration of PMEA and PDEA in stock solutions was determined (taking into account the concentration of P_i in stocks), solutions were then diluted with 0.1 N HCl to 7.5 mM with respect to each phosphobase and then stored at -20°C until required.

The concentrations of PMEA synthesized ranged from 24 to 118 mM, with a mean ± SEM of 71.3 ± 7.8 mM (n=11). The concentrations of PDEA synthesized ranged from 47.7 to 106.6 mM, with a mean ± SEM of 67.8 ± 5.1 mM (n=13). The percent efficiency ($\%_{eff}$) for the synthesis of the phosphobases was determined. The $\%_{eff}$ for PMEA synthesis ranged from 2.69 to 11.2 %, with a mean ± SEM of 6.6 ± 0.6 % (n=11). The $\%_{eff}$ for PDEA synthesis ranged from 4.23 to 9.43 %, with a mean ± SEM of 6.3 ± 0.5 % (n=13).

Analysis of PMEA and PDEA

Each new preparation of PMEA and PDEA was compared to previously prepared phosphobases. First, the purity of new phosphobases was ensured by their co-migration with standard phosphobases on silica G plates during TLC (described later). Next, the suitability of new phosphobases as enzyme substrates was ensured by equal rates of activity

with new and previously prepared phosphobases in phosphobase *N*-methyltransferase assays.

SAM: phosphobase *N*-methyltransferase assays

SAM: phosphobase *N*-methylating activities with PEA, PMEA and PDEA as substrates were quantified using a stopped assay method modified from Datko and Mudd (1988b). In this thesis, the substrate PMEA was used to assay for PMEAMeT activity. The assay contained the following components: 0.1 M HEPES-KOH (pH 7.8, 22°C) or 0.1 M Tris-HCl (pH 8.5, 22°C) buffer containing 1 mM Na_2-EDTA, 200 µM SAM, 40 nM [*methyl*-^{3}H]SAM, 250 µM phosphobase, 16.5 µL distilled H_2O, and 25 µL of enzyme sample (diluted with assay buffer, if necessary) in a final volume of 150 µL. For controls, distilled H_2O replaced the 250 µM phosphobases. The reaction was initiated by the addition of the enzyme sample, at which point the mixture was vortexed briefly and then incubated at 30°C for 30 min. The reaction was stopped by the addition of 1 mL of cold distilled H_2O and vortexed. One mL of the diluted mixture was quickly applied to a 1 mL column of Dowex-50W (H^+) X8-200 resin in an Evergreen disposable column (Diamed, catalogue #208-3384-060). The column was washed with 2 × 0.5 mL of distilled H_20 and the flow-through and washes were discarded. [*methyl*-^{3}H]-labelled and unlabelled phosphobases were eluted with 10 mL 0.1 N HCl and the eluate was mixed by vortexing the tube. One mL of the eluate was added to 10 mL of Formula 989 (Dupont, 40% counting efficiency for [^{3}H]) or 5 mL of Ready Safe (Beckman, 41.3% counting efficiency for [^{3}H]) scintillation cocktail in a vial. The mixture was vortexed and β-radiation emission was quantified using a Beckman LS 1801. The counts per minute (cpm) were measured and 24 h later, a second count was taken. Discrepancies between these counts would reveal problems with quenching and chemiluminescence. However, such differences (ie greater than 20%) were not found. The second value was used to determine enzyme activity. Ideally, enzyme samples were diluted to give approximately 1.36 nmol•min^{-1}•mL^{-1} diluted sample of PMEAMeT activity. The detection limit of the assay is 0.036 nmol•min^{-1}•mL^{-1} sample for phosphobase *N*-methylating activity (Lorenzin, 1998).

Protein and chlorophyll determination

Protein in samples was quantified colorimetrically by the method of Bradford (1976) with BSA as the standard. The Bio-Rad Protein Assay (Bio-Rad), Microassay Procedure, was used and the absorbance was read at 595 nm in disposable semi-micro polystyrene cuvettes (Bio-Rad, catalogue #223-9955). The range of BSA standards used was from 0 to 12.5 $\mu g \bullet mL^{-1}$. A standard curve of OD_{595} versus concentration of standards was generated. However, the OD_{595} value at 12.5 $\mu g \bullet mL^{-1}$ was not included in regression curve calculations as it was frequently beyond the linear range.

Chlorophyll concentration was estimated by the method of Arnon (1949). Twenty-five µL of crude leaf extract were added to 3 mL of 80% (v/v) acetone in aluminium foil-covered test tube. The mixture was vortexed, centrifuged for 5 min at 1,640*g* in an IEC Clinical Centrifuge (IEC, rotor 809 12-No 302). The absorbance of the supernatant was measured at 700, 663 and 645 nm. Chlorophyll concentration in $\mu g \bullet mL^{-1}$ was estimated using the formula: $20.2 ((OD_{645}-OD_{700}) + 8.02 (OD_{663}-OD_{700})) \times 3.025$ mL/ 0.025 mL. The OD_{700} corrects for turbidity. Chlorophyll determinations were done in duplicate.

Plant Material

Spinacia oleracea L. (cv Savoy Hybrid 612, Harris Moran Seeds, Rochester, New York) plants were grown in chambers (Conviron E15) under the following conditions: 8 h, 24°C day, 325 $\mu mol \bullet m^{-2} \bullet s^{-1}$ PAR/ 16 h, 19°C night. The seeds were planted 1 cm deep in moist, medium vermiculite and were not watered for 3 days. The seeds were then watered for 4 days. Each one week-old seedling was transplanted to an individual 350 mL plastic pot filled with vermiculite and watered daily with half-strength Hoagland's solution (Hoaglands and Arnon, 1939). Spinach plants used for PMEAMeT extraction from leaves were between 4 to 7 weeks old. Prior to crude extraction, plants were exposed to 48 h of continuous darkness at 19°C to deplete leaves of light-regulated PEAMeT activities (Weretilnyk et al., 1995; Smith, 1995). Alternatively, leaves of spinach plants purchased from markets were used as a source of PMEAMeT (Weretilnyk, *unpublished*). Plants

purchased from markets were not exposed to prolonged periods of darkness prior to crude extraction since the leaves were already depleted of light-regulated PEAMeT activities (Weretilnyk, *unpublished*).

PMEAMeT Purification

A four-step partial purification strategy for PMEAMeT was developed. The strategy involved bulk crude extraction from leaves, precipitation with ammonium sulfate, and subsequent purification by column chromatography on DEAE Sepharose (anion exchange), phenyl Sepharose (hydrophobic interaction) and High Q Anion Exchanger Support matrices. All procedures were performed at 4°C or on ice. Protein samples of approximately 1 mL were removed after each step. The samples were assayed for phosphobase *N*-methylating activities with PEA, PMEA (PMEAMeT activity) and PDEA as substrates and protein concentration was measured using the method of Bradford (1976). Prior to being used in enzyme assays or for measurement of protein concentration, samples from crude extraction and ammonium sulfate precipitation steps had to be desalted and the buffer was exchanged by centrifugation through 1.2 mL Sephadex G-25 (Pharmacia) columns, pre-equilibrated with 100 mM HEPES-KOH (pH 7.8, 4°C) buffer containing 1 mM Na_2-EDTA and 5 mM DTT (Weigel et al., 1986). Samples were frequently used immediately in enzyme assays or were flash frozen in liquid N_2 and stored at -80°C until required. These freezing and storage conditions did not lead to detectable losses in phosphobase *N*-methylating activities.

Crude leaf extraction and ammonium sulphate precipitation

Spinach leaves were deveined, coarsely chopped with a razor blade (typically 2.0 kg of chopped leaves per bulk extraction) and homogenised (in 100-g batches) in a chilled Waring Blender with 100 mM Tris-HCl (pH 7.8, 4°C) buffer containing 2 mM Na_2-EDTA and 1 mM DTT (buffer A). For homogenisation, the ratio of grams fresh weight of leaf tissue to volume of buffer A used was 1: 2. The homogenate was then squeezed through a filter of four layers of cheesecloth and one of Miracloth (Calbiochem) and the chlorophyll concentration of the filtrate was determined (Arnon, 1949). The remainder of the filtrate

was centrifuged for 10 min at 10,000*g* using a Sorvall GSA rotor. The supernatant was raised to 1.8 M (w/v) ammonium sulfate by additions of solid ammonium sulfate using tables from Wood (1976), stirred for 30 min and then centrifuged for 10 min at 10,000*g*. The supernatant was made to contain 2.6 M (w/v) ammonium sulfate, stirred for 30 min and then centrifuged for 10 min at 10,000*g*. The pellet was dissolved in 1 to 2 volumes of buffer A, transferred to dialysis tubing (Spectra/ Por, VWR Scientific, molecular weight cutoff 12 to 14 kDa, 3.3 $mL \bullet cm^{-1}$) and dialysed against 20 volumes of 20 mM Tris-HCl (pH 7.8, 4°C) buffer containing 1 mM Na_2-EDTA, 1 mM DTT and 10% (v/v) glycerol (buffer B). Buffer B was changed every 5 to 12 h for a total of 4 changes. This fraction, designated the 1.8 to 2.6 M ammonium sulphate fraction, was then transferred to 50 mL plastic tubes, flash frozen in liquid N_2 and stored at -80°C.

Column Chromatography

All procedures were open-bed, low pressure liquid chromatography. The Gilson Model 740 Protech system controller software was used with a Gilson 506B system interface, two Gilson Miniplus 3 pumps, a Gilson 112 UV/ VIS detector and a Gilson FC 204 fraction collector. Protein elution from chromatography columns was continuously monitored at 280 nm and the trace was recorded with a flatbed recorder (Kipp and Zonen).

Selected fractions eluting from columns and all column washes were assayed for phosphobase *N*-methylating activities with PMEA (PMEAMeT activity) and PDEA as substrates. The protein concentration in fractions and column washes was measured using the method of Bradford (1976). Fractions exhibiting high PMEAMeT activity were pooled. Pooled fractions were then divided into 15 and/ or 50 mL plastic tubes, flash frozen in liquid N_2 and stored at -80°C.

Following chromatography on some columns, pooled fractions were concentrated and dialysed using ultrafiltration prior to flash freezing in liquid N_2 and storage at -80°C. For ultrafiltration, a YM30 membrane (Amicon, Publication I-101S) was wetted with distilled H_2O and placed in a 50 mL Amicon 8050 stirred cell (Amicon, Pmax 75 psi, 5.3 $kg \bullet cm^{-2}$). The cell was passivated with 6% (w/v) polyethylene glycol (PEG; molecular

weight 15 to 20 kDa) at 22°C overnight (Amicon, Publication 334) and then the solution was thoroughly rinsed out with distilled H_2O. Under N_2 gas at 60 psi (4°C), buffer B was passed two times through the membrane without allowing the membrane to dry. The cell was then refilled with buffer B and stored at 4°C until required. Using the passivated Amicon cell, pooled fractions were concentrated to a maximum volume of 15 mL and then dialysed extensively with buffer B under N_2 gas at 60 psi (4°C). Concentrated and dialysed protein samples were divided into 15 mL plastic tubes, flash frozen in liquid N_2 and stored at -80°C.

Anion exchange chromatography on DEAE Sepharose CL-6B matrix

DEAE Sepharose CL-6B (Sigma) beads were poured into a column (Bio-Rad, 2.5 cm i.d. × 20 cm, 60 mL bed volume or 5.0 cm i.d. × 20 cm, 300 mL bed volume) and equilibrated with 10 bed volumes of buffer B at a flow rate of 1.0 $mL \bullet min^{-1}$. 1.8 to 2.6 M ammonium sulphate fractions were thawed (a maximum of 50 mg $protein \bullet mL^{-1}$ matrix) and then centrifuged for 10 min at 10,000*g* using a Sorvall GSA rotor to remove insoluble debris. The supernatant was loaded onto the column at a flow rate of 0.5 $mL \bullet min^{-1}$. Non-adsorbed proteins were washed from the column with buffer B at a flow rate of 1.0 $mL \bullet min^{-1}$ until the absorbance of the effluent at 280 nm had decreased to a constant value. The flow rate was then maintained at 1.0 $mL \bullet min^{-1}$. Adsorbed proteins were eluted with a linear, 10 bed volume gradient of 0 to 0.3 M or 0 to 0.5 M NaCl in buffer B followed by a 2 bed volume wash with 0.3 M or 0.5 M NaCl, respectively, also in buffer B. The eluate from the column was collected in 6 mL fractions and fractions exhibiting high PMEAMeT activity were pooled. The pooled fractions were flash frozen in liquid N_2 and stored at -80°C.

Hydrophobic interaction chromatography on phenyl Sepharose CL-4B matrix

Phenyl Sepharose (Sigma, P-7892) beads were poured into a column (Bio-Rad; 2.5 cm i.d. × 20 cm, 100 mL bed volume) and equilibrated with 1 L of buffer B containing 1.0 M (w/v) ammonium sulfate at a flow rate of 1.0 $mL \bullet min^{-1}$. Pooled fractions from DEAE

Sepharose chromatography step were thawed (a maximum of 1500 mg of protein), the concentration of ammonium sulfate made to 1.0 M (w/v) and then stirred for a minimum of 30 min. This solution was then loaded onto the column at a flow rate of 0.5 $mL \bullet min^{-1}$. Non-adsorbed proteins were washed from the column with buffer B containing 1.0 M (w/v) ammonium sulfate at a flow rate of 1.0 $mL \bullet min^{-1}$ until the absorbance of the effluent at 280 nm approached zero. The flow rate was then maintained at 1.0 $mL \bullet min^{-1}$. Adsorbed proteins were eluted with a linear, 1 L gradient of 25 - 0% (w/v) ammonium sulfate/ 0 - 50% (v/v) ethylene glycol in buffer B followed by a 0.2 L wash with 50% (v/v) ethylene glycol in buffer B. The eluate from the column was collected in 6 mL fractions and fractions exhibiting high PMEAMeT activity were pooled. Pooled fractions were concentrated to less than 15 mL and then dialysed 100-fold against buffer B to remove ammonium sulphate and ethylene glycol using a passivated Amicon ultrafiltration cell. Concentrated and dialysed protein samples were then flash frozen in liquid N_2 and stored at -80°C.

Chromatography on High Q Anion Exchanger Support matrix

High Q Anion beads were poured into a column (Bio-Rad; 2.5 cm i.d. × 20 cm, 50 mL bed volume) and equilibrated using 0.5 L of buffer B at a flow rate of 1.0 $mL \bullet min^{-1}$. Concentrated and dialysed protein samples from phenyl Sepharose chromatography step were thawed (a maximum of 600 mg of protein), diluted to less than 10 mg $protein \bullet mL^{-1}$ with buffer B and then loaded onto the column at a flow rate of 0.5 $mL \bullet min^{-1}$. Non-adsorbed proteins were washed from the column with buffer B at a flow rate of 1.0 $mL \bullet min^{-1}$ until the rate of absorbance at 280 nm approached zero. The flow rate was then maintained at 1.0 $mL \bullet min^{-1}$. Adsorbed proteins were eluted with a linear, 0.5 L gradient of 0 to 0.3 M NaCl in buffer B followed by a 0.1 L wash with 0.3 M NaCl in buffer B. The eluate from the column was collected in 6 mL fractions and fractions exhibiting high PMEAMeT activity were pooled. Pooled fractions were concentrated to less than 15 mL and then dialysed 100-fold against buffer B to remove NaCl using a passivated Amicon ultrafiltration cell. Concentrated and dialysed protein samples were flash frozen in liquid N_2 and stored at -80°C.

Native molecular weight determination

Native molecular weights of phosphobase *N*-methyltransferases were determined by comparison to protein molecular weight standards (Sigma, molecular weight GF-200 Kit). An HPLC Protein Pak 300SW gel filtration column (Waters, 7.5 × 300 mm, 13.3 mL bed volume) was used with Baseline 810 software, a Waters 625 LC System, a Waters 486 absorbance detector and a Waters fraction collector. All procedures were carried out at 4°C and at a flow rate of 0.1 mL•min^{-1}. The column was equilibrated with a minimum of 50 mL of 50 mM Tris-HCl (pH 7.4, 4°C) buffer containing 100 mM KCl, 1 mM DTT and 5% (v/v) glycerol (buffer C), prefiltered through a Nucleopore membrane (0.22 µM pore size). Proteins eluting from the column were continuously monitored by the rate of absorbance at 280 nm and the trace recorded with a flat bed recorder (Zipp and Konen).

Sample purified 30-fold after High Q Anion chromatography was centrifuged at 14,000 rpm for 1-2 min in an Eppendorf 5415C microcentrifuge. The supernatant was diluted in buffer C and a 50 µL aliquot was injected onto the column. 100 µL fractions were collected and aliquots from select fractions were assayed for phosphobase *N*-methylating activities with PMEA (PMEAMeT activity) and PDEA as substrates. The elution volume (V_e) for phosphobase *N*-methyltransferases was determined using the fraction containing the maximal activity. As a control, a sample of the supernatant combined with 2 internal protein molecular weight standards was also injected onto the column.

Protein molecular weight standards were used to generate calibration curves. The standards were dissolved in buffer C (as per Technical Bulletin No GF-3, Sigma) and the solutions were mixed together. The mixture was filtered through disposable Acrodisc filters (0.2 µM pore size, Gelman) and then a 50 µL aliquot was injected onto the column. The V_e for standards was determined using the fraction containing maximal protein as shown by the trace. Dextran blue was dissolved in buffer C (as per Technical Bulletin No GF-3, Sigma) and filtered (as per standards). Next, a 50 µL aliquot was injected onto the column and the fraction containing the most dextran blue was used to determine the void volume (V_o) of the column. V_e and V_o estimates were calculated with the following formula: (fraction number

× 100 µL per fraction) + volume of eluate collected between loading the sample and collecting the first fraction - 285 µL for the volume of the tubing leading from the column end to fraction collecting tubes.

Photolabeling with [*methyl*-^{3}H]SAM

Photolabeling of [*methyl*-^{3}H]SAM to protein sample was carried out on ice in pre-cooled Falcon 3911 Microtest III flexible assay plates (approximately 300 µl well volumes, Becton Dickenson) using a Mineralight UV GL-58 lamp (short wave, 115 V, 60 Hz, 0.16 Amps, Ultraviolet Products Inc.). For the photolabeling assay, 0.43 µM [*methyl*-^{3}H]SAM (70.1 Ci•mmole^{-1}; 0.55 µC•µL^{-1}) and 60 µg of protein were mixed in 0.15 M Tris-HCl (pH 8.5, 22°C) buffer containing 1.5 mM Na_2-EDTA in a final volume of 53 µL. The mixture was irradiated with 254 nm UV light for 1 h at a height of 1.0 cm. After UV irradiation, a 40 µL aliquot of the mixture was added to 40 µL of SDS sample buffer (see below Merrick, 1983) to stop the reaction. Then, a 40 µL aliquot was removed and denatured by heating at 90°C for 3 min. The samples were then separated by SDS-PAGE and [*methyl*-^{3}H]SAM-labeled peptides were detected by fluorography (as described below).

Polyacrylamide Gel Electrophoresis, Fluorography

Discontinuous gel electrophoretic analysis of protein samples was performed using 7.5 to 15% SDS-polyacrylamide gradient gels (Chua, 1980) with the buffer system of Neville (1971). Protein samples were diluted with SDS sample buffer containing 60 mM Tris-HCl (pH 6.8, 22°C), 10% (v/v) glycerol, 1% (w/v) SDS, 1% (w/v) DTT and 0.002% (w/v) bromophenol blue (Merrick, 1983). SDS-PAGE molecular weight standards, low range (Bio-Rad, catalogue # 161-1034) were diluted with SDS sample buffer 1:100, by volume, for silver-stained gels and 1:20, by volume, for Coomassie R-250-stained gels. Protein samples and molecular weight standards were then denatured by heating at 90°C for 3 min and loaded onto gels. Electrophoresis was conducted at a constant current of 15 mAmps per gel at 15°C (temperature maintained by RM 6 LAUDA) until the bromophenol

blue dye ran off the gel (approximately 7 to 8 h). Gels were silver-stained by the method of Wray et al., (1982) and then placed for at least 3 h in gel drying solution containing 40% (v/v) methanol, 7% (v/v) glacial acetic acid and 3% (v/v) glycerol. Gels were then dried between 2 sheets of cellophane (BioRad, Model 583 No. 165-0963) using the method of Wallevick and Jensenius (1982).

SDS-polyacrylamide gels used to separate proteins exposed to UV light and [*methyl*-^{3}H]SAM (as described above) were stained with 0.1% (w/v) Coomassie Brilliant Blue R-250 dye, 25% (v/v) isopropanol, 10% (v/v) glacial acetic acid and 0.1% (w/v) cupric acetate. The gels were then destained with 40% methanol and 7% (v/v) glacial acetic acid. Destained gels were exposed to the fluorographic reagent Amplify (Amersham) for 15 min with agitation and then dried as above. The positions of molecular weight standards were marked with [^{14}C]choline-spiked ink. Peptides linked to [*methyl*-^{3}H]SAM were detected by exposure of dried gels to Kodak X-OMAT-AR films at -80°C for varying lengths of time. The X-rays were developed using a Kodak M35A X-OMAT Diagnostic Imaging Processor.

Identification and quantification of phosphobase *N*-methyltransferase assay products

To produce assay products for characterization, phosphobase *N*-methyltransferase assays were performed with PEA, PMEA and PDEA as substrates using sample purified 30-fold after High Q Anion chromatography. Next, the 0.1 N HCl eluates from PMEA and PDEA *N*-methyltransferase assays that had a minimum of 1.36 nmol•min^{-1}•mL^{-1} diluted sample of PMEAMeT activity were evaporated (separately) to dryness at 40°C under N_2 gas using a Meyer N-Evap Analytical Evaporator (Organomation). The 0.1 N HCl eluates from PEA *N*-methyltransferase assays contained no radioactivity but were still evaporated to dryness at 40°C under N_2 gas. The dried samples were then resuspended in 10 µL of 0.1 N HCl and carriers of PEA (30 mM), PMEA (59 mM), PDEA (70 mM) and PCho (30 mM) were added in 1 µL aliquots to 7 µL of each sample. The samples combined with carrier phosphobases were then evaporated to dryness at 40°C under N_2 gas and the mixture resuspended in 4 µL 0.1 N HCl.

To identify the assay products, the above mixtures were separated by TLC (as described below). More specifically, 2.0 μL of each mixture was applied to a silica G plate and, as migration patterns of compounds can differ when a mixture is chromatographed, carrier phosphobases were also applied both individually and in the following combinations: a) PDEA and PCho, b) PMEA, PDEA and PCho and c) all four phosphobases. Following chromatography, which also involved staining for carrier phosphobases, the plate was cut into lanes. The lanes separating mixtures of sample combined with carrier phosphobases were cut into zones according to the positions of the carrier phosphobases (Figure 5). Radioactivity associated with each zone was determined by scrapping off the silica which was then added to a vial containing 5 mL Ready Safe scintillation cocktail (Beckman). The vial was vortexed to mix the contents and radioactivity (cpm) was measured using a Beckman LS 1801 liquid scintillation counter. To account for any radioactivity slowly released from the silica, radioactivity in vials was measured one or two times a day over approximately three days by which point counts remained relatively stable

Counts associated with each zone were expressed as a percentage of total counts recovered from the lane, which indicated the type and amount of *N*-methylated phosphobase product produced in phosphobase *N*-methyltransferase assays. To provide an estimate of the amount of radioactivity in each mixture applied to the plate, 1.0 μL of the remaining mixture was added to a vial containing 5 mL of Ready Safe scintillation cocktail (Beckman). The vial was then vortexed and radioactivity measured (cpm) using a Beckman LS 1801 counter. Thus, the total amount of radioactivity recovered from the plate for each mixture could be expressed as a percentage of radioactivity in the mixture applied to the plate.

Thin Layer Chromatography

Thin layer chromatography (TLC) was carried out in a single dimension with a polar solvent system using a method modified from Andriamampandry et al. (1989). Silica G plates (Machenreg-Nachel, 20 × 20 cm) were "activated" for a minimum of 40 h at 40°C in an oven. The developing tank was lined with two pieces of 3MM chromatography paper (Whatman). "Activated" plate(s) were equilibrated overnight in the tank with 110 mL of 1-

FIGURE 5: Cartoon highlighting the zones on silica G plates

Mixtures of phosphobase *N*-methyltransferase assay products and carrier phosphobases were applied to silica G plates at the origin, separated by TLC and then plates were sprayed with a P_i-specific spray. The lanes were cut into zones (indicated by dashed lines) according to the position of the carrier phosphobases (shaded ovals). The average R_f values for phosphobases were: 0.60 for PEA, 0.52 for PMEA, 0.37 for PDEA and 0.22 for PCho.

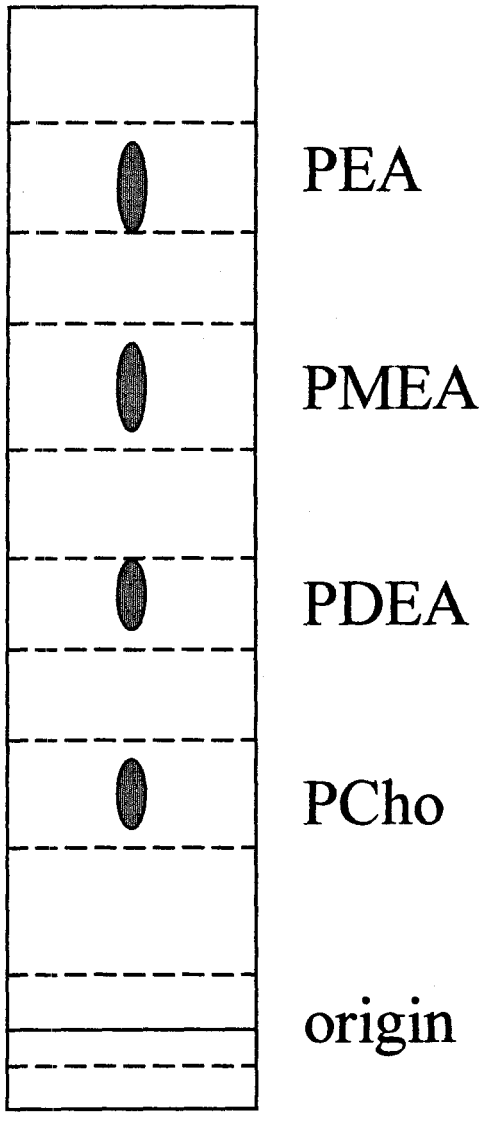
PEA
PMEA
PDEA
PCho
origin

butanol/ MeOH/ concentrated HCl/ H_2O (5: 5: 1: 1, by vol). Plates, chromatography papers and the tank were then air-dried. The tank and chromatography papers were equilibrated for a minimum of 1 h with 120 mL of 1-butanol/ MeOH/ concentrated HCl/ H_2O (10: 10: 1: 1, by vol).

A pencil line was drawn 1.5 cm from the bottom edge of the dried plate and points were marked at 1.0 cm intervals along the line. 0.5 μL of samples dissolved in 0.1 N HCl were applied to plate on designated points and the sample solvent was allowed to evaporate. For samples requiring multiple 0.5 μL applications, the sample solvent was allowed to evaporate between applications. Plates were developed in the equilibrated tank by ascending solvent for 6 h and then air-dried. Dried plates were reversibly stained with iodine vapour in a closed chamber overnight. Plates were photocopied and the bound iodine was allowed to sublime. Plates were then evenly sprayed with a P_i-specific acid molybdenum blue reagent that consisted of 85.6 mM $(NH_4)_6MO_7O_{24}{\cdot}4H_2O$, 0.0076% (v/v) concentrated HCl, 0.05% (v/v) perchloric acid made up to 50 mL with acetone. After air-drying, plates were exposed to UV light from a Mineralight UV GL-58 lamp (short wave, 115V, 60Hz, 0.16 A, Ultraviolet Products Inc.) for approximately 30 min at a distance of 5.7 cm. All phosphorous-containing compounds were stained blue and their relative mobility (R_f) determined by measuring the distance from the origin to the midpoint of the respective blue spot. The plates were then photocopied and stored.

Kinetic, metabolite and metal ion requirement studies

Typically, studies of phosphobase *N*-methyltransferase activities with PMEA (PMEAMeT activity) and PDEA as substrates were performed using sample purified 30-fold after High Q Anion chromatography and if other samples were used, the samples are described. The assays were performed in 0.1 M Tris-HCl buffer at pH 8.5 (22°C), except for studies on the effect of pH since the assay buffer varied according to the pH required. For studies requiring additions to assays or omissions of standard assay components, the standard assay volume of 150 μL was maintained by adjusting the volume of distilled H_20 (16.5 μL) normally included in assays.

The effect of pH in the range from 6 to 10 on enzyme activities was examined using a series of buffers that overlapped in pH. The following buffers were used at a final assay concentration of 0.1 M adjusted to the indicated pHs at 22°C: Biscine-Tris-HCl (pH 6, 6.5 and 7), HEPES-KOH (pH 7, 7.5, 7.8 and 8), Tris-HCl (pH 7, 7.5, 8, 8.5, 8.8 and 9.0), Biscine-Tris-Propane-HCl (pH 7.8, 8.3. 8.5, 8.8 and 9) and CHES-NaOH (pH 9, 9.5 and 10). The incubation time over which enzyme activities remained linear was also examined over the range from 0 to 60 min, with 30 min being the standard incubation time of phosphobase *N*-methyltransferase assays (Datko and Mudd, 1988b).

The concentration-dependant effect of SAH and various end products of choline and glycinebetaine biosynthesis on enzyme activities was determined. All metabolites were dissolved in distilled H_2O, except for SAH which was dissolved in 0.01 N H_2SO_4: ethanol (9:1, by vol). Stock solutions of PCho (Na-salt), choline (Cl-salt) and glycinebetaine (Cl-salt) were buffered to the assay pH (8.5 at 22°C) with either NaOH or HCl. P_i (Na-salt) stock solution was buffered to the assay pH (8.5 at 22°C) by mixing equimolar solutions of NaH_2PO_4 (acidic) and Na_2HPO_4 (basic). Metal ion requirements for enzyme activities were examined by (1) omission from assays of Na_2-EDTA, a metal ion chelator normally included at a final assay concentration of 1 mM (Datko and Mudd, 1988b), and (2) by addition to assays of $MgCl_2$ and $MnCl_2$ at final assay concentrations of 1 and 10 mM, in the absence of Na_2-EDTA.

RESULTS

PARTIAL PURIFICATION OF PMEAMeT

Purification of PMEAMeT from spinach leaves was followed by assaying for PMEA *N*-methylating activity (PMEAMeT activity) and the possibility (proposed by Weretilnyk and Summers, 1992) that PMEAMeT has a second associated activity that *N*-methylates PDEA was investigated. However, spinach leaves also have a light-regulated enzyme PEAMeT that has three associated activities of PEA, PMEA and PDEA *N*-methylations (Smith, 1995). The fact that PEA *N*-methylations should be a distinguishing activity between the two enzymes was used as a basis for the purification. It was previously noted that exposure of plants to prolonged periods of darkness (48 h) results in a substantial decrease (over 90%) in PEA *N*-methylations (Figure 4C; Weretilnyk et. al, 1995). In principle, leaf material depleted of PEA *N*-methylations suggests PMEA and PDEA *N*-methylations associated with PEAMeT are also depleted in such tissue (Smith, 1995). It was also noted that leaves purchased from markets already have low levels of PEA *N*-methylating activity (Weretilnyk, *unpublished*). Therefore, leaves from plants exposed to prolonged periods of darkness and those plants purchased from the market were used for enzyme purification.

PMEAMeT was partially purified 21 to 43-fold using a four-step strategy which involved, in sequence: bulk crude extractions from leaves with low PEA *N*-methylating activity, ammonium sulphate fractionation, and column chromatography on DEAE Sepharose (anion exchange), Phenyl Sepharose (hydrophobic interaction) and High Q Anion Exchanger Support matrices. The summaries of purification trials are reported in Tables I to IV, with the best fold improvement of specific activity of 43-fold for PMEAMeT reported in Table III. The results of each step are described in detail using data from all four purification trials in the following sections. Although a typical or best purification trial could have been reported, all four are included because partially purified enzyme from the various trials were used in experiments reported elsewhere in this thesis.

Table I: Partial purification of PMEAMeT-Trial I using leaves from market spinach plants

Purification Step (column elution conditions)	Total Volume	Total Protein[a]	Total PMEA *N*-methylating Activity[a]	Specific Activity	Fold Purification
	mL	mg	nmol•min^{-1}	nmol•min^{-1}•mg^{-1} protein	
Crude	10430	42017 (100)	2607 (100)	0.062	1
1.8 to 2.6 M ammonium sulfate fraction	372	12970 (31)	3494 (134)	0.269	4.3
DEAE Sepharose (0 to 0.3 M NaCl)	440	2664 (6)	2070 (79)	0.777	12.5
Phenyl Sepharose (25-0% AS/ 0-50% EG)[b]	76	919 (2)	4401 (169)	4.789	77.2
High Q Anion (0 to 0.3 M NaCl)	10	210 (0.5)	420 (16)	2.000	32.3

[a] Values in parentheses are % recoveries relative to the Crude step.
[b] AS and EG refer to ammonium sulfate and ethylene glycol, respectively.

Table II: Partial purification of PMEAMeT-Trial II using leaves from dark-exposed spinach plants

Purification Step (column elution conditions)	Total Volume	Total Protein[a]	Total PMEA *N*-methylating Activity[a]	Specific Activity	Fold Purification
	mL	mg	nmol•min^{-1}	nmol•min^{-1}•mg^{-1} protein	
Crude	13105	26078 (100)	11766 (100)	0.451	1
1.8 to 2.6 M ammonium sulphate fraction	420	10538 (40)	10201 (87)	0.968	2.1
DEAE Sepharose (0 to 0.3/ 0.5 M NaCl)[b]	680	2712 (10)	9577 (81)	3.531	7.8
Phenyl Sepharose (25-0% AS/ 0-50% EG)[c]	49	1110 (4)	7420 (63)	6.685	14.8
High Q Anion (0 to 0.3 M NaCl)	10	152 (0.6)	1456 (12)	9.579	21.2

[a] Values in parentheses are % recoveries relative to Crude step.
[b] A 0 to 0.3 M NaCl gradient was used for one column and a 0 to 0.5 M NaCl gradient was used for other columns.
[c] AS and EG refer to ammonium sulfate and ethylene glycol, respectively.

Table III: Partial purification of PMEAMeT-Trial III using leaves from dark-exposed spinach plants

Purification Step (column elution conditions)	Total Volume	Total Protein[a]	Total PMEA *N*-methylating Activity[a]	Specific Activity	Fold Purification
	mL	mg	nmol•min^{-1}	nmol•min^{-1}•mg^{-1} protein	
Crude	6889	17904 (100)	6179 (100)	0.345	1
1.8 to 2.6 M ammonium sulphate fraction	332	5560 (31)	5899 (95)	1.061	3.1
DEAE Sepharose (0 to 0.3 M NaCl)	284	2380 (13)	3023 (49)	1.270	3.7
Phenyl Sepharose (25-0% AS/ 0-50% EG)[b]	56	709 (4)	3316 (54)	4.677	13.6
High Q Anion (0 to 0.3 M NaCl)	10	74 (0.4)	1093 (18)	14.770	42.8

[a] Values in parentheses are % recoveries relative to Crude step.
[b] AS and EG refer to ammonium sulfate and ethylene glycol, respectively.

Table IV: Partial purification of PMEAMeT-Trial IV using leaves from dark-exposed spinach plants

Purification Step (column elution conditions)	Total Volume	Total Protein[a]	Total PMEA *N*-methylating Activity[a]	Specific Activity	Fold Purification
	mL	mg	nmol•min^{-1}	nmol•min^{-1}•mg^{-1} protein	
Crude	3493	9078 (100)	3133 (100)	0.345	1
1.8 to 2.6 M ammonium sulphate fraction	168	2819 (31)	2991 (95)	1.061	3.1
DEAE Sepharose (0 to 0.3 M NaCl)	144	1207 (13)	1533 (49)	1.270	3.7
Phenyl Sepharose (25-0% AS/ 0-50% EG)[b]	18	663 (7)	1702 (54)	2.567	7.4
High Q Anion (0 to 0.3 M NaCl)	13	178 (2)	1822 (58)	10.236	29.7

[a] Values in parentheses are % recoveries relative to Crude step.
[b] AS and EG refer to ammonium sulfate and ethylene glycol, respectively.

Protein samples recovered after each step were also assayed for PEA and PDEA *N*-methylating activities (Table V). PEA *N*-methylating activity was assayed in crude leaf extracts (step 1) to ensure that leaves harvested from plants had low levels of this activity and then this activity was also assayed in samples from all subsequent steps. PDEA *N*-methylating activity was assayed in samples after each step to determine whether the activity co-purified with PMEAMeT.

It is noteworthy that for each of the four purification trials, more than one bulk crude extraction experiment (first step) was performed to yield enough protein for the single run on the High Q Anion chromatography column (last step; Tables I to IV). Each crude leaf extract was individually and immediately fractionated by ammonium sulfate (second step). For DEAE Sepharose column chromatography (third step), ammonium sulfate fractions were then either individually applied to the column or several were combined and then applied to the column. Protein recovered from each run on the DEAE Sepharose column was either applied directly to the Phenyl Sepharose column (fourth step), divided and applied individually, or preparations from several runs were combined and then applied to the column. Combining or dividing samples was based on pragmatic considerations, such as column loading capacities. Thus for the Crude step (first step) to the Phenyl Sepharose step (fourth step), the data reported for the total volume, protein and PMEA *N*-methylating activity were the sum of more than one crude extraction/ ammonium sulfate fractionation experiment and generally also of more than one run on the respective chromatography column.

Crude extraction from leaves and ammonium sulfate fractionation

PMEAMeT activity (average 0.30 nmol•min^{-1}•mg^{-1} protein) was detected in desalted, crude leaf extracts from market plants (Table I) and plants exposed to prolonged periods of darkness (Table II to IV). PDEA *N*-methylating activity (average 0.33 nmol•min^{-1}•mg^{-1} protein) was also detected in desalted, crude leaf extracts. These activity levels approach those previously reported for PMEAMeT and PDEA *N*-methylating activities for dark-exposed plants (0.85 ± 0.05 and 0.62 ± 0.04 nmol•min^{-1}•mg^{-1} protein, respectively;

Table V: Average ratio of PEA and PDEA *N*-methylating specific activities relative to PMEAMeT after each purification step[a]

Purification Step	Average PMEAMeT activity [b]	Ratio of specific activities relative to PMEAMeT activity		
		PEA	PMEA	PDEA
	$nmol \bullet min^{-1} \bullet mg^{-1}$ protein			
Crude	0.30 ± 0.08	0.07 ± 0.04	1	1.21 ± 0.20
1.8 to 2.6 M ammonium sulfate fraction	0.84 ± 0.18	0.05 ± 0.00	1	0.99 ± 0.06
DEAE Sepharose	1.71 ± 0.62	0.05 ± 0.01	1	0.99 ± 0.03
Phenyl Sepharose	4.68 ± 0.84	0.02 ± 0.01	1	1.12 ± 0.06
High Q Anion	9.15 ± 2.65	nd[c]	1	1.15 ± 0.11

[a] PMEAMeT activity assayed with PMEA as substrate
[b] PMEAMeT specific activities for each step are reported in Tables I to IV.
[c] nd refers to not detected, the activity was at or below the detection limit of the assay (0.036 $nmol \bullet min^{-1} \bullet mL^{-1}$ sample).

Lorenzin, 1998). In contrast, the activity level detected for PEA *N*-methylating activity was only approximately 7% that of PMEAMeT activity which contrasts with the value from light-exposed plants (0.51 ± 0.03 nmol•min^{-1}•mg^{-1} protein; Lorenzin, 1998) suggesting the light-regulated enzyme PEAMeT was substantially reduced in leaves from these plants. Therefore, this plant material was deemed suitable for purification of PMEAMeT and for investigating the possibility that PMEAMeT also *N*-methylated PDEA (Weretilnyk and Summers, 1992; Weretilnyk et al., 1995). Thus, PDEA *N*-methylating activity was assayed during the purification of PMEAMeT in each trial and the data are reported in Table VI (Trials I and II) and VII (Trials III and IV). For the ease of comparison, the corresponding PMEAMeT activity reported in Tables I to IV is also reported in Tables VI and VII.

Each crude leaf extract was fractionated using ammonium sulfate. The 1.8 to 2.6 M ammonium sulfate fraction contained 33% of protein and, on average, 100% (range, 87 to 134%) of PMEAMeT activity present in crude leaf extracts. In comparison, approximately 5% (range, 0 to 11%) and 3% (range, 0 to 10%) of PMEAMeT activity in crude leaf extracts was detected in the 0 to 1.8 M and ≥ 2.6 M ammonium sulfate fractions, respectively. The 1.8 to 2.6 M ammonium sulfate fractionation led to a 83% (range, 73% to 87%) recovery of PDEA *N*-methylating activity. A low level of PEA *N*-methylating activity was also detected in the 1.8 to 2.6 ammonium sulfate fraction (Table V). Thus, ammonium sulphate fractionation had purified the average sample 3.2-fold for PMEAMeT activity and 2.5-fold for PDEA *N*-methylating activity over the crude leaf extract.

Anion exchange chromatography on DEAE Sepharose matrix

The dialysed 1.8 to 2.6 M ammonium sulphate fraction was centrifuged for 10 min at 10,000*g* to remove particulates and then the supernatant was loaded onto a DEAE Sepharose column (Methods and Methods). Approximately 75% of the protein applied was adsorbed onto the matrix. Figure 6 shows a typical elution profile of protein and *N*-methylating activities using PMEA and PDEA as substrates. PMEAMeT and PDEA *N*-methylating activities co-eluted from the column during application of a linear gradient of increasing NaCl concentration (0 to 0.3 M in buffer B) and the elution profiles of both

Table VI: PMEAMeT and PDEA *N*-methylating activities at each step of partial purification trials I and II[a]

Purification Step	Trial I				Trial II			
	Total Activity[b]		Fold Purification		Total activity[b]		Fold purification	
	PMEA	PDEA	PMEA	PDEA	PMEA	PDEA	PMEA	PDEA
	nmol•min^{-1}				nmol•min^{-1}			
Crude	2607 (100)	4524 (100)	1	1	11766 (100)	15599 (100)	1	1
1.8 to 2.6 M ammonium sulfate fraction	3495 (134)	3798 (84)	4.3	2.7	10201 (87)	11333 (73)	2.1	1.8
DEAE Sepharose	2070 (79)	2276 (50)	12.5	7.9	9577 (81)	10068 (65)	7.8	6.2
Phenyl Sepharose	4401 (169)	4905 (108)	77.2	49.4	7420 (63)	8168 (52)	14.8	12.3
High Q Anion	420 (16)	548 (12)	32.3	24.1	1456 (12)	1834 (12)	21.2	20.2

[a]PMEAMeT activity was assayed using PMEA as substrate.
[b]Values in parentheses are % recoveries relative to the Crude step.

Table VII: PMEAMeT and PDEA *N*-methylating activities at each step of partial purification trials III and IV[a]

Purification Step	Trial III				Trial IV			
	Total Activity[b]		Fold Purification		Total activity[b]		Fold purification	
	PMEA	PDEA	PMEA	PDEA	PMEA	PDEA	PMEA	PDEA
	nmol•min^{-1}				nmol•min^{-1}			
Crude	6179 (100)	5499 (100)	1	1	3133 (100)	2788 (100)	1	1
1.8 to 2.6 M ammonium sulfate fraction	5899 (95)	4757 (87)	3.1	2.8	2991 (95)	2495 (89)	3.1	2.8
DEAE Sepharose	3023 (49)	2809 (51)	3.7	3.8	1533 (49)	1695 (61)	3.7	3.8
Phenyl Sepharose	3316 (53)	4228 (77)	13.6	19.4	1702 (54)	1688 (61)	7.4	8.3
High Q Anion	1093 (18)	1334 (24)	42.8	58.7	1822 (58)	1595 (57)	29.7	29.2

[a]PMEAMeT activity was assayed using PMEA as substrate.
[b]Values in parentheses are % recoveries relative to the Crude step.

FIGURE 6: Anion exchange chromatography on DEAE Sepharose (CL-6B) column.

Representative elution profiles of PMEAMeT activity (●, with PMEA as substrate), PDEA *N*-methylating activity (O) and protein (...) from a 60 mL DEAE Sepharose matrix. Adsorbed protein was eluted from the column with a 600 mL linear gradient of 0 to 0.3 M NaCl in buffer B followed with a 200 mL wash of 0.3 M NaCl in buffer B (solid line). The eluate was collected in 6 mL fractions. Selected fractions were assayed for PMEAMeT and PDEA *N*-methylating activities as described (Materials and Methods) and protein concentration was measured in fractions using the method of Bradford (1976).

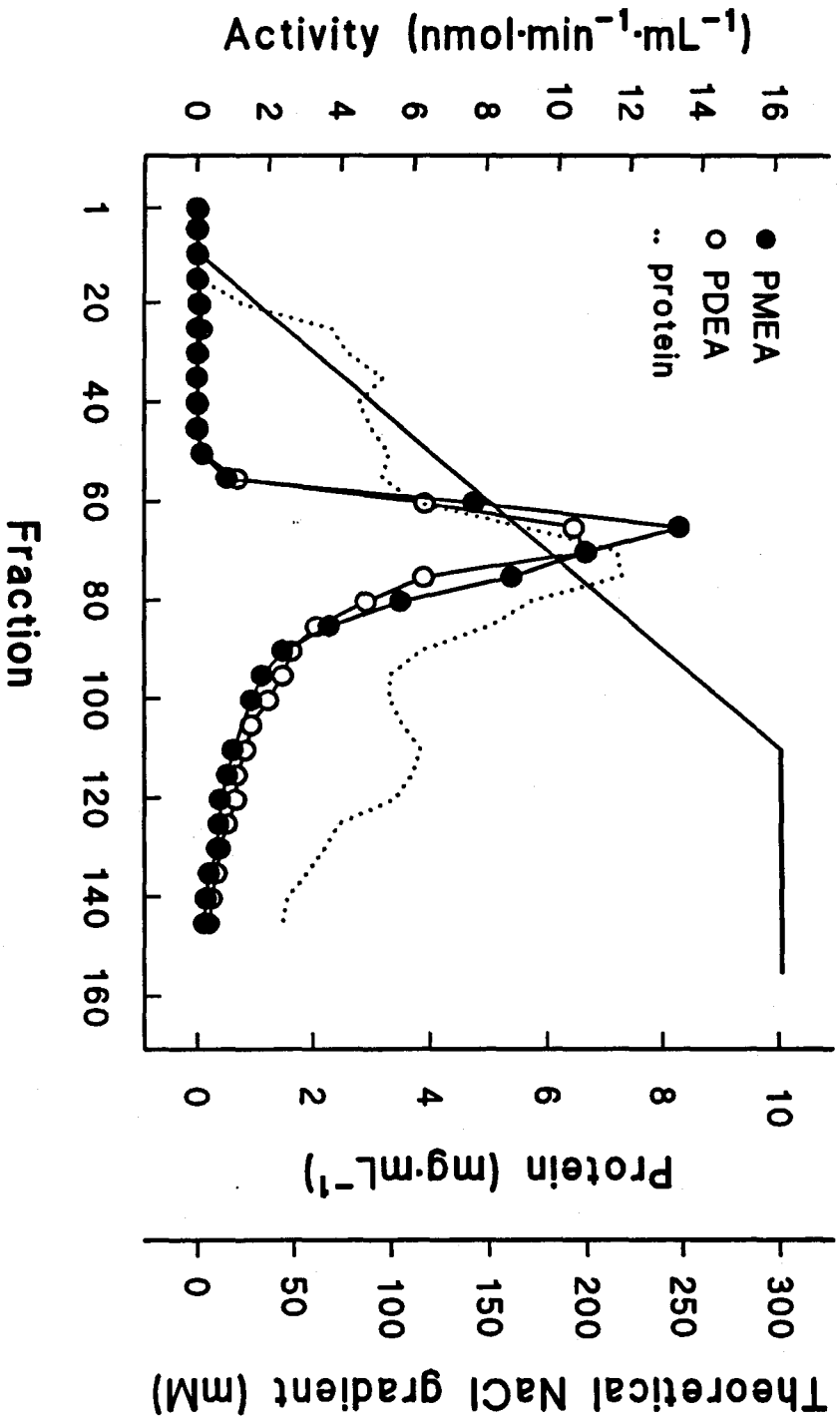
Activity (nmol·min⁻¹·mL⁻¹)
0
2
4
6
8
10
12
14
16
● PMEA
○ PDEA
·· protein
1
20
40
60
80
100
120
140
160
Fraction
0
2
4
6
8
10
Protein (mg·mL⁻¹)
0
50
100
150
200
250
300
Theoretical NaCl gradient (mM)

activities were uni-modal. The fractions containing the highest amounts of both activities were estimated to contain approximately 0.17 M NaCl and this value was based on elution volume, as the concentration of NaCl in fractions was not measured directly. Figure 6 also shows the activities were found in fractions that slightly preceded those containing the highest concentrations of protein. Fractions that exhibited a minimum of 0.72 nmol•min^{-1}•mL^{-1} of PMEAMeT activity were pooled for further purification. There was no apparent difference in the elution profiles of either the activities or protein from the DEAE Sepharose column when a 0 to 0.5 M NaCl gradient was applied in two experiments (Table II) in comparison to the 0 to 0.3 M NaCl gradient applied otherwise (data not shown).

The average pooled sample contained 33% of protein and 64% of PMEAMeT activity present in the 1.8 to 2.6 ammonium sulfate fraction. There was a 67% recovery of PDEA *N*-methylating activity in the sample over the previous step and a low level of PEA *N*-methylating activity was also detected in these samples (Table V). Thus, the use of DEAE Sepharose chromatography resulted in an approximate 2-fold purification for both PMEAMeT and PDEA *N*-methylating activities over the 1.8 to 2.6 ammonium sulfate fractionation.

Hydrophobic interaction chromatography on Phenyl Sepharose matrix

Typically, samples purified by DEAE Sepharose chromatography contained approximately 0.17 M NaCl and as these proteins were already in a salt-containing buffer, Phenyl Sepharose hydrophobic interaction chromatography was used as the next step. To maximise adsorption, samples were adjusted to 1.0 M ammonium sulphate and then loaded onto the phenyl Sepharose column. Typically, 85% of protein present in samples loaded onto the column was adsorbed onto the matrix. Figure 7 shows a typical elution profile of protein and *N*-methylating activities using PMEA and PDEA as substrates. PMEAMeT activity and PDEA *N*-methylating activity co-eluted from the column during the application of a linear gradient of concomitant decreasing ammonium sulphate (25 to 0%) and increasing ethylene glycol (0 to 50%) concentration in buffer B. The peaks of both

FIGURE 7: Hydrophobic interaction chromatography on Phenyl Sepharose (CL-4B) column.

Representative elution profiles of PMEAMeT activity (●, with PMEA as substrate), PDEA *N*-methylating activity (O) and protein (...) from a phenyl Sepharose matrix. Samples recovered after DEAE Sepharose anion exchange chromatography (sample shown is described in Table IV) was made to contain 1.0 M ammonium sulfate and then loaded onto 100 mL Phenyl Sepharose column, pre-equilibrated in buffer B containing 1.0 M ammonium sulfate (Materials and Methods). Adsorbed proteins were then eluted with a 1000 mL linear gradient of 25-0% (w/v) ammonium sulfate/ 0 to 50% ethylene glycol in buffer B followed by a 200 mL wash with 50% ethylene glycol in buffer B (solid line). The eluate was collected in 6 mL fractions. Selected fractions were assayed for PMEAMeT and PDEA *N*-methylating activities as described (Materials and Methods) and protein concentration in fractions was measured using the method of Bradford (1976). Abbreviations: AS, ammonium sulfate; EG, ethylene glycol.

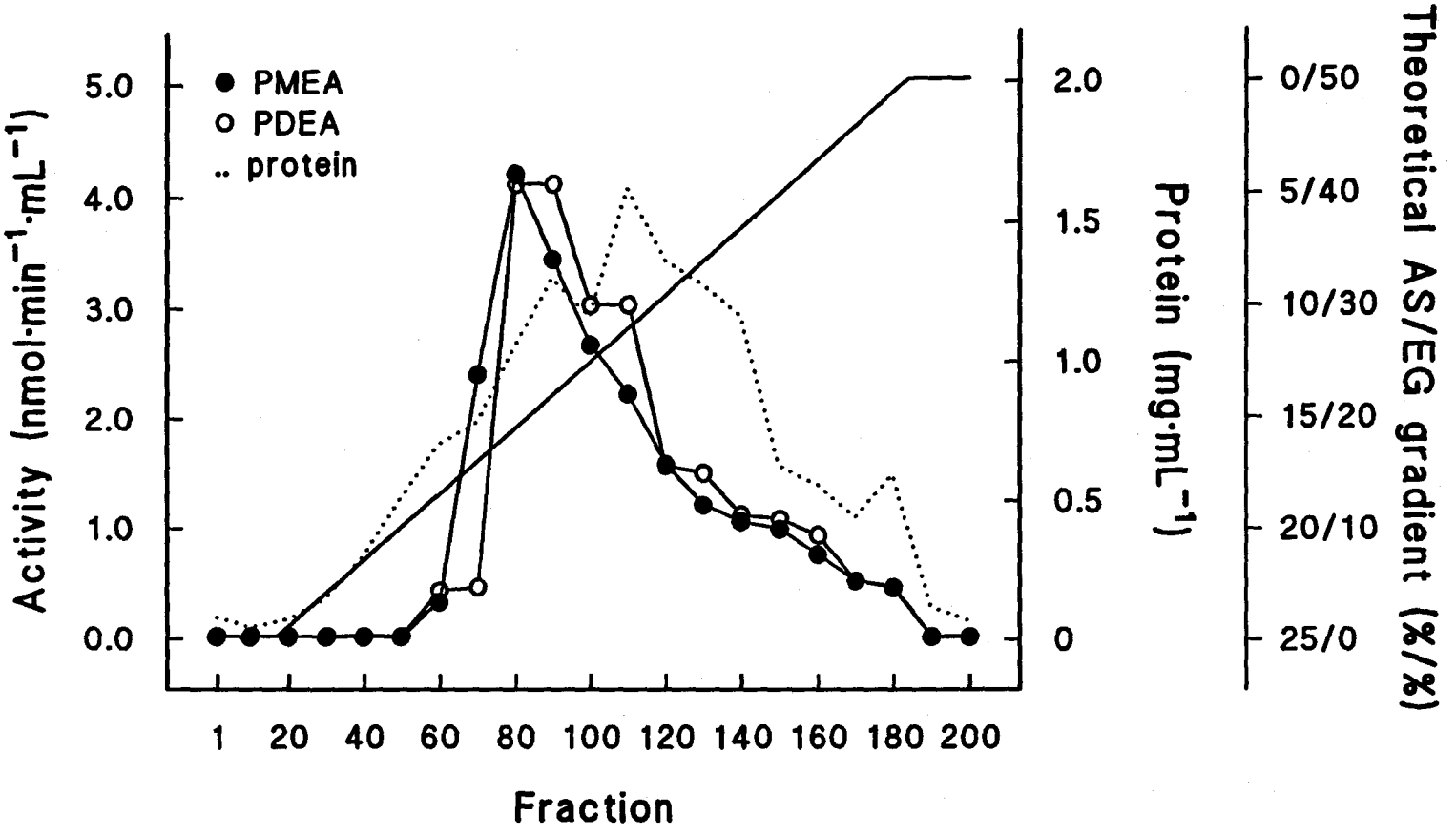
PMEA
PDEA
protein
Activity (nmol·min⁻¹·mL⁻¹)
Protein (mg·mL⁻¹)
Theoretical AS/EG gradient (%/%)
Fraction
5.0
4.0
3.0
2.0
1.0
0.0
2.0
1.5
1.0
0.5
0
0/50
5/40
10/30
15/20
20/10
25/0
1
20
40
60
80
100
120
140
160
180
200

activities overlapped, eluting with an estimated 15% ammonium sulphate/ 20% ethylene glycol (estimate based on elution volume). Figure 7 also shows the activities that were found in fractions that preceded those containing the highest concentrations of protein. Fractions that exhibited a minimum of 0.72 nmol•min^{-1}•mL^{-1} of PMEAMeT activity were pooled, concentrated to less than 20 mL and then the concentrate was dialyzed 100-fold against buffer B to remove ammonium sulphate and ethylene glycol.

The average sample contained 40% of protein and 127% of PMEAMeT activity of the original sample applied to the column. The sample also had a 142% recovery of PDEA *N*-methylating activity over the previous step and PEA *N*-methylating activity was detected at low levels in the pooled, concentrated and dialyzed samples (Table V). Thus, samples were purified approximately 2.0 to 6.2-fold for both PMEAMeT and PDEA *N*-methylating activities over DEAE Sepharose purified samples.

Chromatography on High Q Anion Exchanger Support matrix

For the last step, concentrated and dialysed sample from the phenyl Sepharose chromatography step were diluted to a maximum of 10 mg protein•mL^{-1} with buffer B and then loaded onto a column containing High Q Anion matrix. All protein loaded onto the column was adsorbed to the matrix and Figure 8 shows that PMEAMeT and PDEA *N*-methylating activities co-eluted from the column during application of a linear gradient of increasing NaCl concentration (0 to 0.3 M in buffer B). The elution profiles of PMEAMeT and PDEA *N*-methylating activities were uni-modal and the peak of each activity overlapped, eluting with approximately 0.11 M NaCl (estimated using the elution volume). Figure 8 also shows the peaks of the activities were found in fractions that had the second highest concentrations of protein and preceded those fractions containing the highest concentrations of protein. Fractions that exhibited a minimum of 0.72 nmol•min^{-1}•mL^{-1} of PMEAMeT activity were pooled, concentrated to less than 20 mL and then the concentrate was dialysed 100-fold against buffer B to remove NaCl.

The order of Tables I to IV reflect increasing recoveries of PMEAMeT activity in samples over the phenyl Sepharose purified samples, which can likely be attributed to better

FIGURE 8: Chromatography on High Q Anion Exchanger Support column.

Representative elution profiles of PMEAMeT activity (●, with PMEA as substrate), PDEA *N*-methylating activity (O) and protein (...) from a High Q Anion matrix. Samples recovered after Phenyl Sepharose hydrophobic interaction chromatography (sample shown is outlined in Table IV) were diluted to 10 mg protein•mL^{-1} with buffer B (Materials and Methods) and then loaded onto 50 mL High Q Anion column pre-equilibrated in buffer B. Adsorbed proteins were then eluted with a linear, 500 mL gradient of 0 to 0.3 M NaCl in buffer B followed with a 100 mL wash with 0.3 M NaCl in buffer B (solid line). The eluate was collected in 6 mL fractions. Selected fractions were assayed for PMEAMeT and PDEA *N*-methylating activities as described (Materials and Methods) and protein concentration in fractions was measured using the method of Bradford (1976).

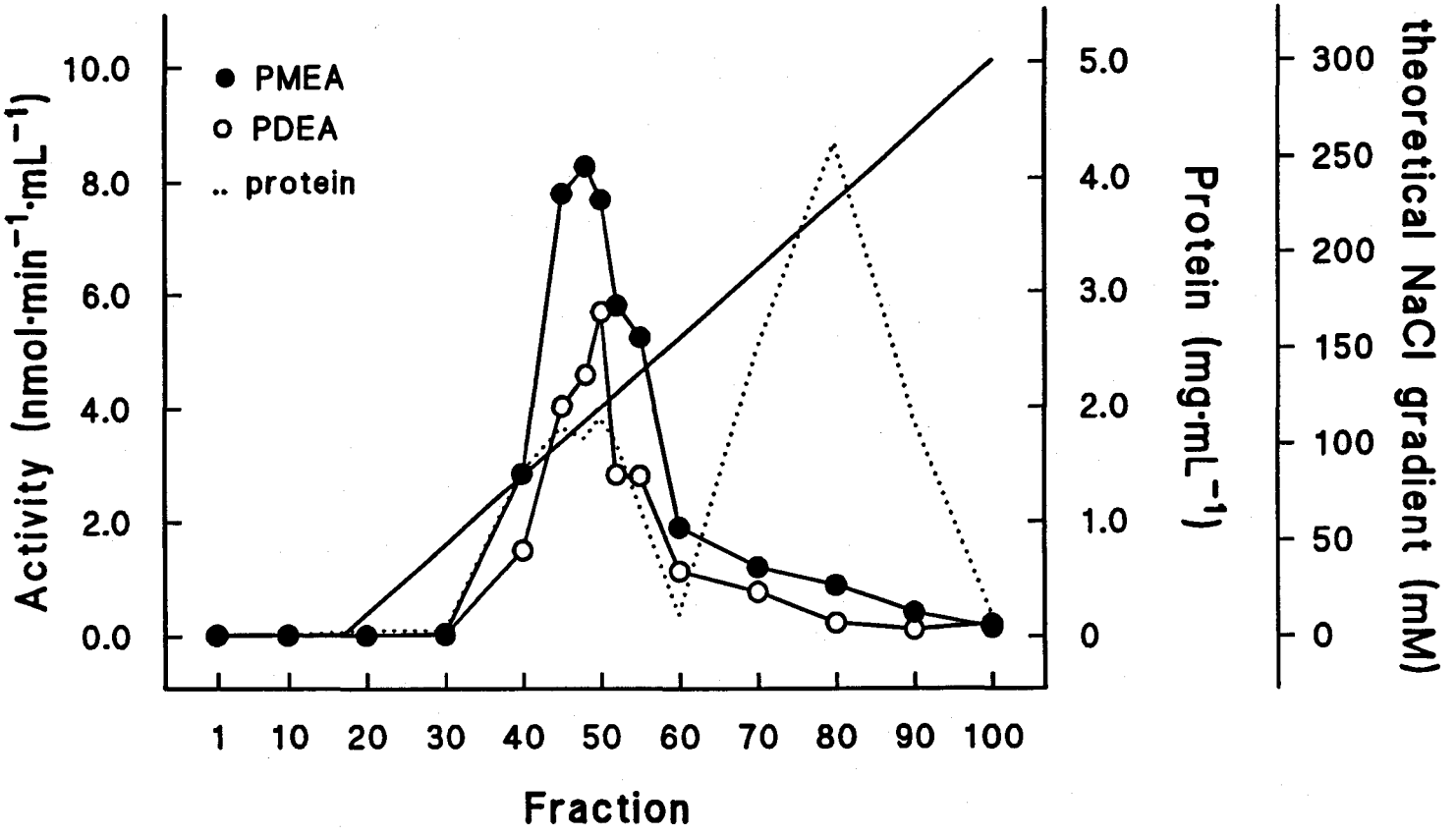
PMEA
PDEA
.. protein
Activity (nmol·min⁻¹·mL⁻¹)
Protein (mg·mL⁻¹)
theoretical NaCl gradient (mM)
Fraction
10.0
8.0
6.0
4.0
2.0
0.0
5.0
4.0
3.0
2.0
1.0
0
300
250
200
150
100
50
0
1
10
20
30
40
50
60
70
80
90
100

skill in handling the column separation with experience. The sample described in Table IV gave the best separation achieved over the phenyl Sepharose purified sample with a 107% recovery of PMEAMeT activity and only a 27% recovery of protein. This last sample also showed a 94% recovery of PDEA *N*-methylating activity over sample from the previous step. This reflects an improvement in specific activities of 4-fold for PMEAMeT activity and 3.8-fold for PDEA *N*-methylating activity over the phenyl Sepharose purified samples. PEA *N*-methylating activity was not detected in pooled, concentrated and dialyzed samples (Table V).

After this last step, samples were purified 21 to 43-fold for PMEAMeT activity over crude leaf extracts. The sample purified to the highest extent of 43-fold had an 18% recovery of PMEAMeT activity and 0.4% recovery of protein present in crude leaf extracts (Table III). This sample was also purified to the highest extent for PDEA *N*-methylating activity of 59-fold and had a 24% recovery of the activity present in crude leaf extracts (Table VII).

Ratio of phosphobase *N*-methylating activities after each purification step

Table V provides the average ratio of specific activities of PEA and PDEA *N*-methylating activities relative to PMEAMeT activity after each step of the purification trials. In crude leaf extracts, the ratio of PEA: PMEA: PDEA *N*-methylating specific activities was approximately 0.07: 1: 1.21. Thus, the phosphobase *N*-methylating specific activities can be ranked in the order from lowest to highest as PEA < PMEA < PDEA in crude leaf extracts. After High Q Anion chromatography, the ratio of PEA: PMEA *N*-methylating specific activities was 0: 1 because PEA N-methylating activity was no longer detected and therefore, the ratio was significantly different from that in crude leaf extracts. In contrast, the ratio of PMEA: PDEA *N*-methylating specific activity after High Q Anion chromatography was approximately 1: 1.15 and was not significantly different from that in crude leaf extracts.

ENZYME CHARACTERIZATION

PMEA and PDEA *N*-methyltransferase assays

Effect of pH

During the purification of PMEAMeT, phosphobase *N*-methylating activities were assayed at pH 7.8 in HEPES-KOH buffer (as in Mudd and Datko, 1988b). However, the optimal pH for PMEAMeT activity and PDEA *N*-methylating activity in leaves depleted of PEA *N*-methylating activity, as used during this study, has not been previously determined. Figure 9 shows the effect of pH on PMEAMeT and PDEA *N*-methylating activities determined using a sample purified 14-fold after phenyl Sepharose chromatography (sample described in Table III). The pH profile of PMEAMeT activity was unimodal and the activity exhibited an apparent pH optimum between 8.5 and 9.0 with 0.1 M Tris-HCl buffer (Panel A, Figure 9). The pH profile of PDEA *N*-methylating activity was also unimodal and the activity similarly exhibited an apparent pH optimum between 8.5 and 9.0 with 0.1 M Tris-HCl buffer (Panel B, Figure 9). Thus while during the purification of PMEAMeT, both activities were assayed at a suboptimal pH, namely pH 7.8, all subsequent phosphobase *N*-methyltransferase assays used to characterize PMEAMeT employed an assay pH of 8.5 with 0.1 M Tris-HCl buffer.

Despite purification and storage of the enzyme for prolonged periods at pH 7.8, no decline in the enzyme activities was found upon repeated freeze/thaw cycles and re-assays which suggested that this pH was not damaging to the enzyme (data not shown). A reason for the decline in activities below pH 8.5 down to pH 7.8 is likely due to formation of a reversible, improper ionic state of either the substrate and/ or enzyme (Segel, 1976). The pH values, both below and above the optimal range, at which irreversible enzyme inactivation plays a role in the observed activity decline would be determined through a study of the effect of pH on enzyme stability (Segel, 1976).

Linearity of PMEA and PDEA *N*-methyltransferase assays with incubation time

When elution profiles for PMEAMeT and PDEA *N*-methylating activities from

FIGURE 9: pH profiles of PMEAMeT and PDEA *N*-methylating activities

PMEAMeT activity (with PMEA as the substrate, Panel A) and PDEA *N*-methylating activity (Panel B) were determined as a function of pH using a series of buffers that overlapped with respect to pH (22°C). The sample used was purified 14-fold after the phenyl Sepharose step (sample described in Table III) and the buffers were at a final assay concentration of 0.1 M. The values shown are the means of two measurements ± SE; except at pH 7.8 with HEPES-KOH buffer which is the mean of eight measurements ± SE. Standard error bars that do not extend beyond the symbols are not shown.

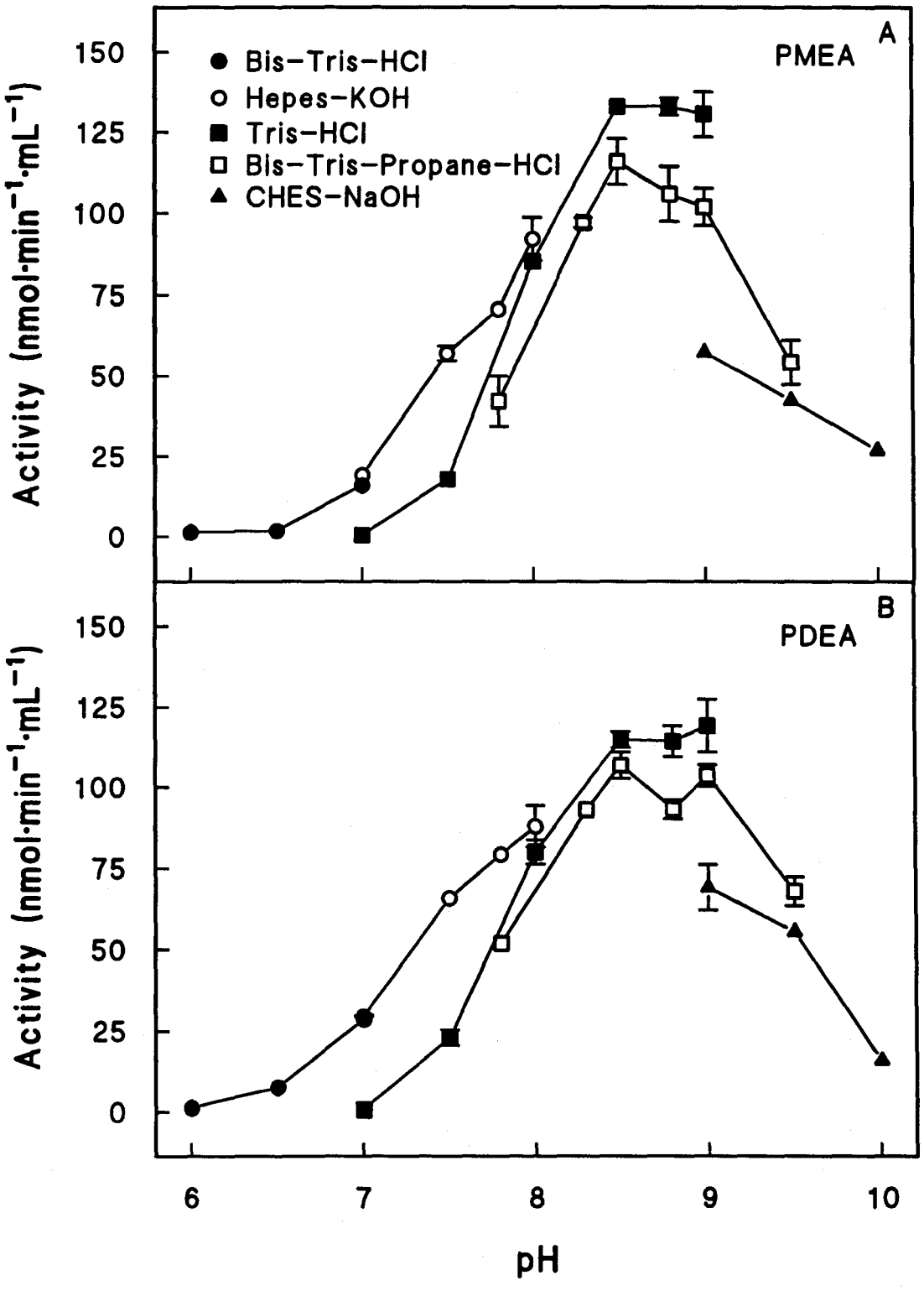
A
PMEA
Bis-Tris-HCl
Hepes-KOH
Tris-HCl
Bis-Tris-Propane-HCl
CHES-NaOH
Activity (nmol·min⁻¹·mL⁻¹)
150
125
100
75
50
25
0
B
PDEA
Activity (nmol·min⁻¹·mL⁻¹)
150
125
100
75
50
25
0
6
7
8
9
10
pH

various chromatographic columns were being determined, undiluted samples from select fractions were added directly to the assays and the length of the incubation period was 30 min as described in Mudd and Datko (1988b). Dilutions of these samples yielded higher estimates of enzyme activity showing the assays were non-linear with time. Therefore, determinations of total activity recovered after each purification step and for characterization studies required diluting samples with assay buffer before addition of the sample to the assay. It has been determined that a sample diluted so that substrate-dependant enzyme activity did not exceed 55 nmol•mL^{-1} by the end of the incubation period at either assay pH 7.8 or 8.5 provided the highest rate of enzyme activity which does not change upon further sample dilution (data not shown). Samples purified through the last step of High Q Anion chromatography were diluted to approximate this rate per minute and used to test the linearity of PMEAMeT and PDEA *N*-methylating activities over a 60 minute incubation interval (Figure 10). Linearity of reaction rates of these samples were tested because they were used for all subsequent characterization studies. Figure 10 shows the PMEA *N*-methyltransferase assay was linear ($r^2 = 0.988$) for up to 30 min using sample purified 30-fold (sample described in Table IV). Figure 10 also shows the PDEA *N*-methyltransferase assay although more variable was reasonably linear ($r^2 = 0.957$) for up to 30 min using sample purified 43-fold (sample described in Table III).

Comparison of phosphobase *N*-methylating activities assayed at pH 7.8 and 8.5

Phosphobase *N*-methylating activities were assayed at pH 8.5 with 0.1 M Tris-HCl using samples from the High Q Anion step from each purification trial, diluted to yield activity in a linear range (data not shown). This was done to provide a comparison of PEA: PMEA: PDEA *N*-methylating activities at pH 7.8 and 8.5 (Table VIII) and the data reported for pH 7.8 is from Table V. The average ratio of PEA: PMEA: PDEA *N*-methylating specific activities was approximately 0: 1: 1.06 after the High Q Anion step when the activities were assayed at pH 8.5, a ratio which was not significantly different from that at pH 7.8 and one which indicated that PEA *N*-methylating activity was still not detected.

FIGURE 10: Effect of incubation time on PMEA and PDEA *N*-methyltransferase assays.

PMEAMeT activity (●, with PMEA as substrate) and PDEA *N*-methylating activity (O) were assayed using protein purified 30 and 43-fold, respectively, after High Q Anion chromatography (samples described in Tables IV and III, respectively). The assay incubation period was varied from between 0 to 60 min. The values for both activities are means of two measurements ± SE. Standard error bars that do not extend beyond the symbols are not shown. The line of best fit for PMEAMeT activity through data points 0 to 30 min gives an equation of $y = 3.822x + 2.116$ with an r^2 of 0.988. The line of best fit for PDEA *N*-methylating activity through data points from 0 to 30 min gives an equation of $y = 2.141x + 6.666$ with an r^2 of 0.957.

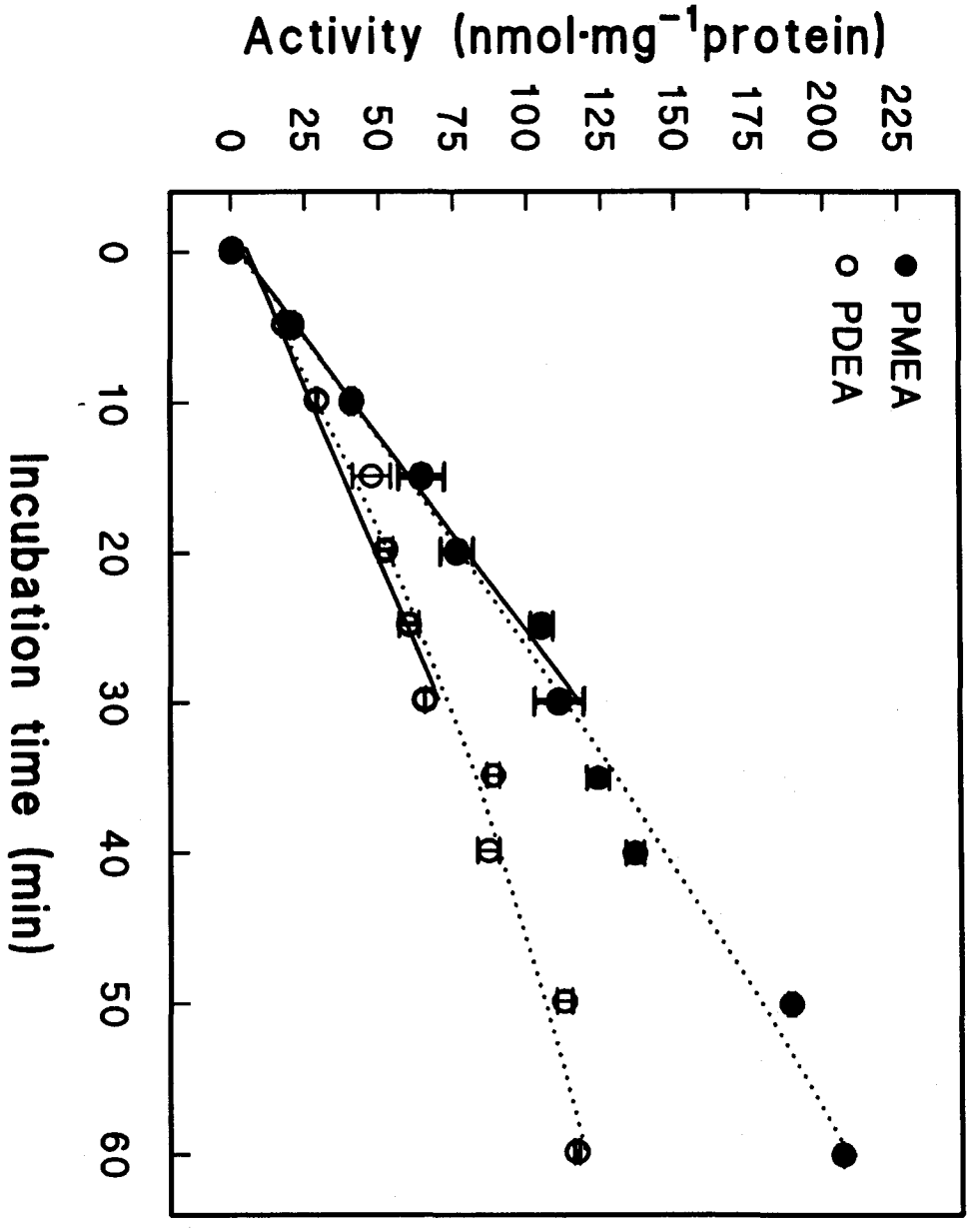
Activity (nmol·mg⁻¹protein)
0
25
50
75
100
125
150
175
200
225
● PMEA
o PDEA
0
10
20
30
40
50
60
Incubation time (min)

Table VIII: Average ratio of PEA and PDEA *N*-methylating specific activities relative to PMEAMeT at pH 7.8 and 8.5 in samples purified after High Q Anion chromatography[a]

Purification step	Assay pH	Ratio of specific activities relative to that of PMEAMeT activity		
		PEA	PMEA	PDEA
High Q Anion	7.8	nd[b]	1[c]	1.15 ± 0.11
	8.5	nd[b]	1[d]	1.06 ± 0.10

[a] PMEAMeT activity assayed with PMEA as substrate.
[b] The activity was at or below the assay detection limit (0.036 nmol•min^{-1}•mL^{-1} sample).
[c] Average PMEAMeT specific activity was 9.1 ± 2.6 nmol•min^{-1}•mg^{-1} protein and calculated from data reported in Table I to IV.
[d] Average PMEAMeT specific activity was 14.2 ± 3.3 nmol•min^{-1}•mg^{-1} protein.

Molecular weight estimation

Gel filtration chromatography

The native molecular weight of PMEAMeT was estimated by HPLC gel filtration chromatography with a sample purified 30-fold after High Q Anion chromatography (sample described in Table IV). Figure 11 (Panel A) shows the elution profile of PMEAMeT activity from the gel filtration column. A native molecular mass of 76.4 ± 0.9 kDa for PMEAMeT was estimated by comparing the V_e/ V_o estimate for the maximal peak of PMEAMeT activity to the calibration curve (Figure 12) showing log molecular weight versus V_e/ V_o for standards applied to the column. Figure 12 also shows V_e/ V_o positions for internal molecular weight standards of alcohol dehydrogenase (ADH) and carbonic anhydrase (CA) which were co-chromatographed with the 30-fold partially purified sample. The native molecular mass estimates were 148 ± 2 kDa for ADH and 34 ± 0.3 kDa for CA, which are in complete agreement with the values estimated from the calibration curve (ADH, 147 ± 0 kDa; CA, 34.1 ± 0.3 kDa). In the last experiment with the gel filtration column, fractions eluting from the column were also assayed for PDEA *N*-methylating activity and the elution profile for this activity is given in Figure 11 (Panel B). The fraction that contained the maximal peak of PMEAMeT activity also contained maximal PDEA *N*-methylating activity. Thus, a native molecular mass of 76.4 ± 0.9 kDa was also estimated for the enzyme associated with the maximal peak of PDEA *N*-methylating activity and the enzyme was designated as PDEAMeT in Figure 12.

SDS-PAGE, Fluorography

Photolabeling with [*methyl*-^{3}H]SAM in the presence of UV light is considered to be a common characteristic of SAM-dependent methyltransferases (Dixon et al., 1992; Hanson et al., 1995), while enzymes that do not use SAM are not photolabeled (Som and Friedman, 1989; Guschlbauer et al., 1991). The whole SAM molecule is considered to bind covalently and irreversibly specifically at the SAM-binding site of active enzymes (Som and Friedman, 1989; Guschlbauer et al., 1991; Higman and Niles, 1994),

FIGURE 11: Elution profiles for PMEAMeT and PDEA *N*-methylating activties from an HPLC gel filtration chromatography column.

A sample purified 30-fold for PMEAMeT by High Q Anion chromatography (sample described in Table IV) was applied in buffer C to a 7.5 × 300 mm, 13.3 mL bed volume HPLC Protein Pak gel filtration chromatography column, pre-equilibrated in buffer C (Materials and Methods). The sample was chromatographed at a flow rate of 0.1 $mL \bullet min^{-1}$ and the column eluate was collected in 100 μL fractions. Select fractions were assayed for PMEAMeT activity and PDEA *N*-methylating activity and the elution profiles of the activities are shown in Panel A and Panel B, respectively, as a function of elution volume, V_e. Panel A is a representative elution profile based on two measurements; whereas Panel B represents the outcome of a single experiment.

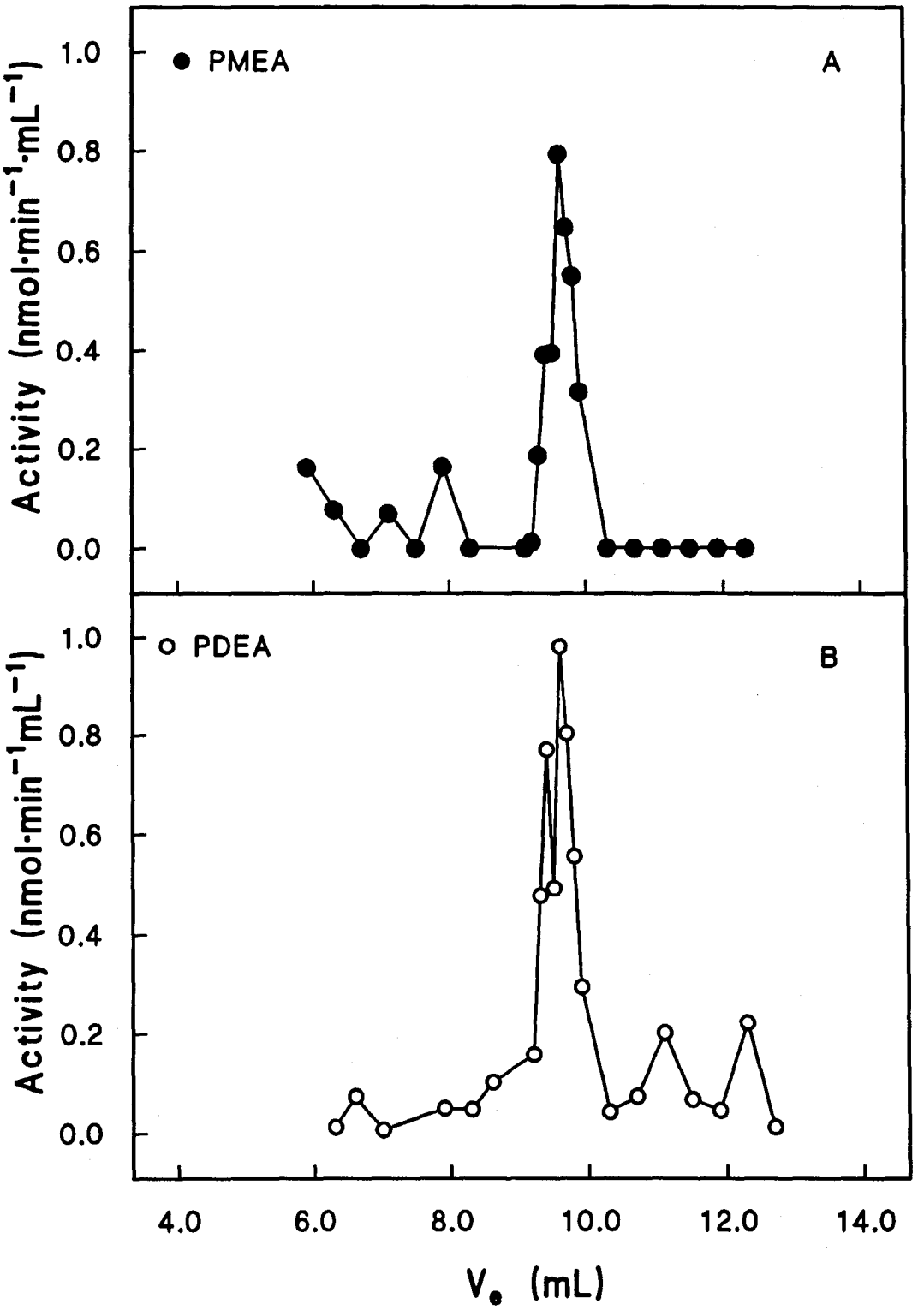
PMEA
A
PDEA
B
Activity (nmol·min⁻¹·mL⁻¹)
1.0
0.8
0.6
0.4
0.2
0.0
4.0
6.0
8.0
10.0
12.0
14.0
Ve (mL)

FIGURE 12: Estimation of native molecular weight of PMEAMeT and the enzyme associated with PDEA *N*-methylation (PDEAMeT).

The HPLC Protein Pak gel filtration chromatography column, pre-equilibrated in buffer C, was calibrated using molecular weight standards (●) of β-amylase (200 kDa), alcohol dehydrogenase (150 kDa), bovine serum albumin (132 kDa), carbonic anhydrase (29 kDa) and cytochrome c (12.4 kDa) dissolved in buffer C (Materials and Methods). The calibration curve was constructed using the average estimate of elution volume of standards/ void volume (V_e/ V_o) from two repeat runs using only the standards and V_o was estimated using blue dextran (2,000 kDa). Regression analysis of the curve generated by each run of standards gave the following two equations: $y = 4.86 - 0.683x$ with a fit of $r^2 = 0.993$; and $y = 4.873 - 0.688x$ with a fit of $r^2 = 0.991$. A native molecular mass of 76.4 ± 0.9 kDa (□) for PMEAMeT coincides with the estimate for the enzyme that *N*-methylates PDEA, designated as PDEAMeT, as determined using the V_e/ V_o value for the maximal peak of both activities. The positions of two internal standards (○) co-injected with the protein sample are also shown and provide molecular weight estimates of 148 ± 2 kDa and 34 ± 0.9 kDa for alcohol dehydrogenase and carbonic anhydrase, respectively.

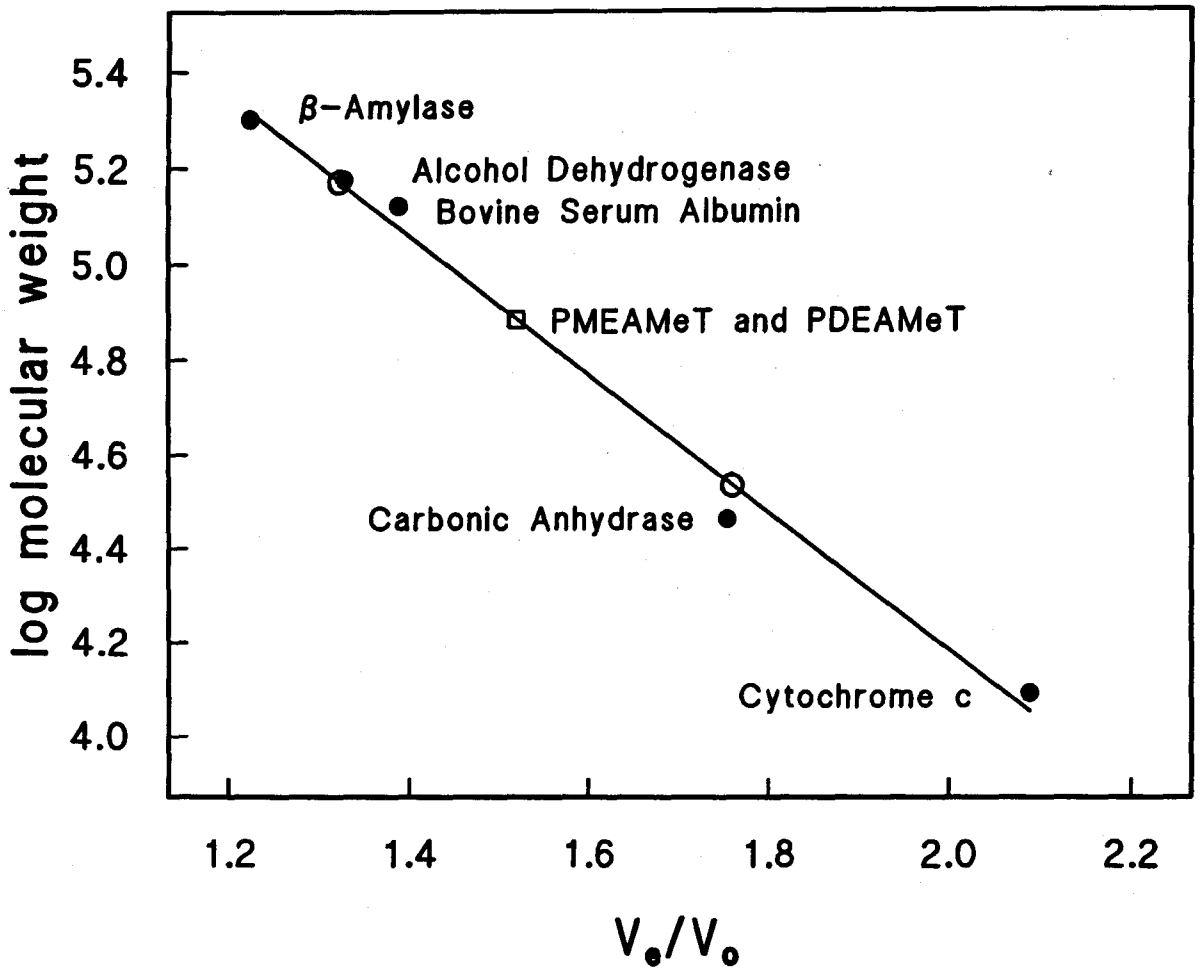
log molecular weight
5.4
5.2
5.0
4.8
4.6
4.4
4.2
4.0
β–Amylase
Alcohol Dehydrogenase
Bovine Serum Albumin
PMEAMeT and PDEAMeT
Carbonic Anhydrase
Cytochrome c
1.2
1.4
1.6
1.8
2.0
2.2
V_e/V_o

presumably through the methyl group (Som and Friedman, 1990; Subbaramaiah and Simms, 1992). This technique was employed to try to identify PMEAMeT or its SAM-binding component by photolabeling samples from each purification step and then using SDS-PAGE and fluorography (see Som and Friedman, 1989 and Shockey et al., 1995). Panel A of Figure 13 shows the SDS-polyacrylamide gel used to analyze samples that had been photolabeled with [*methyl*-^{3}H]SAM and Coomassie-stained while Panel B shows a fluorograph of the same gel.

The fluorograph (Panel B, Figure 13) shows that polypeptides of differing molecular weight were radiolabeled by [*methyl*-^{3}H]SAM in samples from the various steps (*lanes* 1 to 5). However, only one labeled polypeptide of approximately 28.6 kDa (highlighted by arrow) faintly detected first in *lane* 2, which was loaded with a sample of the ammonium sulfate fraction, was also detected at all subsequent steps (*lanes* 3 to 5). Also, the intensity of the band at 28.6 kDa increased with each step which coincides with an increased activity of PMEAMeT. Thus, the polypeptide could be a good candidate for the SAM-binding component of the enzyme. The polypeptide would, though, have a molecular mass of less than 28.6 kDa by at least 0.48 kDa, if a theoretical [*methyl*-^{3}H]SAM: peptide binding ratio of 1: 1 is applied leaving an estimated molecular mass of 28.1 kDa.

The appearance of another polypeptide of approximately 26 kDa (below the above labeled peptide) was noted in protein samples from the last two steps (*lanes* 4 and 5) with the label being more intense in sample from the last step of High Q Anion chromatography (*lane* 5). Thus, this polypeptide could also be a potential candidate for the SAM-binding component of the enzyme. Although, the molecular mass of the polypeptide would be approximately 25 kDa, taking into account the consideration outlined above.

Samples which were not photolabeled with [*methyl*-^{3}H]SAM were also resolved using SDS-polyacrylamide gel electrophoresis and the gel stained with a silver reagent (Figure 14). As there were a number of polypeptides of 24 to 28 kDa molecular mass

FIGURE 13: Photolabeling of [*methyl*-^{3}H]SAM to samples from each purification step.

A sample equivalent to 60 μg protein from each purification step was mixed with 0.43 μM [*methyl*-^{3}H]SAM (70.1 Ci•mmole^{-1}; 0.55 μCi•μL^{-1}) in 0.15 M Tris-HCl (pH 8.5, 22°C) buffer containing 1.5 mM Na_2-EDTA in a final volume of 53 μL. The mixture was then irradiated on ice for 1 h at a distance of 1.0 cm with 254 nm UV light. 40 μL of the irradiated mixture was added to 40 μL of SDS sample buffer to stop the reaction. One half volume of the stopped reaction mixture (equivalent to 22.6 μg protein) was denatured by heating at 90°C for 3 min, then separated electrophoretically using a 7.5 to 15% SDS polyacrylamide gradient gel. The gel was stained with Coomassie dye, destained and then dried (Panel A). A fluorograph was developed after exposing the Coomassie-stained gel to X-ray film for 3 months at -80°C (Panel B). *Lane 1*, Crude; *lane 2*, Ammonium sulfate fraction; *lane 3*, DEAE Sepharose; *lane 4*, Phenyl Sepharose; *lane 5*, High Q Anion. The amount of PMEAMeT activity and PDEA *N*-methylating activity (pmol•min^{-1}) in each lane is reported below Panel B. The positions of the molecular weight standards are indicated to the right of each Panel. The arrow on the right of Panel B highlights the position of the most prominent [*methyl*-^{3}H]SAM-labeled band.

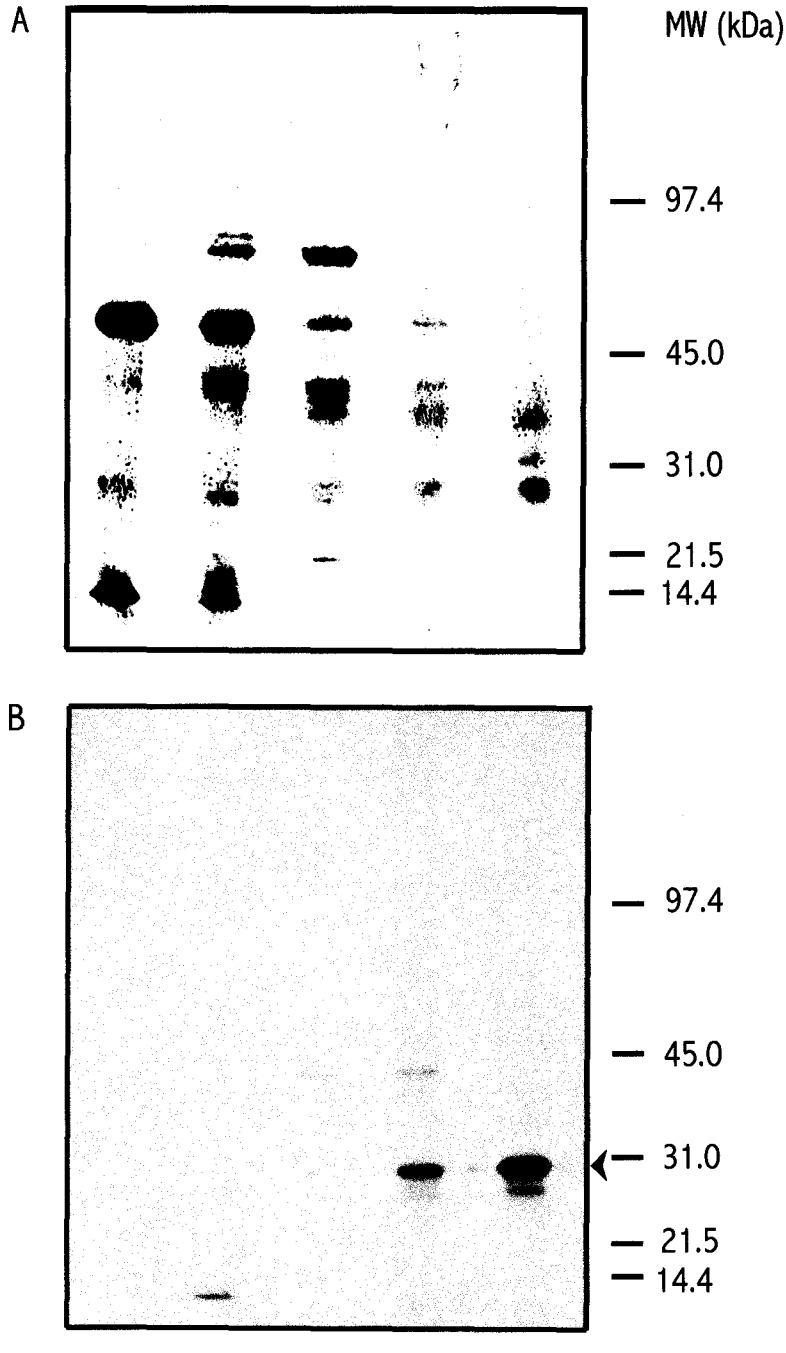

PMEAMeT activity (pmol•min^{-1})	3.8	15.5	68.4	122.2	202.3
PDEA *N*-methylating activity (pmol•min^{-1})	5.5	17.6	73.1	128.2	170.6

FIGURE 14: SDS-PAGE of samples from each purification step.

A sample equivalent to 2.5 μg protein from each purification step was added to SDS sample buffer in a final volume of 20 μL. The mixtures were denatured by heating at 90°C for 3 min, separated in a 7.5 to 15% SDS polyacrylamide gradient gel and the gel was then silver-stained. *Lane 1*, Crude; *lane 2*, Ammonium sulfate fraction; *lane 3*, DEAE Sepharose; *lane 4*, Phenyl Sepharose; *lane 5*, High Q Anion. The amount of PMEAMeT activity and PDEA *N*-methylating activity ($pmol \bullet min^{-1}$) in each lane is reported below the gel. The positions of the molecular weight standards are indicated to the right of the gel. The arrow at the right of the gel highlights the approximate position of 28 to 25 kDa polypeptides.

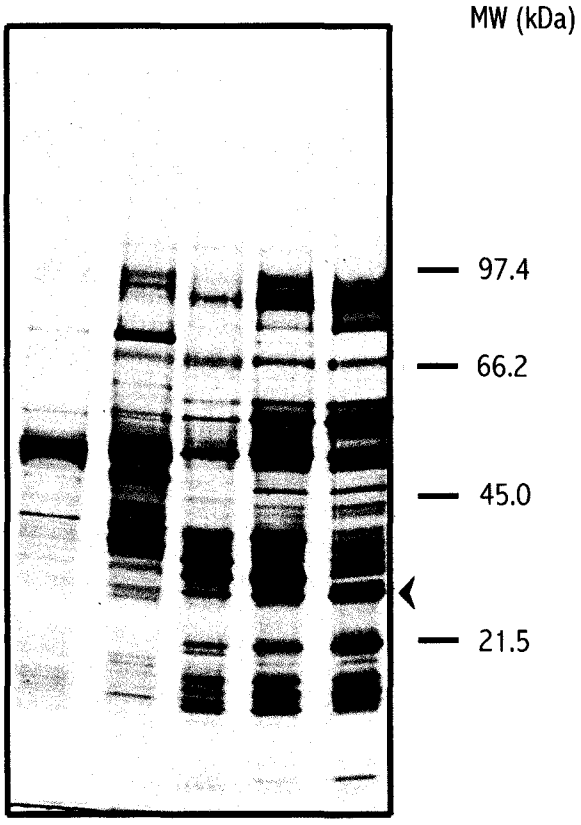

PMEAMeT activity (pmol•min^{-1})	0.8	3.4	11.9	27.0	23.9
PDEA *N*-methylating activity (pmol•min^{-1})	1.2	3.8	19.6	28.0	30.2

range even in *lane* 5 (position highlighted by arrow), it was not possible to identify a specific one as being a SAM-binding component of PMEAMeT.

Product identification and quantification of PEA, PMEA and PDEA *N*-methyltransferase assays

The amount of [*methyl*-^{3}H]phosphobase in the 0.1 N HCl eluate from Dowex columns of phosphobase *N*-methyltransferase assays with PEA, PMEA and PDEA as substrates provides information about the rate of transfer of methyl groups from [*methyl*-^{3}H]SAM to the substrate (Mudd and Datko, 1988b). Furthermore, the eluate can be used to identify and quantify the radiolabeled phosphobase products using TLC.

Phosphobase *N*-methyltransferase assays were performed using sample purified 30-fold after the last step of High Q Anion chromatography (sample described in Table IV). As is typical for these samples, with PEA as the substrate no radioactivity was detected in the 0.1 N HCl eluate (Table VIII) and when concentrated eluates were separated on silica G plates by TLC, no radioactivity was associated with zones to which any of the phosphobases migrated.

With PMEA as the substrate, of the radioactivity applied to a TLC plate, an average 51% was recovered with the silica scraped from the plates after chromatography and the radioactivity was associated with the zones to which PDEA and PCho migrated (Table IX). The ratio of [*methyl*-^{3}H]PDEA: [*methyl*-^{3}H]PCho produced was approximately 9:1, so PDEA was the dominant *N*-methylated product of PMEA *N*-methyltransferase assays in a 30 min incubation period. To provide this ratio, the cumulative amounts of [*methyl*-^{3}H]PDEA and [*methyl*-^{3}H]PCho produced in these assays were calculated and these values were determined as follows (Audubert and Vance, 1983): for [*methyl*-^{3}H]PDEA = (cpm associated with PDEA zone) + 1/2 (cpm associated with PCho zone) and for [*methyl*-^{3}H]PCho = (cpm associated with PCho zone).

With PDEA as the substrate, of the radioactivity applied to a TLC plate, an average 48% was recovered with silica scraped from the plate after chromatography and the radioactivity was only associated with the zone to which PCho migrated (Table IX). Thus,

Table IX: Identification and quantification of [*methyl*-^{3}H]labeled *N*-methylated Phosphobases products[a]

Phosphobase substrate	Radioactivity[b]		[*methyl*-^{3}H]labeled phosphobase product[c]		
	Applied	Recovered	PMEA	PDEA	PCho
	cpm			%	
PMEA	3710 ± 220	1878 ± 106	0	88 ± 2	12 ± 2
PDEA	3336 ± 134	1586 ± 149	0	0	100

[a] Phosphobase *N*-methylating activities were assayed at pH 8.5 using sample purified 30-fold (Table IV). Sample preparation and analysis by TLC as described in Materials and Methods.

[b] Values are means of two measurements ± SE.

[c] Expressed as a percentage of the total [*methyl*-^{3}H] recovered from the plate.

PCho was the product of PDEA *N*-methyltransferase assays in the 30 min incubation period. As a precautionary measure, zones associated with PEA were also scraped and no radioactivity was recovered with any of the phosphobase substrates.

Effect of metal ions

Table X shows the effect of various chloride salts and Na_2-EDTA on PMEAMeT and PDEA *N*-methylating activities determined using sample purified 43-fold (sample described in Table III). The addition of NaCl at 30 and 140 mM inhibited PMEAMeT activity by 7 and 25%, respectively; but did not inhibit PDEA *N*-methylating activity. The omission of Na_2-EDTA, normally included in assays at a final concentration of 1 mM (Mudd and Datko, 1988b), had no effect on either activity. In the absence of Na_2-EDTA, the effect of $MgCl_2$ and $MnCl_2$ at 1 and 10 mM was tested. $MgCl_2$ at 1 mM inhibited PMEA-dependent methylation in the range from 10 to 20% but had no effect on PDEA-dependent methylation. $MgCl_2$ at 10 mM inhibited PMEAMeT and PDEA *N*-methylating activities by approximately 49 and 32%, respectively. $MnCl_2$ at 1 and 10 mM completely inhibited both activities. The inhibition was a result of Mg^{2+} and Mn^{2+} ions and not Cl^- ions because NaCl at 20 mM should inhibit PMEAMeT activity at most by 5% and should not inhibit PDEA *N*-methylating activity.

Effect of metabolites

Figures 15 to 19 show the effect of various metabolites on PMEAMeT and PDEA *N*-methylating activities determined using sample purified 30-fold (sample described in Table IV) and the data is also reported in Table XI. Figure 15 shows SAH was added to the assays in the range from 0.001 and 0.2 M and both activities were inhibited with increasing concentrations of SAH. At 0.2 M SAH, which was equivalent to the concentration of SAM in the assays, both activities were reduced by approximately 92%. The metabolites PCho (Na-salt), choline (Cl-salt) and P_i (Na-salt) were added to the assays in the range from 0.5 to 10 mM and any effect on the activities was due to the metabolites because NaCl at 10 mM should have no effect on either activity (Table X). Figure 16 shows both activities were

Table X: Effect of metal ions on PMEAMeT and PDEA *N*-methylating activities[a]

Addition or modification	n	Final assay concentration	*N*-methylating activity	
			PMEA	PDEA
		mM	% of control	
None			100	100
+ NaCl	4	30	93 ± 2	105 ± 2[b]
		140	75 ± 3	112 ± 0[b]
- Na_2-EDTA	6		99 ± 3	98 ± 5
+ $MgCl_2$	6	1	86 ± 6	99 ± 14
		10	51 ± 5	68 ± 8
+ $MnCl_2$	2	1	0[c]	0[c]
		10	0[c]	0[c]

[a] PMEAMeT activity assayed with PMEA as substrate. The sample used was purified 43-fold (Table III) with control PMEAMeT and PDEA *N*-methylating activities ranging from 76 to 166 and 96 to 190 nmol•min^{-1}•mL^{-1}, respectively.

[b] Values are means of two measurements ± SE.

[c] The activity was at or below the detection limit of the assay (0.036 nmol•min^{-1}•mL^{-1} sample).

FIGURE 15: Inhibition by SAH of PMEAMeT and PDEA *N*-methylating activities.

PMEAMeT activity (■, with PMEA as substrate) and PDEA *N*-methylating activity (□) were assayed in the presence of increasing final assay concentrations of SAH (0.001 to 0.2 mM) with sample purified 30-fold after the High Q Anion step (sample described in Table IV). The concentration of SAM was held constant at a final assay concentration of 0.2 mM (standard concentration in phosphobase *N*-methyltransferase assays as in Mudd and Datko [1998b]). Values are means of three measurements ± SE. In the absence of SAH, control PMEAMeT activity was 187 ± 4 nmol•min^{-1}•mL^{-1} and control PDEA *N*-methylating activity was118 ± 24 nmol•min^{-1}•mL^{-1}.

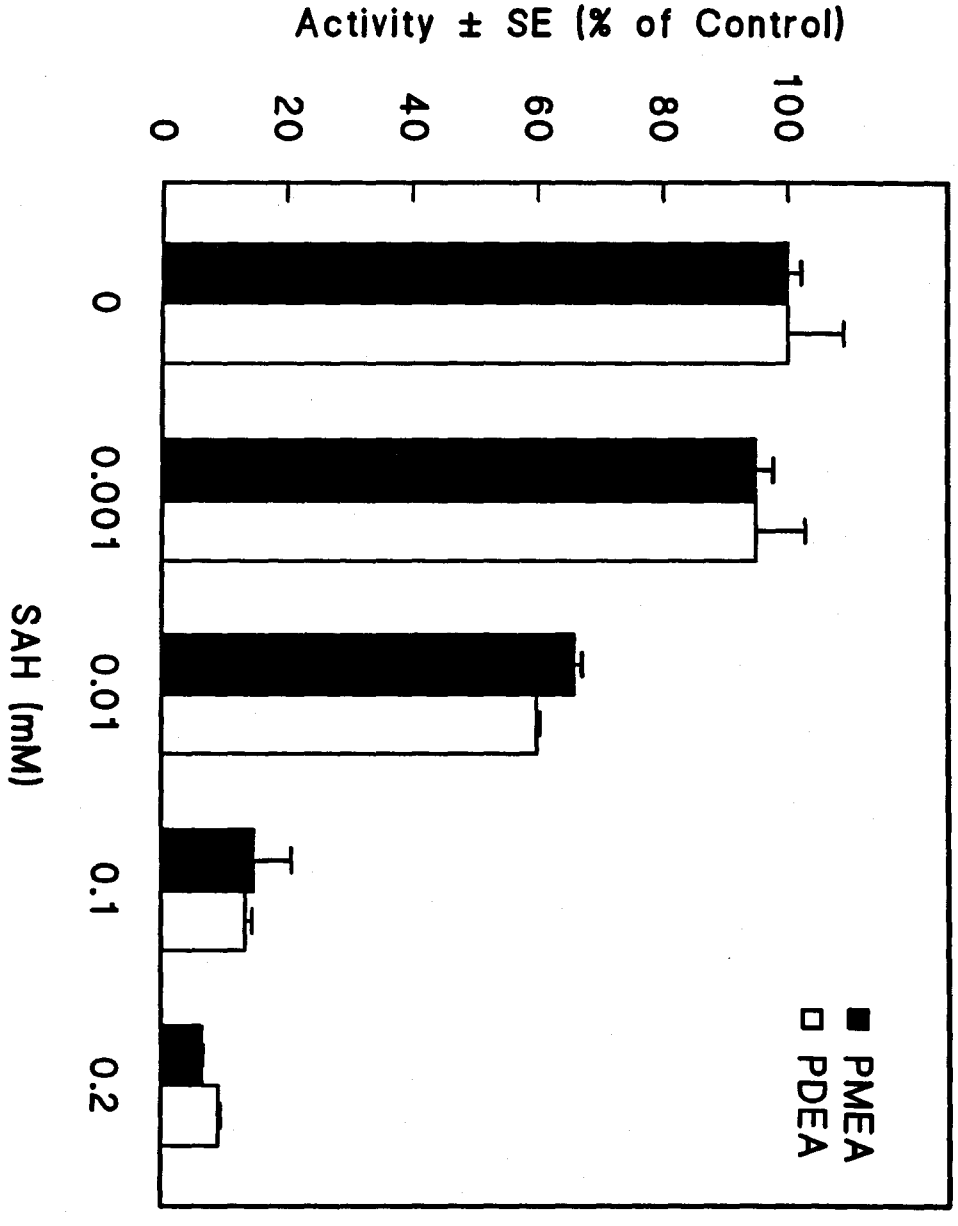
Activity ± SE (% of Control)
0
20
40
60
80
100
SAH (mM)
0
0.001
0.01
0.1
0.2
PMEA
PDEA

FIGURE 16: Inhibition by PCho (Na-salt) of PMEAMeT and PDEA *N*-methylating activities.

PMEAMeT activity (■, with PMEA as substrate) and PDEA *N*-methylating activity (□) were assayed in the presence of increasing final assay concentrations of PCho from 0.5 to 10 mM with sample purified 30-fold after the High Q Anion step (sample described in Table IV). Values are means of four measurements ± SE; except, for at a final assay concentration of 10 mM which are means of two measurements ± SE. In the absence of PCho, control PMEAMeT activity was between 102 and 107 $nmol \bullet min^{-1} \bullet mL^{-1}$; and control PDEA *N*-methylating activity was between 117 and 142 $nmol \bullet min^{-1} \bullet mL^{-1}$.

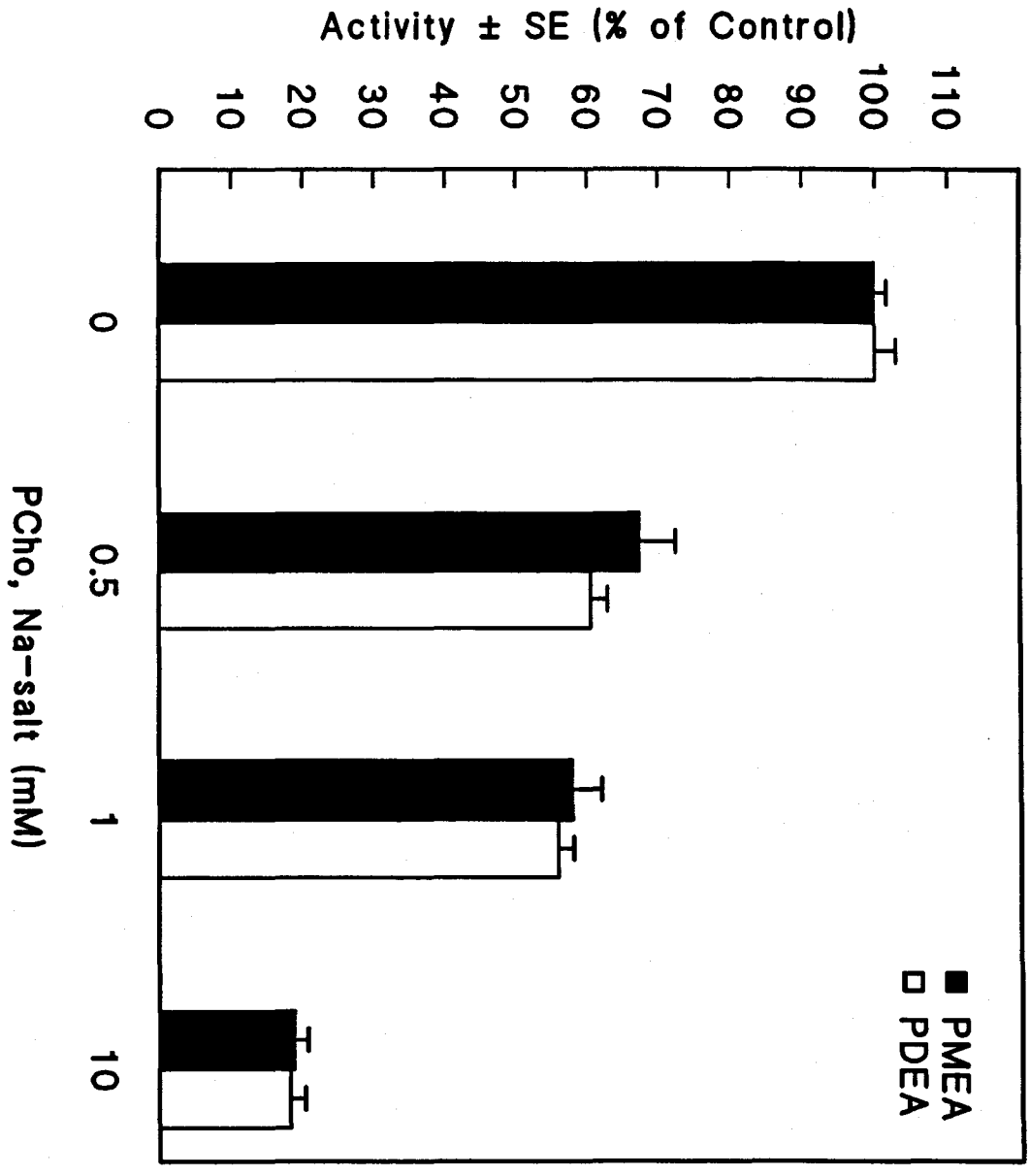
Activity ± SE (% of Control)
0
10
20
30
40
50
60
70
80
90
100
110
PCho, Na-salt (mM)
0
0.5
1
10
PMEA
PDEA

FIGURE 17: Effect of choline (Cl-salt) on PMEAMeT and PDEA *N*-methylating activities.

PMEAMeT activity (■, with PMEA as substrate) and PDEA *N*-methylating activity (□) were assayed in the presence of increasing final assay concentrations of choline from 0.5 to 10 mM with sample purified 30-fold after the High Q Anion step (sample described in Table IV). Values are means of four measurements ± SE. In the absence of choline, control PMEAMeT activity was between 80 and 107 $nmol \bullet min^{-1} \bullet mL^{-1}$ and control PDEA *N*-methylating activity was between 84 and 118 $nmol \bullet min^{-1} \bullet mL^{-1}$.

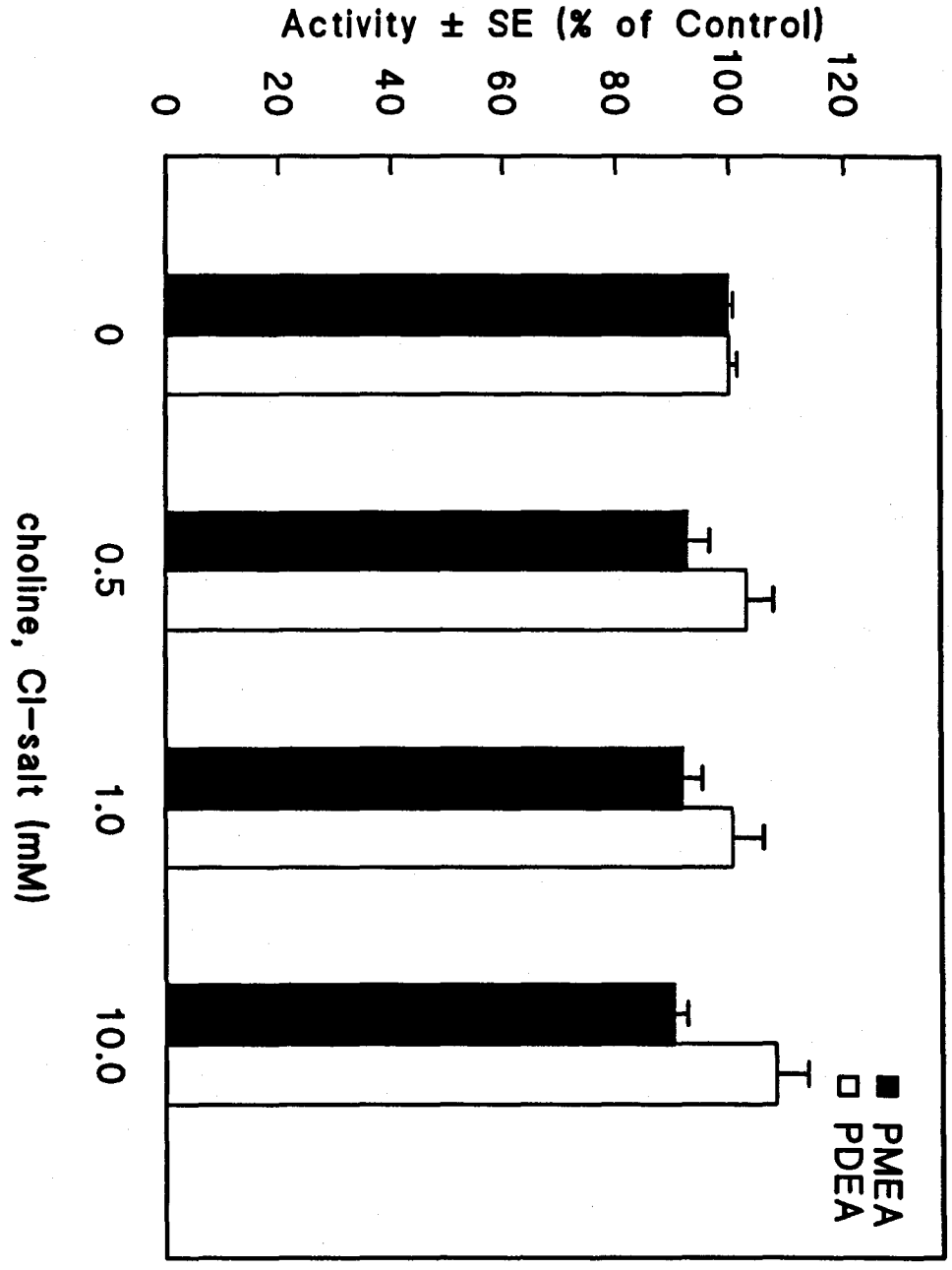
Activity ± SE (% of Control)
0
20
40
60
80
100
120
0
0.5
1.0
10.0
choline, Cl-salt (mM)
PMEA
PDEA

FIGURE 18: Effect of P_i (Na-salt) on PMEAMeT and PDEA *N*-methylating activities.

PMEAMeT activity (■, with PMEA as substrate) and PDEA *N*-methylating activity (□) were assayed in the presence of increasing final assay concentrations of P_i from 0.5 to 10 mM with sample purified 30-fold after the High Q Anion step (sample described in Table IV). Values are means of four measurements ± SE. In the absence of P_i, control PMEAMeT activity was between 122 and 204 $nmol \bullet min^{-1} \bullet mL^{-1}$ and control PDEA *N*-methylating activity was between 94 and 206 $nmol \bullet min^{-1} \bullet mL^{-1}$.

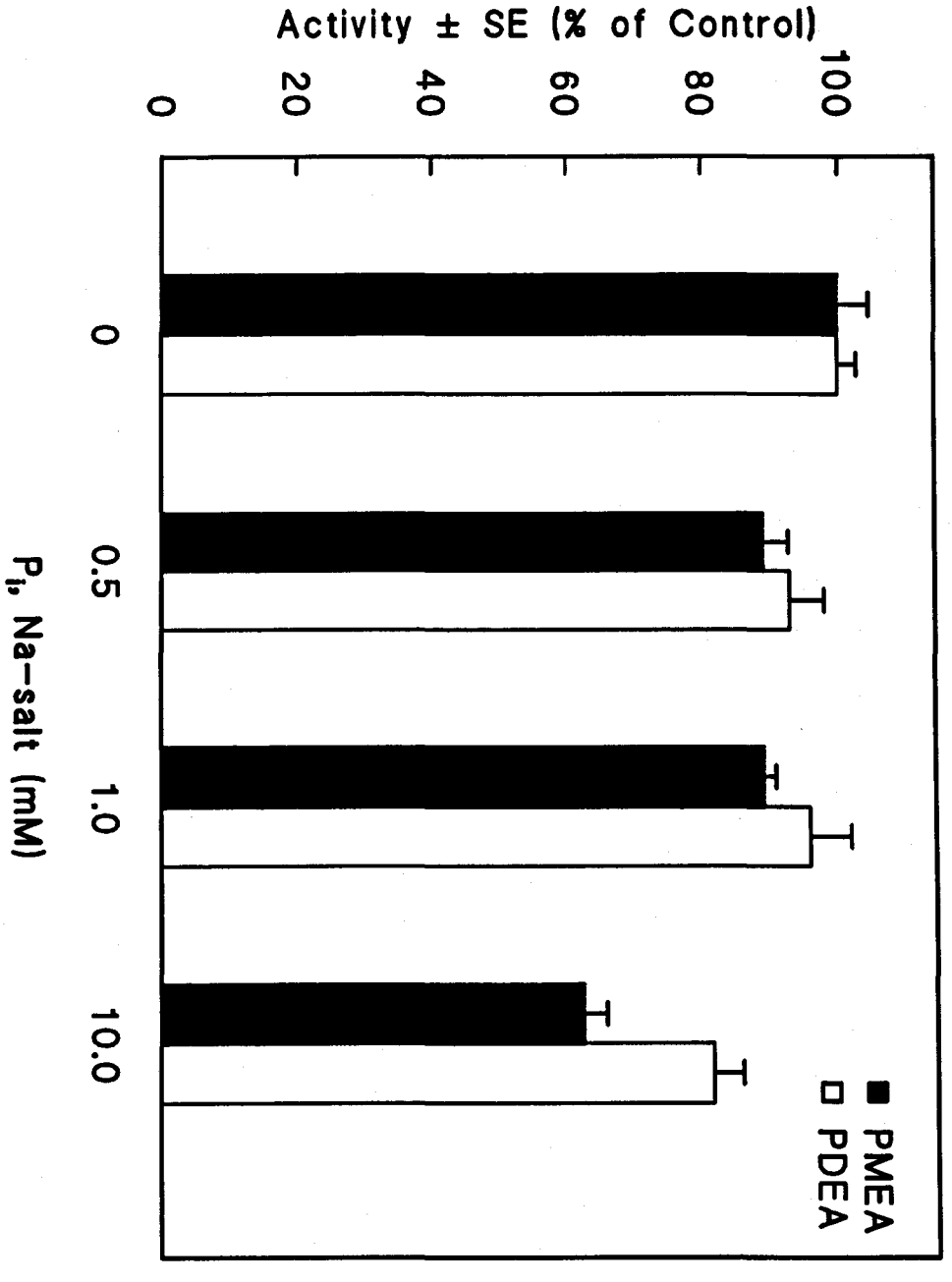
Activity ± SE (% of Control)
0
20
40
60
80
100
0
0.5
1.0
10.0
P_i, Na-salt (mM)
PMEA
PDEA

FIGURE 19: Effect of glycinebetaine (Cl-salt) on PMEAMeT and PDEA *N*-methylating activities.

PMEAMeT activity (■, with PMEA as substrate) and PDEA *N*-methylating activity (□) were assayed in the presence of increasing final assay concentrations from 1 to 140 mM of glycinebetaine with sample purified 30-fold after the High Q Anion step (sample described in Table IV). Values are means of six measurements ± SE; except for the control value for PDEA *N*-methylating activity which is the mean of five measurements ± SE. In the absence of glycinebetaine, control PMEAMeT activity was between 86 and 197 $nmol \bullet min^{-1} \bullet mL^{-1}$ and control PDEA *N*-methylating activity was between 91 and 217 $nmol \bullet min^{-1} \bullet mL^{-1}$.

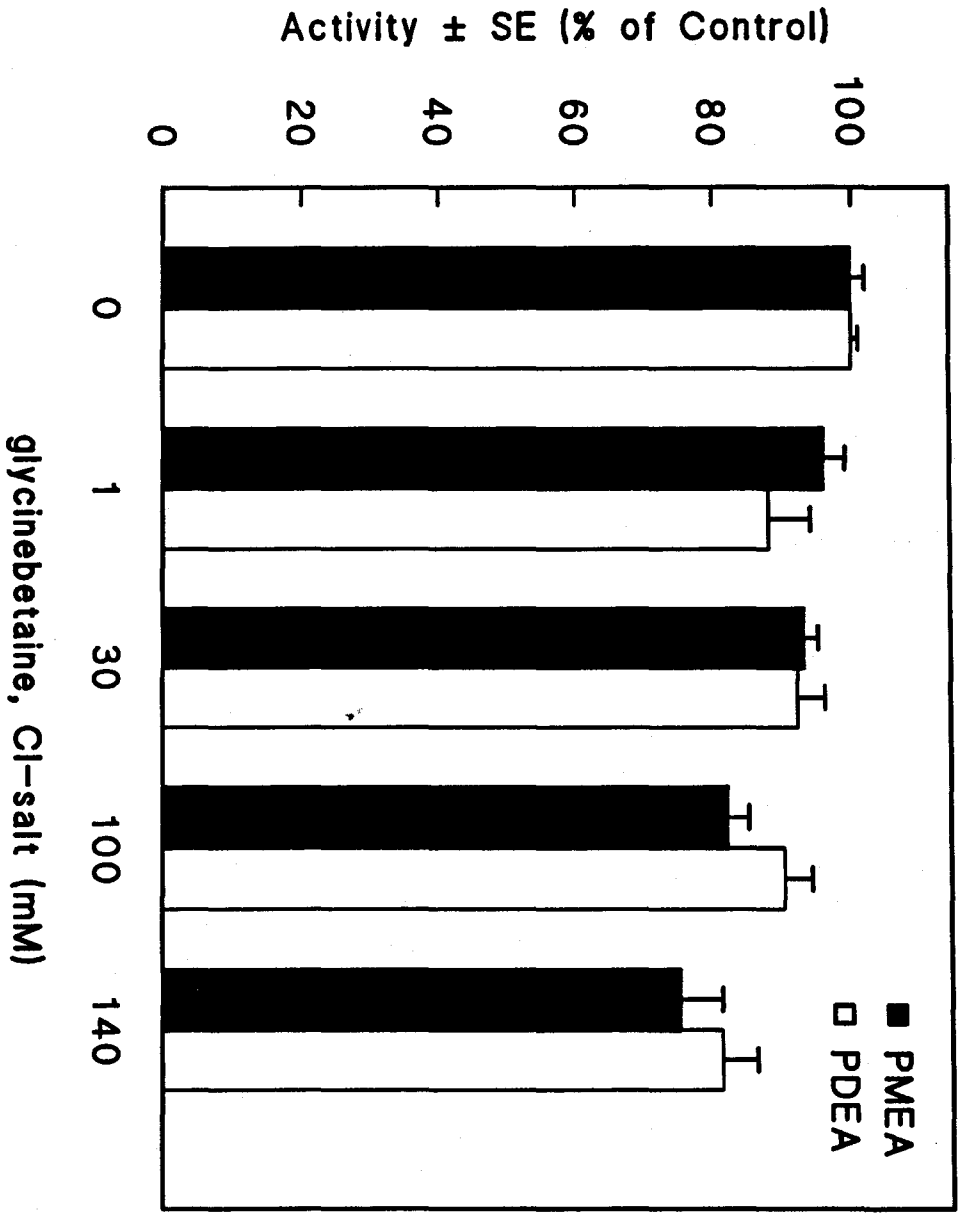
Activity ± SE (% of Control)
0
20
40
60
80
100
0
1
30
100
140
glycinebetaine, Cl-salt (mM)
PMEA
PDEA

Table XI: Effect of metabolites on PMEAMeT and PDEA *N*-methylating activities[a]

Addition	n	Final assay Concentration	*N*-methylating activity	
			PMEA	PDEA
		mM	% of control	
SAH	3	0	100 ± 2	100 ± 9
		0.001	95 ± 3	95 ± 8
		0.01	66 ± 1	60 ± 1
		0.1	15 ± 6	14 ± 1
		0.2	6 ± 0	9 ± 0
PCho	4	0	100 ± 2	100 ± 3
		0.5	67 ± 5	60 ± 2
		1	58 ± 4	56 ± 2
		10	19 ± 2[b]	18 ± 2[b]
Choline	4	0	100 ± 1	100 ± 1
		0.5	93 ± 4	103 ± 5
		1	92 ± 3	100 ± 5
		10	90 ± 2	108 ± 6
P_I	4	0	100 ± 5	100 ± 3
		0.5	89 ± 4	93 ± 5
		1	89 ± 1	96 ± 6
		10	62 ± 3	81 ± 5
Glycinebetaine	6	0	100 ± 2	100 ± 1[c]
		1	96 ± 3	88 ± 6
		30	93 ± 2	92 ± 4
		100	82 ± 3	90 ± 4
		140	75 ± 6	81 ± 3

[a] PMEAMeT activity assayed with PMEA as substrate. The sample used was purified 30-fold (Table IV) with control PMEAMeT and PDEA *N*-methylating activities ranging from 80 to 122 and 84 to 217 $nmol \bullet min^{-1} \bullet mL^{-1}$, respectively.

[b] Values are means of two measurements ± SE.

[c] Value is the mean of five measurements ± SE.

inhibited with increasing concentrations of PCho and at 10 mM PCho, both activities were reduced by approximately 82%. Figure 17 shows only PMEAMeT activity was inhibited with increasing concentrations of choline and at 10 mM choline, the activity was reduced by 10%. Figure 18 shows both activities were inhibited with increasing concentrations of P_i and at 10 mM P_i, PMEAMeT activity was reduced by 38% and PDEA *N*-methylating activity by 19%. Figure 19 shows the compatible osmolyte glycinebetaine (Cl-salt) was added to the assays in the range from 1 to 140 mM and both activities were inhibited with increasing concentrations of glycinebetaine. So at 140 mM glycinebetaine (Cl-salt), PMEAMeT activity was reduced by 25% and PDEA *N*-methylating activity was reduced by 19%. However, the inhibition of PMEAMeT activity was not due to the added glycinebetaine because NaCl at 140 mM reduced PMEAMeT activity by 25% (Table X). Whereas, the inhibition of PDEA N-methylating activity was caused by the added glycinebetaine because NaCl at 30 and 140 mM did not inhibit this activity (Table X).

DISCUSSION

Number of phosphobase *N*-methyltransferases in spinach leaves.

Two phosphobase *N*-methyltransferases are believed to synthesize PCho from PEA in spinach leaves (Figure 3). The enzyme PEAMeT which is light-regulated, has been partially purified and shown to convert PEA → PMEA → PDEA → PCho (Smith, 1995). The second enzyme PMEAMeT converts PMEA → PDEA, has not been purified or characterized and thus may also convert PDEA → PCho (Weretilnyk and Summers, 1992; Weretilnyk et al., 1995). A consideration in the selection of leaf tissue for the purification of PMEAMeT was to use material depleted of the light-regulated enzyme PEAMeT. Therefore, leaves of plants exposed to prolonged periods of darkness (Weretilnyk et al., 1995) or those of plants purchased from markets (Weretilnyk, *unpublished*) were used to reduce the level of PEA *N*-methylating activity in crude leaf extracts (Table V).

Starting with crude leaf extracts, PMEAMeT was purified on the basis of PMEA *N*-methylating activity (Tables I to IV). At the onset it was not apparent whether the activity was catalyzed by more than one enzyme but as the purification proceeded, some observations were best explained by the presence of a single enzyme. For example, 100% of the activity in crude leaf extracts was subsequently recovered in the 1.8 to 2.6 M ammonium sulfate fraction. This fraction was then further purified by column chromatography using matrices that exploited different properties of protein, such as ionic and hydrophobic interactions. Despite using these different matrices, the chromatographic profiles from the columns of DEAE Sepharose (Figure 6), Phenyl Sepharose (Figure 7) and High Q Anion (Figure 8) showed PMEA *N*-methylating activity was always resolved as a single peak. The activity was also resolved as a single peak when sample purified by High Q Anion chromatography was separated on the basis of size using gel filtration chromatography (Figure 11).

PDEA *N*-methylating activity was also detected in these crude leaf extracts and 1.8 to 2.6 M ammonium sulfate fractions (Tables VI, VII). During subsequent chromatographic steps, PDEA *N*-methylating activity co-eluted with PMEAMeT activity from columns of DEAE Sepharose (Figure 6), Phenyl Sepharose (Figure 7), High Q Anion (Figure 8) and gel filtration (Figure 11). The inability to separate the two activities argues that PMEAMeT has a second associated activity, namely the *N*-methylation of PDEA → PCho. Table V shows samples most purified for the enzyme had no PEA *N*-methylating activity and so the low levels of this activity detected in crude leaf extracts were presumably associated with the light-regulated enzyme PEAMeT. Therefore, the enzyme does not have a third associated activity that can *N*-methylate PEA → PMEA. The data, thus, supports the hypothesis that PMEAMeT could convert PMEA → PDEA → PCho in spinach leaves (by Weretilnyk and Summers, 1992; Weretilnyk et al., 1995).

The function of two enzymes PEAMeT and PMEAMeT with overlapping PMEA and PDEA *N*-methylating activities in spinach leaves is not known (Smith, 1995). However, glycinebetaine accumulating plants need to produce more choline than non-glycinebetaine accumulating plants and so choline biosynthetic pathways are suggested to be specialized in the former to accommodate the increased flux (Rhodes and Hanson, 1993). Perhaps, the overlapping activities are a 'specialization' of choline biosynthesis in spinach plants.

The number of *N*-methyltransferases involved in choline synthesis is not known for any other higher plant. However, the existence of at least two *N*-methyltransferases is probably not an unique property of spinach since different routes of choline synthesis are found in higher plants (Figure 2; Weretilnyk and Summers, 1992; Weretilnyk et al., 1995), which is unusual for a primary metabolic pathway (Mudd and Datko, 1989b). For instance in castor bean endosperm, the first *N*-methyltransfer is of ethanolamine → MEA and the subsequent *N*-methylations occur at phosphobase and phosphatidylbase levels (Prud'homme and Moore, 1992a). In leaves of several higher plants, the first *N*-methyltransfer is of PEA → PMEA and the subsequent *N*-methylations occur at phosphobase and/ or phosphatidylbase levels (Hitz et al., 1981; Hanson and Rhodes,

1983; Mudd and Datko, 1986; Datko and Mudd, 1988; Summers and Weretilnyk, 1993). Thus, the results of the above studies are difficult to reconcile with the existence of a single enzyme in most higher plants (Weretilnyk and Summers, 1992).

For clarity, in the following discussion, the enzyme names are abbreviated according to the first substrate used and so the abbreviations are not necessarily synonymous with those used by the authors. There are also at least two phosphobase *N*-methyltransferases involved in choline synthesis in mammalian brain cytosol and both are partially purified (Andriamampandry et al., 1992; Mukherjee et al., 1995). However unlike those from spinach leaves (Smith, 1995), each enzyme is associated with only a single activity: the enzyme PEAMeT is suggested to convert PEA → PMEA (Mukherjee et al., 1995) and the second enzyme PDEAMeT to convert PDEA → PCho (Andriamampandry et al., 1992). In mammalian liver, a single phosphatidylbase *N*-methyltransferase (PtdEAMeT) converts PtdEA → PtdMEA → PtdDEA → PtdCho (Ridgeway and Vance, 1987). In yeast, two phosphatidylbase *N*-methyltransferases with an overlapping activity convert PtdEA → PtdMEA → PtdDEA → PtdCho (Yamashita et al., 1982; Kodaki and Yamashita, 1987; Gaynor and Carmen, 1990) which is a similar situation to spinach leaves (Smith, 1995). The yeast enzyme PtdEAMeT converts PtdEA → PtdMEA → PtdDEA → PtdCho and so has three associated activities; whereas, the other enzyme PtdEAMeT II converts only PtdEA → PtdMEA.

PMEAMeT purification: Strategy, precautions and future steps

The four-step strategy used to partially purify PMEAMeT involved considering the subcellular location of the enzyme and exploiting properties of proteins such as their differential solubility in salt solutions and their differential interaction with columns of anion (weak and strong) and hydrophobic interaction matrices (Tables I to IV). After the phenyl Sepharose step, a 1 mL column of a strong cation exchanger (High S, BioRad) was tested but none of the protein was adsorbed onto this matrix (data not shown) and so High Q Anion (strong anion exchanger) to which the enzyme bound was employed instead. Also, there was no one step that routinely resulted in more than 3-fold purification of the

enzyme. Overall, PMEAMeT was partially purified a maximum of 43-fold with a 18% recovery of activity present in crude leaf extracts (Table III). In this sample, PMEAMeT has a specific activity of 14.7 nmol•min^{-1}•mg^{-1} protein with PMEA as substrate and 18.0 nmol•min^{-1}•mg^{-1} protein with PDEA as substrate (Table III, VII). Three other protein samples were also produced using the strategy and these samples were purified between 21 and 32-fold for PMEAMeT over crude leaf extracts (Tables I, II, IV).

A large quantity of spinach leaves (in total over 12 kg) was harvested to produce crude extracts that contained in total 95 g of protein and the four samples purified by the last step of High Q Anion chromatography contained in total 0.6 g protein (Tables I to IV). Whether these samples alone will be sufficient to yield enough pure enzyme will depend on the abundance of the enzyme in crude leaf extracts and the amount of enzyme lost during purification. Although, PMEAMeT is probably not an abundant enzyme in accord with other choline and glycinebetaine biosynthetic enzymes from spinach. That is, substantially pure ethanolamine kinase and substantially pure PEAMeT account for 0.02% and less than 0.0003% of protein in crude leaf extracts, respectively (Mercer, 1994; Smith, 1995). Purified enzymes CMO and BADH account for 0.0004-0.0007% and 0.006% of protein in crude leaf extracts, respectively (Burnet et al.,1995; Weretilnyk and Hanson, 1989).

A number of precautionary measures were taken to maintain enzyme stability during extraction and purification. For instance, the extraction buffer (buffer A) was at a pH of 7.8 which is close to that of the cytoplasm (pH 7.5) of spinach leaf cells (Bligny et al., 1990). The buffer also contained Na_2-EDTA to chelate divalent metal cations that could be inhibitory to enzyme activity and DTT to prevent possible formation of disulfide bonds between cysteine residues (Scopes, 1982; Stryer, 1981). After ammonium sulfate fractionation, 10% (v/v) glycerol was added to the buffer (buffer B) also to maintain enzyme stability (Linn, 1990). It is good practice to keep proteins concentrated (>1 mg•mL^{-1}) during purification (Linn, 1990). Therefore as a precaution, ultrafiltration using a stirred cell was used to concentrate fractions collected after chromatography on phenyl Sepharose (fourth step) and High Q anion (fifth step) columns prior to freezing protein samples in liquid N_2 and storage at -80°C. Since solutes concentrate during freezing and

the enzyme may be exposed to high concentrations that may affect its stability, samples were generally desalted prior to freezing and storage. Thus, after ammonium sulfate fractionation, samples were desalted by dialysis. Also, after chromatography on phenyl Sepharose and High Q anion columns, samples that were concentrated by ultrafiltration using a stirred cell were desalted using the same apparatus.

SDS-PAGE showed that sample purified after the last step of High Q Anion chromatography was still composed of numerous polypeptides (Figure 14, *lane 5*) which suggested that PMEAMeT shared similar biochemical properties with other proteins in the sample. Consequently, other techniques will have to be employed to further purify PMEAMeT. Affinity chromatography with ligands of adenosine (Dumas, 1997) and SAH (Mazzafera et al., 1994) has been used as a very effective purification step for many SAM-dependent methyltransferases, including the spinach enzyme PEAMeT (Smith et al., *in press*). Therefore, 1 mL columns of these affinity matrices were tested using sample purified after the High Q Anion step (data not shown). Adenosine agarose chromatography was excluded because none of the proteins were adsorbed onto the column. PMEAMeT has been adsorbed to the SAH-agarose matrix and eluted with a gradient increasing in NaCl concentration and so this column may afford additional purification of the enzyme (Weretilnyk, *personal communication*).

Physical property: molecular weight

PMEAMeT has a native molecular mass of 76 ± 1 kDa as estimated by HPLC gel filtration chromatography (Figure 12) and may have a SAM-binding subunit of approximately 25 or 28 kDa as shown by a fluorograph (Figure 13, Panel B) of a SDS-polyacrylamide gel separating samples photolabed with [*methyl*-^{3}H]SAM (Figure 13, Panel A). Therefore, at the simplest, PMEAMeT could be a heterodimeric protein with a non SAM-binding subunit of either 48 or 51 kDa. Spinach PEAMeT is probably a monomer with a minimum molecular mass of 54 kDa as shown by SDS-PAGE and fluorography and a maximum molecular mass of 77 kDa as estimated by HPLC gel filtration chromatography (Smith et al., *in press*).

The only other phosphobase *N*-methyltransferases that have been characterized are from mammalian brain cytosol but their native molecular weights are not known (Andriamampandry et al., 1992; Mukherjee et al., 1995). However, estimates are available for phosphatidylbase *N*-methyltransferases from yeast and mammalian liver. For the two yeast enzymes, PtdEAMeT (PtdEA → PtdMEA → PtdDEA → PtdCho) has a molecular mass of 23 kDa and PtdEAMeT II (PtdEA → PtdMEA) of 101 kDa as determined by nucleotide analysis of gene coding frames (Kodaki and Yamashita, 1987). The single enzyme in mammalian brain PtdEAMeT (PtdEA → PtdMEA → PtDEA → PtdCho) is a monomer with a molecular mass of 18.3 kDa as determined by SDS-PAGE (Ridgeway and Vance, 1987). It is interesting that both yeast PtdEAMeT and mammalian PtdEAMeT which catalyze all three *N*-methylations have similar molecular weights. The authors also found the molecular weight of mammalian PtdEAMeT unusually small for an enzyme that catalyzes a fairly complex series of reactions (Ridgeway and Vance, 1987). *In vitro* data suggests that mammalian PtdEAMeT has a single, not multiple, active site for the three phosphatidylbase substrates (Ridgeway and Vance, 1987) and it will be interesting to determine whether spinach PMEAMeT has one or two active sites for the substrates PMEA and PDEA.

In the case of yeast, the larger enzyme PtdEAMeT II (PtdEA → PtdMEA) exhibits internal homology and homology to the smaller enzyme PtdEAMeT (PtdEA → PtdMEA → PtdDEA → PtdCho) which suggests the two enzymes may have evolved through a gene duplication event (Kodaki and Yamashita, 1987). Considering the two spinach enzymes catalyze partly overlapping activities (Smith, 1995; this thesis) as do the yeast enzymes (Kodaki and Yamashita et al., 1987), perhaps spinach PMEAMeT shares homology with spinach PEAMeT and the two enzymes have arisen through a gene duplication event.

A large group of SAM-dependent methyltransferases share conserved motifs suggested to be part of an evolutionarily conserved SAM-binding site (Kagan and Clarke, 1994). Once available, analysis of the amino acid sequence of spinach PMEAMeT will reveal if the enzyme also has the conserved motifs. Alternatively, the enzyme may be part of a much smaller group of enzymes lacking these motifs that are suggested to have

evolved a novel or independent approach to SAM-dependent methylations (Kagan and Clarke, 1994). This latter group of enzymes includes the yeast phosphatidyl *N*-methyltansferase enzymes (Kagan and Clarke, 1994). In general, it would be interesting to determine if the *N*-methyltransferases involved in choline synthesis from the various organisms fall into that latter group.

Effect of pH and metal ion requirements.

PMEAMeT activities are localized to the cytosol in spinach leaf cells (Weretilnyk et al., 1995) and the pH of the cytoplasm is around 7.5 in spinach leaf cells (Bligny et al., 1990). Both PMEAMeT activities have an alkaline pH optimum of between 8.5 and 9.0 (Figure 9) and so the activities may likely be functioning at a sub optimal pH *in vivo*. The rates of PMEAMeT activities *in vivo* may be approximately 50% of the maximal rates observed *in vitro*, when the *in vitro* rates at pH 7.5 and 8.5 are compared for each activity using partially purified enzyme (Figure 9). The pH optimum of spinach PEAMeT activities is also slightly alkaline (7.8), so this enzyme is likely to be functioning at a near optimal pH *in vivo* as the activities are also localized to the cytosol (Smith, 1995; Weretilnyk et al., 1995).

Interestingly, the pH optima are also alkaline for the *N*-methyltransferase activities involved in choline synthesis in yeast and mammals. From mammalian brain, PEAMeT activity (PEA → PMEA) and PDEAMeT activity (PDEA → PCho) have a pH optimum of 9.5 and 11 or greater, respectively (Andriamampandry et al., 1992; Mukherjee et al., 1995). From mammalian liver, PtdEAMeT activities (PtdEA → PtdMEA → PtDEA → PtdCho) all have the same pH optimum of 10 (Ridgeway and Vance, 1987). Similarly from yeast, PtdEAMeT activities (PtdEA → PtdMEA → PtdDEA → PtdCho) have the same pH optimum of 8.1 and PtdEAMeT II activity (PtdEA → PtdMEA) has a pH optimum of 9.9 (Kodaki and Yamashita, 1987). The observed alkaline pH optimum of the *N*-methyltransferase activities may reflect the fact that protonation of the substrate's amino group (phosphobase or phosphatidylbase) could cause poor binding to the active site (Ridgeway and Vance, 1987).

Over 25% of enzymes require metal ions such as K^+, Mg^{2+}, Mn^{2+}, Ca^{2+}, Zn^{2+} or $Fe^{2+/\ 3+}$ for activity and the enzymes are either metal-activated, require added ions, or metalloenzymes which contain a definite quantity of ion (Rodwell, 1985; Das, 1978). Some SAM-dependent plant methyltransferases are known to be metal-activated (Poulton, 1981). However, like spinach PEAMeT (Smith, 1995), PMEAMeT activities may not be metal-activated since the omission of Na_2-EDTA had no effect and the addition of Mg^{2+} and Mn^{2+} ions did not enhance either activities (Table X). Mg^{2+} is predominantly tested as a cofactor for many SAM-dependent plant methyltransferases and some enzymes require the divalent cation for activity; whereas, others are not affected or are inhibited (eg Poulton, 1981; Presing et al., 1989; O'Keefe and Beecher, 1994). Since Mg^{2+} ions are suggested to have a strong affinity for phosphate groups (Harrison and Hoarce, 1980), the inhibition by 10 mM Mg^{2+} ions of PMEAMeT activities may be a result of the ions complexing with the phosphobase substrate (0.25 mM) making the latter unavailable for binding or *N*-methylation. PMEAMeT activities were completely inhibited by the addition of 1 and 10 mM Mn^{2+} ions and a reason for the stronger inhibition in comparison to Mg^{2+} ions is not known.

From mammalian brain, PEAMeT activity (PEA $\rightarrow$ PMEA) is activated by both $MgCl_2$ and $MnCl_2$; whereas, PDEAMeT activity (PDEA $\rightarrow$ PCho) is activated by $MgCl_2$ and inhibited by $MnCl_2$ (Andriamampandry et al., 1992; Mukherjee et al., 1995). From yeast, PtdEAMeT activities (PtdEA $\rightarrow$PtdMEA $\rightarrow$ PtdDEA $\rightarrow$ PtdCho) are activated by Mg^{2+} and inhibited by Mn^{2+} ions and PtdEAMeT II activity (PtdEA $\rightarrow$ PtdMEA) is inhibited both by Mg^{2+} and Mn^{2+} ions (Gaynor and Carmen, 1990). Other divalent metal cations, such as Ca^{2+}, Cu^{2+}, Co^{2+}, $Ni^{2+}$and Zn^{2+}, have been tested as cofactors for the *N*-methyltransferases involved in choline synthesis from spinach, yeast and mammalian brain (Gaynor and Carmen, 1990; Andriamampandry et al., 1992; Mukherjee et al., 1995; Smith, 1995). The above cations are shown to be inhibitory to enzyme activity, with the exception of Ca^{2+}, which increased the activity of the phosphobase *N*-methyltransferases from mammalian brain. It will be interesting to test the effect of such divalent metal cations on

spinach PMEAMeT activities to obtain a more comprehensive analysis of the enzyme's metal ion requirements, if any.

Spinach PMEAMeT may not be completely excluded from being a metalloenzyme by the data in Table X. Although considering color was not associated with PMEAMeT-containing fractions, the enzyme was probably not an iron-containing protein (red-brown) or a cuproprotein (blue, pink). Also, no SAM-dependent plant methyltransferase or any *N*-methyltransferases involved in choline synthesis from yeast or mammalian brain or liver are suggested to be metalloenzymes. Among the enzymes involved in glycinebetaine synthesis, CMO, which oxidizes choline → betaine aldehyde in spinach chloroplasts, is found to be an iron-sulfur protein (Russell et al., 1998). CMO contains a [2Fe-2S] cluster and maybe mononuclear Fe (Russell et al., 1998) and has a red-brown color (Figure 3; Burnet et al., 1995).

Inhibition by reaction products.

SAH (Figure 20).

Typically, SAM-dependent methyltransferases are strongly inhibited *in vitro* at low concentrations of the demethylated reaction product SAH (Cossins, 1980; Poulton, 1981). The inhibition is usually competitive with SAM and the K_i value for SAH is several-fold lower than the K_m value for SAM (Poulton, 1981). This type of inhibition would also be consistent with the similar structures of the two nucleotides as well as that of their proposed binding sites (Carmen and Gaynor, 1990; Schlubier et al., 1995). These features have been suggested to point to a general mechanism for *in vivo* regulation of these methyltransferases ie the intracellular ratio of SAM: SAH (Poulton, 1981).

The concentrations of SAM and SAH in the cytosol of spinach leaf cells are not known, but the concentration of SAM was 0.2 mM in phosphobase *N*-methyltransferase asssays. Therefore, the effect of 0.001 to 0.2 mM SAH was examined on PMEAMeT activities and both activities were inhibited with increasing concentrations of the added SAH (Figure 15, Table XI). Thus, PMEAMeT activities could be regulated *in vivo* by the ratio of SAM: SAH if the *in vitro* inhibition is determined to be competitive with SAM

FIGURE 20: Possible inhibition of PMEAMeT activities by reaction products SAH and PCho in leaves of the glycinebetaine accumulator spinach (Figure modified from Figure 3).

Choline biosynthesis from the precusor ethanolamine occurs mainly in the cytosol and that of glycinebetaine from choline in chloroplasts (Weretilnyk et al., 1995; Hanson et al., 1995). The enzymes involved are: step 1, ethanolamine kinase; steps 2, 3 and 4, PEA *N*-methyltransferase (PEAMeT); steps 3 and 4, PMEA *N*-methyltransferase (PMEAMeT); step 5, PCho phosphatase; step 6, choline monoxygenase (CMO); and step 7, betaine aldehyde dehydrogenase (BADH).

Abbreviations: PEA, phosphoethanolamine; PMEA, phosphomethylethanolamine; PDEA, phosphodimethylethanolamine; PCho, phosphocholine; SAM, *S*-adenosyl-L-methionine; SAH, *S*-adenosyl-L-homocysteine; P_i, inorganic orthophosphate; Fd, ferredoxin; NAD^+, nicotinamide adenine dinucleotide (oxidized form); NADH; nicotinamide adenine dinucleotide (reduced form).

ethanolamine
ATP
1
ADP
PEA
SAM
2
SAH
PMEA
SAM
3
SAH
?
PDEA
SAM
4
SAH
?
PCho
5
P_i
cytosol
?
choline
2Fd red
2Fd ox
O_2
H_2O
NAD+
NADH
betaine aldehyde
glycinebetaine
6
7
chloroplast

(Poulton, 1981). More specifically, an *in vivo* SAM: SAH ratio of 200: 1 could have no effect on either activity; whereas, a change in the ratio to 1: 1 could reduce both activities by more than 90% (Figure 15, Table XI). Alternatively, if the *in vitro* inhibition is found to be noncompetitive, then the enzyme activities may be regulated *in vivo* by a second mechanism that involves only the concentration of SAH (Knogge and Weisenbock, 1984). That is, if the pool size of SAH can increase to over 0.001 mM, then PMEAMeT activities could be inhibited by the reaction product SAH (Figure 15, Table XI).

In any case, the strong inhibition requires that the concentration of SAH be regulated for continuation of SAM-dependant methylations *in vivo* (Poulton, 1981). This is especially true when spinach plants are salt-stressed because the rate of choline synthesis increases (Summers and Weretilnyk, 1993) which means an increase in SAM usage and SAH production. SAH may be removed from the cytosol and be sequestered in another subcellular compartment or alternatively, SAH may be cleaved to adenosine and L-homocysteine by SAH hydrolase (Cossins, 1980; Poulton, 1981). Since this reaction is freely reversible, sustained hydrolysis requires removal or metabolism of the products: adenosine is most probably converted to ADP (Poutlon, 1981) and L-homocysteine can be methylated to L-methionine using N_5-methyltetrahydrofolate (Cossins, 1980; Poulton, 1981).

The effect of SAH has been examined on SAM-dependent *N*-methyltransferase activities involved in choline synthesis from other organisms. The spinach enzyme PEAMeT is also inhibited *in vitro* by SAH (Smith et al., *in press*), as are the phosphobase *N*-methyltransferases from mammalian brain (Andriamampandry et al., 1992; Mukerjee et al., 1995). The phosphatidylbase *N*-methyltransferases from yeast and mammalian liver are inhibited competitively by SAH with respect to SAM and thus, the intracellular ratio of SAM: SAH is suggested to be an important regulatory factor (Carmen and Gaynor, 1990; Ridgeway and Vance, 1987).

PCho (Fgure 20).

PCho is suggested to regulate choline synthesis probably through feedback inhibition of phosphobase *N*-methyltransferase activities in glycinebetaine accumulating and non-glycinebetaine accumulating plants (Hanson and Rhodes, 1983; Mudd and Datko, 1989ab; Rhodes and Hanson, 1993; Smith et al., *in press*).

The flux through the phosphobase *N*-methylation sequence is down-regulated when a large trapping pool of PCho is infiltrated into salinized sugarbeet leaves, suggesting that PCho can feedback inhibit its own synthesis (Hanson and Rhodes, 1983). An almost complete down-regulation of flux through PEA is also associated with an increase in PCho pool size from 58 μM to 592 μM and a reduction in phosphobase *N*-methyltransferase activities in the choline-grown duckweed (Mudd and Datko, 1989a). More specifically, PEA *N*-methylating activity is reduced by 80%, PMEA *N*-methylating activity by 30% and PDEA *N*-methylating activity by 40% in this plant. Also *in vitro* data shows the addition of 175 μM PCho inhibits PEA *N*-methylating activity from duckweed by 27% and considering the *in vivo* PCho pool is estimated to expand to 592 μM, the expanded PCho pool could greatly inhibit PEA *N*-methylating activity resulting in the down-regulation of choline synthesis in choline-grown duckweed. Therefore, it would be interesting to determine whether PCho could serve to down-regulate its own synthesis from PEA through feedback inhibition at the enzymatic level in spinach leaves.

To date, there is no *in vivo* work to show the effect of an expanded PCho pool size on the flux through PEA or on phosphobase *N*-methyltransferase activities in spinach leaves. Although the pool size of PCho is not known in the cytosol, PCho is shown to be a cytoplasmic metabolite (Bligny et al., 1990) found at 2 to 5 mM in the light (calculated using a cytoplasm: vacuole ratio of 1: 10 from Coughlan and Wyn Jones, 1980) and at 2.3 mM in the dark (Bligny et al., 1990). Therefore, the effect of 0.5 to 10 mM PCho was tested on PMEAMeT activities and both activities were inhibited by PCho, with an average 40% inhibition at 1 mM (Figure 16, Table XI). Also, PCho was shown to be a reaction-product of PMEAMeT using TLC (Table IX). Considering the *in vivo* PCho pool sizes (Coughlan and Wyn Jones, 1982; Bligney et al., 1990) and the *in vitro* inhibition data

(Figure 16, Table XI), PCho could down-regulate its synthesis from PEA through reaction-product inhibition of PMEAMeT activities in the cytosol of spinach leaf cells.

An 'expanded' PCho pool could mean that glycinebetaine synthesis is being reduced in leaf cells, at least in salinized sugar beet (Hanson and Rhodes, 1983). Interestingly, a storage pool of PCho and not a metabolically-accessible pool of PCho is suggested to be the down-regulatory effector of PCho synthesis in salinized sugar beet leaves (Hanson and Rhodes, 1983). Experimental data and computer simulations suggest that there is a metabolic and storage pool of PCho and when glycinebetaine synthesis is decreased, the 'excess' PCho enters the storage pool which then 'expands' and down-regulates the flux through PEA to PCho (Hanson and Rhodes, 1983). Theoretical estimates (calculated using a cytoplasm: vacuole ratio of 1: 10 from Hanson and Rhodes, 1983) for the storage pool of PCho are 300 μM when the rate of PCho utilization is constant and up to 750 μM when PCho is accumulating as a result of reduced rate of glycinebetaine synthesis. In contrast, theoretical estimates for the metabolic pool size of PCho are between 56 and 100 μM with no correlation of the higher values with a decreased rate of glycinebetaine synthesis (Hanson and Rhodes, 1983). It would be interesting to determine whether a similar situation may exist in spinach leaves, ie where there is a metabolic and a storage pool of PCho and the latter is the effector of the down-regulation of PCho synthesis.

Effect of products of PCho hydrolysis: choline and P_i (Figure 21).

It is not known whether PCho hydrolysis to produce choline and P_i occurs in the cytosol (site of PCho synthesis; Weretilnyk et al., 1995), chloroplasts (site of glycinebetaine synthesis; Hanson et al., 1985) or another subcellular compartment in spinach leaf cells. A pool of PCho is found in chloroplasts as shown by ^{31}P NMR in spinach leaf cells (Bligny et al., 1990). If PCho hydrolysis is cytosolic, then choline and/ or P_i could act as regulatory effectors of PCho synthesis *in vivo*.

FIGURE 21: Possible regulation of PMEAMeT activities by endproducts choline, P_i and glycinebetaine in leaves of the glycinebetaine accumulator spinach (Figure modified from Figure 3).

Choline biosynthesis from the precusor ethanolamine occurs mainly in the cytosol and that of glycinebetaine from choline in chloroplasts (Weretilnyk et al., 1995; Hanson et al., 1995). The enzymes involved are: step 1, ethanolamine kinase; steps 2, 3 and 4, PEA *N*-methyltransferase (PEAMeT); steps 3 and 4, PMEA *N*-methyltransferase (PMEAMeT); step 5, PCho phosphatase; step 6, choline monoxygenase (CMO); and step 7, betaine aldehyde dehydrogenase (BADH).

Abbreviations: PEA, phosphoethanolamine; PMEA, phosphomethylethanolamine; PDEA, phosphodimethylethanolamine; PCho, phosphocholine; SAM, *S*-adenosyl-L-methionine; SAH, *S*-adenosyl-L-homocysteine; P_i, inorganic orthophosphate; Fd, ferredoxin; NAD^+, nicotinamide adenine dinucleotide (oxidized form); NADH; nicotinamide adenine dinucleotide (reduced form).

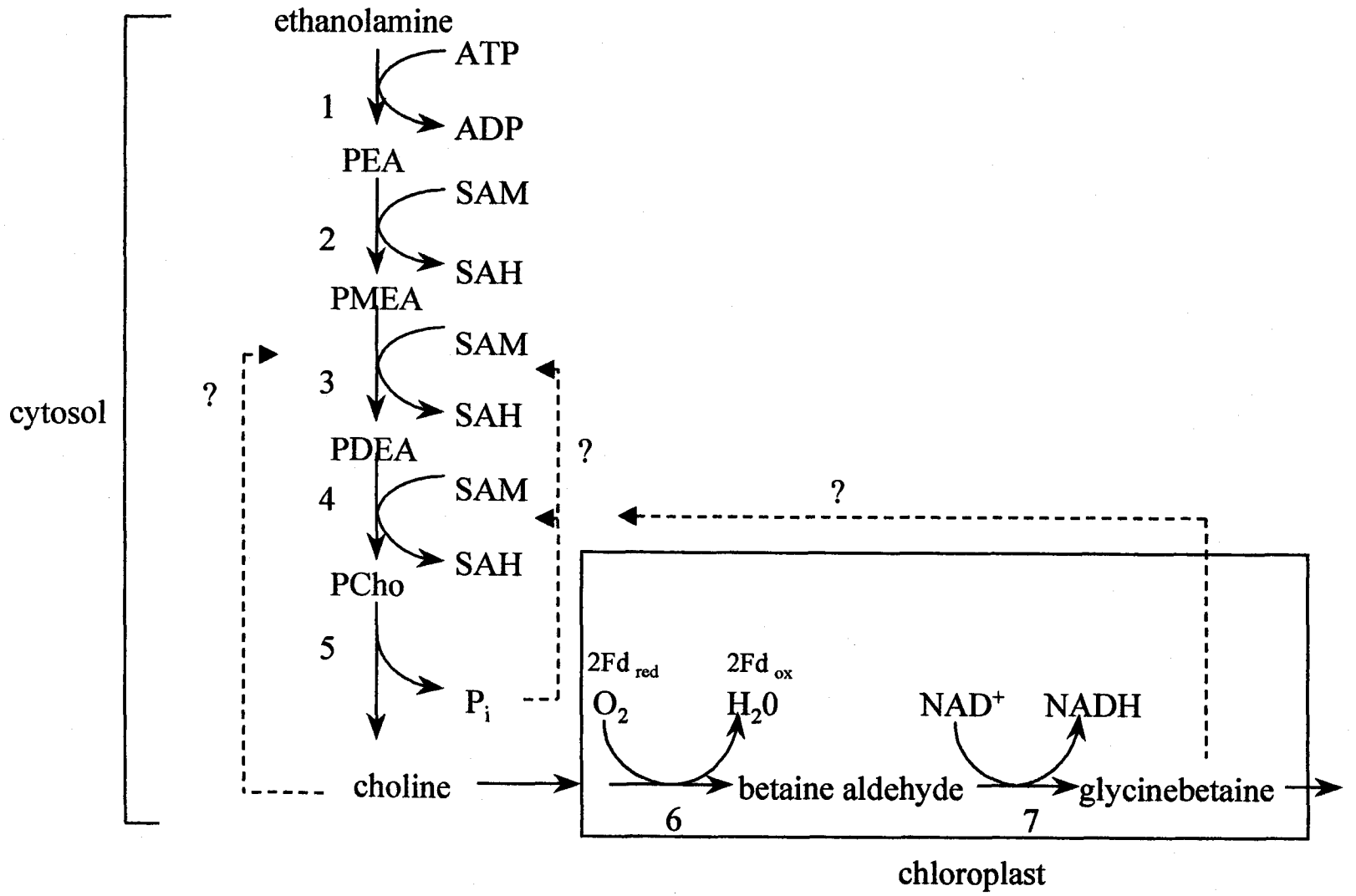
ethanolamine
ATP
1
ADP
PEA
SAM
2
SAH
PMEA
SAM
3
SAH
PDEA
SAM
4
SAH
PCho
5
P_i
cytosol
?
?
?
choline
$2Fd_{red}$
$2Fd_{ox}$
O_2
H_2O
NAD^+
NADH
betaine aldehyde
glycinebetaine
6
7
chloroplast

Choline is suggested to be a possible feedback inhibitor of choline synthesis, at least in non-glycinebetaine accumulating plants (Mudd and Datko, 1989ab). More specifically, *in vivo* choline synthesis from PEA is completely down-regulated in duckweed grown in 1.4 μM choline (Mudd and Datko, 1989a) and in soybean and carrot cultures grown in 50 μM choline (Mudd and Datko, 1989b). The tissue pool of choline is shown to have increased from 102 μM to 544 μM in choline-grown duckweed (Mudd and Datko, 1989a) and also increased greatly in both choline-grown soybean and carrot cultures (Mudd and Datko, 1989b). Interestingly, *in vitro* PEA *N*-methylating activity from duckweed fronds is inhibited only 26% by 10 mM choline. Nevertheless, the authors did not preclude choline (or a pool of choline) from being an effector in the observed down-regulation of choline synthesis in these choline-grown plants. Thus, the possibility that choline could serve as a regulatory effector of choline synthesis in spinach leaves was examined.

Although, the concentration of choline is not known in the cytosol, a value of between 5 to 10 mM can be calculated for the cytoplasmic pool of choline (estimated using a cytoplasm: vacuole ratio of 1: 10 from Coughlan and Wyn Jones, 1982). The effect of 0.5 to 10 mM choline was tested on PMEAMeT activities and only PMEA *N*-methylating activity was inhibited by 10% at 10 mM (Figure 17, Table XI). Considering the upper limit (10 mM) for cytoplasmic choline (Coughlan and Wyn Jones, 1982) and the *in vitro* inhibition data (Figure 17, Table XI), choline may play a role in regulating PMEA *N*-methylating activity of PMEAMeT in spinach leaves if the cytosolic pool exceeds 10 mM.

To date, there is some evidence that P_i serves as a regulatory effector of choline synthesis in higher plants (Smith et al., *in press*). The cytosolic pool size for P_i is below 1 mM in spinach leaf cells (Bligny et al., 1990) and as P_i at a concentration of 1 mM inhibits spinach PEAMeT activities by 14%, this metabolite was proposed to be a possible *in vivo* regulatory metabolite (Smith et al., *in press*). Therefore, the effect of 0.5 to 10 mM P_i was tested on PMEAMeT activities and both activities were inhibited with increasing concentrations of P_i (Figure 18, Table XI). At 10 mM P_i, PMEA *N*-methylating activity was inhibited by 38% and PDEA *N*-methylating activity by 19%. Considering the cytosolic *in vivo* pool estimate of 1 mM P_i (Bligny et al., 1990), PMEAMeT activities

could be feedback inhibited *in vivo* by P_i if the pool 'expands'. Thus, P_i may have a regulatory role in PCho synthesis from PEA in spinach leaves.

Effect of compatible osmolyte glycinebetaine (Figure 21).

To date, there is no evidence that glycinebetaine regulates choline synthesis in higher plants (Smith et al, *in press*). The compatible osmolyte glycinebetaine is synthesized from choline in chloroplasts of spinach leaf cells (Brousquisse et al., 1989; Weigel et al., 1986) and preferentially accumulates in the cytoplasm, as opposed to the vacuole (see references in McCue and Hanson, 1990; and Hanson and Rhodes, 1993). Although the cytosolic pool size of glycinebetaine is not known, there are values for the cytoplasm. The *in vivo* pool estimate of glycinebetaine is 50 mM in the cytoplasm and the pool expands when spinach plants are salt-stressed (calculated using a cytoplasm: vacuole ratio of 1: 10 from Weigel et al., 1986). More specifically, the pool size increases to 150 mM in response to 100 mM NaCl stress, to 217 mM in response to 200 mM NaCl, and to 267 mM in response to 300 mM NaCl (calculated using a cytoplasm: vacuole ratio of 1: 10 from Weigel et al., 1986). Therefore, the effect of 1 up to 140 mM glycinebetaine (Cl-salt) was tested on PMEAMeT activities (Figure 19, Table XI).

PMEA *N*-methylating activity was not inhibited by up to 140 mM glycinebetaine, because NaCl at 30 and 140 mM inhibited this activity (Table X and Results text). Therefore, either the Cl^- ions (glycinebetaine added as a Cl-salt) or Na^+ ions (glycinebetaine chloride stock solution buffered with NaOH to the assay pH of 8.5) present in the assay likely can explain the observed inhibition of activity. The data is in accord with the fact that high concentrations of glycinebetaine (up to 1 M) typically do not inhibit the activities of various enzymes from halophytic cyanobacteria (Incharoensakdi et al., 1986), plants (Wyn Jones et al., 1977; Pollard and Wyn Jones, 1979; Manetas et al., 1986) and animals (Yancey et al, 1982), in keeping with its role as a compatible osmolyte (Wyn Jones et al., 1977; Hanson and Rhodes, 1993).

Interestingly, PDEA *N*-methylating activity was inhibited with the addition of up to 140 mM glycinebetaine and the inhibition was not caused by the Na^+ or Cl^- ions present in

the assay because NaCl did not inhibit this activity at 30 and 140 mM (Table X and Results text). At 140 mM glycinebetaine, the activity was inhibited by 19%. Two enzyme activities are shown to be inhibited by high concentrations of glycinebetaine, bovine liver glutamate dehydrogenase is inhibited by 15% at 0.5 M and *Chromatium vinosium* ribulose biphosphate carboxylase is inhibited by 50% at 1 M (Pollard and Wyn Jones, 1979; Incharoensakdi et al., 1986). Therefore, this activity may be part of a minor group of enzymes that are inhibited by the compatible osmolyte. However, this observation is difficult to reconcile with the fact that glycinebetaine accumulation under conditions of salt-stress is a result of increased flux through both choline and glycinebetaine biosynthetic pathway (Summers and Weretilnyk, 1993). More specifically, PMEA and PDEA *N*-methylations are 2-fold higher in crude leaf extracts from spinach plants salinized with 200 mM NaCl in comparison to control plants (Weretilnyk and Summers, 1992) and the glycinebetaine pool size is expected to reach approximately 200 mM in these salinized plants (Weigel et al., 1986). So, if anything, an activating effect on PMEAMeT activities by glycinebetaine may have been expected. The observation may reflect an *in vivo* mechanism that decreases the involvement of PMEAMeT in PCho synthesis for glycinebetaine accumulation under conditions of salt-stress and so PMEAMeT may only play a role in PCho synthesis for PtdCho production.

Concluding remarks.

This thesis provides the first study on the enzyme PMEAMeT involved in choline synthesis and its properties from spinach leaves. Two salient contributions to understanding choline synthesis in leaves of the glycinebetaine accumulator spinach were: (1) providing evidence that a second enzyme PMEAMeT converts PMEA → PDEA and may also *N*-methylate PDEA → PCho *in vitro* and thus, insight into the number of enzymes that convert PEA → PMEA → PDEA → PCho *in vivo*; and (2) providing evidence for inhibition of PMEAMeT activities by reaction products SAH and PCho *in vitro* and thus, two putative rapid regulatory mechanisms of PCho synthesis from PEA *in vivo*. With regards to the second point, choline synthesis seems to be tightly regulated in

higher plants (Hanson and Rhodes, 1983; Mudd and Datko, 1989ab; Weretilnyk et al., 1995; Yang et al., 1995) probably because of the significant demand it could place on the methyl budget and the use of one ATP for each SAM formed (Weretilnyk et al., 1995).

Interestingly, PMEAMeT exhibited many similar properties to the light-regulated enzyme PEAMeT that could convert PEA → PMEA → PDEA → PCho *in vivo* (Smith, 1995). Both enzymes have identical native molecular weights, neither seemed to require divalent metal cations for activity, both were inhibited *in vitro* by reaction products SAH and PCho and by endproduct P_i (Smith, 1995; Smith et al., *in press*).

One future research direction should be the continued purification of PMEAMeT to homogeneity to obtain antibodies and the amino acid sequence. The latter is necessary to generate oligonucleotide probes to clone cDNA encoding PMEAMeT from a spinach cDNA library. The antibodies and mRNA probe will be useful in exploring PMEAMeT regulation at a protein and mRNA level especially with respect to salt-stress. That is, does PMEAMeT contribute to the up-regulation of choline synthesis for glycinebetaine accumulation in leaves of salinized spinach (Summers and Weretilnyk, 1993)? Such information will be helpful to develop a model for the regulation of choline synthesis with respect to PtdCho (primary metabolism) and glycinebetaine synthesis (secondary metabolism) in chenopods at least. These studies are important to both genetic engineering studies aimed at introducing the glycinebetaine-accumulating trait into crop as an approach to osmotic-stress resistance and to basic research on plant metabolism.

LITERATURE CITED

Andriamampandry C, Freysz L, Kanfer JN, Dreyfus H, Masserelli R (1989) Conversion of ethanolamine, monomethylethanolamine and dimethylethanolamine to choline-containing compounds by neurons in culture and by the rat brain. Biochem J **264**: 555-562

Andriamampandry C, Masserelli R, Freysz L, Kanfer JN (1990) A rat brain cytosolic *N*-methyltransferase(s) activity converting phosphorylethanolamine into phosphorylcholine. Biochem Biophys Res Comm **171**: 758-763

Andriamampandry C, Masserelli R, Kanfer JN (1992) Properties of a partially purified phosphodimethylethanolamine methyltransferase from rat brain cytosol. Biochem J **288**: 267-272

Arakawa K, Takabe T, Sugiyama T, Akazawa T (1987) Purification of betaine aldehyde dehydrogenase from spinach leaves and preparation of its antibody. J Biochem **101**: 1485-1488

Arnon DI (1949) Copper enzymes in isolated chloroplasts. Polyphenoloxidase in *Beta vulgaris*. Plant Physiol **24**: 1-15

Audubert F, Vance DE (1983) Pitfalls and problems on the studies of methylation of phosphatidylethanolamine. J Biol Chem **258**: 10695-10701

Bligny R, Gardenestrom P, Roby C, Douce R (1990) ^{31}P NMR studies of spinach leaves and their chloroplasts. J Biol Chem **265**: 1319-1326

Boch J, Kempf B, Bremer E (1994) Osmoregulation in *Bacillus subtilis*: Synthesis of the osmoprotectant glycine betaine from exogenously provided choline. J Bacteriol **176**: 5364-5371

Borowitzka LJ (1981) Solute accumulation and regulation of cell wall activity. *In*, Paleg LG, Aspinall D, ed.s, The Physiology and Biochemistry of Drought Resistance in Plants. Academic Press, Australia, pp 97-127

Boyer JS (1982) Plant productivity and environment. Science **218**: 443-448

Bradford MM (1976) A rapid and sensitive method for the quantification of microgram quantities of protein utilizing the principles of protein-dye binding. Anal Biochem **72**: 248-254

Brady CJ, Gibson TS, Barlow EWR, Spiers J, Wyn Jones RG (1984) Salt tolerance in plants. I. Ions, compatible organic solutes and the stability of plant ribosomes. Plant Cell Environ. **7**: 571-578

Brousquisse R, Weigel P, Rhodes D, Yocum CF, Hanson AD (1989) Evidence for a ferredoxin-dependant choline monoxgenase from spinach chloroplast stroma. Plant Physiol **90**: 322-329

Brown AD, Simpson JR (1972) Water relations of sugar-tolerant yeasts: the role of intracellular polyols. J Gen Microbiol **72**: 589-591

Burnet M, Lafontaine PJ, Hanson AD (1995) Assay, purification and partial characterization of choline monoxygenase from spinach. Plant Physiol **108**: 581-588

Chambers ST, Kunin CM (1987) Osmoprotective activity for *Escherichia coli* in mammalian inner renal medulla and urine: correlation of glycine and proline betaines and sorbitol with response to osmotic loads. J Clin Invest **80**: 1255-1260

Chua N-H (1980) Electrophoretic analysis of chloroplast proteins. Methods Enzymol **69**: 434-446

Coughlan SJ, Wyn Jones RG (1980) Some responses of *Spinacea oleracea* to salt-stress. J Exp Bot **31** (123): 883-893

Coughlan SJ, Wyn Jones RG (1982) Glycinebetaine biosynthesis and its control in detached secondary leaves of spinach. Planta **154**: 6-17

Csonka LN (1989) Physiological and genetical responses of bacteria to osmotic stress. Microbiological Reviews **53**: 121-147

Csonka LN, Hanson AD (1990) Prokaryotic osmoregulation: Genetics and physiology Annu Rev Microbiol **45**: 596-606

Cui Z, Vance JE, Chen MH, Voelker DR, Vance DE (1993) Cloning and expression of a novel phosphatidylethanolamine *N*-methyltransferase. A specific biochemical and cytological marker for a unique membrane fraction in rat liver. J Biol Chem **286**: 16655-16663

Das D (1978) Enzymes. *In*, Das D, ed., Biochemistry. Academic Publishers, Calcutta, New Delhi, pp 104-137

Datko AH, Mudd SH (1988a) Phosphatidylcholine synthesis. Differing patterns in soybean and carrot. Plant Physiol **88**: 854-861

Datko AH, Mudd SH (1988b) Enzymes of phosphatidylcholine synthesis in *Lemna*, soybean and carrot. Plant Physiol **88**: 1338-1348

Delauney AJ, Verma DP (1993) Proline biosythesis and osmoregulation in plants. Plant J **4:** 215-223

Deshnium P, Los DA, Hayashi H, Mustardy L, Murata N (1995) Transformation of *Synechococcus* with a gene for choline oxidase enhances tolerance to salt stress. Plant Mol Biol **29**: 897-907

Eloranta TO, Kajander EO, Raina AM (1976) A new method for the assay of tissue *S*-adenosylhomocysteine and *S*-adenosylmethionine. Biochem J **160**: 287-294

Flower TJ, Troke PF, Yeo AR (1977) The mechanisms of salt tolerance in halophytes. Annu Rev Plant Physiol **28**: 89-121

Garcia-Perez A, Burg MB (1990) Importance of organic osmolytes for osmoregulation by renal medullary cells. Hypertension **16**: 595-602

Gaynor PM, Carmen GM (1990) Phosphatidylethanolamine methyltransferase and phospholipid methyltransferase activities from *Saccharomyces cerevisiae*. Enzymological and kinetic properties. Biochem Biophys Acta **1045**: 156-163

Gibson TS, Spiers J, Brady CJ (1984) Salt-tolerance in plants. II. In vitro translation of m-RNAs from salt-tolerant and salt-sensitive plants in wheat germ ribosomes. Responses to ions and compatible organic solutes. Plant Cell Environ **7**: 579-587

Giddings TH, Hanson AD (1982) Water stress provokes a generalised increase in phosphatidylcholine turnover in barley leaves. Planta **155**: 493-501

Greenway H, Munns R (1980) Mechanisms of salt tolerance in nonhalophytes Annu Rev Plant Physiol **31**: 149-90

Hanson AD, Nelsen CE (1978) Betaine accumulation and [^{14}C] formate metabolism in water-stressed barley leaves. Plant Physiol **62**: 305-312

Hanson AD, Scott NA (1980) Betaine synthesis from radioactive precursors in attached, water-stressed barley leaves Plant Physiol **66**: 342-348

Hanson AD, Hitz WD (1982) Metabolic responses of mesophytes to plant water deficits. Annu Rev Plant Physiol **33**: 163-203

Hanson AD, Wyse R (1982) Biosynthesis, translocation and accumulation of betaine in sugar beet and its progenitors in relation to salinity. Plant Physiol **70**: 1191-1198

Hanson AD, Rhodes D (1983) ^{14}C Tracer evidence for synthesis of choline and betaine via phosphoryl base intermediates in salinized spinach sugar beet leaves. Plant Physiol **71**: 692-700

Hanson AD, May AM, Grumet R, Bode J, Jamieson GC, Rhodes D (1985) Betaine synthesis in chenopods: Localization in chloroplasts. Proc Natl Acad Sci USA **82**: 3678-3682

Hanson AD (1992) Compatible solute synthesis and compartmentation in higher plants. *In*, Somero G, Osmond CB, Bolis CL, eds, Water and Life. Springer-Verlag, Berlin, Heidelberg, pp 52-60

Hanson AD, Rathinasabapathi B, Rivoal J, Burnet M, Dillon MO, Gage DA (1995) Osmoprotective compounds in the Plumbaginaceae: A natural experiment in metabolic engineering of stress tolerance Proc Natl Acad Sci USA **91**: 306-310

Hanson AD, Rivoal J, Burnet M, Rathinasabapathi B (1995) Biosynthesis of quarternary ammonium and tertiary sulphonium compounds in response to water deficit. *In*, N Smirnoff, ed., Environment and Plant Metabolism: Flexibility and Acclimation. BIOS Scientific Publishers Ltd, Oxford, UK, pp 189-198

Hayashi H, Alia, Mustardy L, Deshnium P, Ida M, Murata N (1997) Transformation of Arabidopsis thaliana with the codA gene for choline oxidase; accumulation of glycinebetaine and enhanced tolerance to salt and cold stress. Plant J. **12**: 133-142

Hoaglands DR, Arnon DI (1939) The water-culture method for growing plants without soil. Agri Exp Stn Berkeley, Cal. Circular 347

Higman MA, Niles EG (1994) Location of the *S*-adenosyl-L-methionine binding region of the vaccina virus mRNA (Guanine-7-)methyltransferase. J Biol Chem **269**: 14982-14987

Hitz WD, Rhodes D, Hanson AD (1981) Radiotracer evidence implicating phosphoryl and phosphatidyl bases as intermediates in betaine synthesis by water-stressed barley leaves. Plant Physiol **68**: 814-822

Hitz WD, Ladyman JAR, Hanson AD (1982) Betaine synthesis and accumulation in barley during field water stress. Crop Sci **22**: 47-54

Incharoensakdi A, Takabe T, Akazawa, T (1986) Effect of betaine on enzyme activity and subunit interaction of ribulose-1, 5-biphosphate carboxylase/ oxygenase from *Aphanothece halophytica.* Plant Physiol **81**: 1044-1049

Ishitani M, Nakamura T, Han SY, Takabe T (1995) Expression of the betaine aldehyde dehydrogenase gene in barley in response to osmotic stress and abscisic acid. Plant Mol Biol **27**: 307-315

Kagan RM, Clarke S (1994) Widespread occurrence of three sequence motifs in diverse *S*-adenosyl-dependent methyltransferases suggests a common structure for these enzymes. Arch Biochem Biophys **310**: 417-427

Kempf B, Bremer E (1995) OpuA, an osmotically regulated binding protein-dependant transport system for the osmoprotectant glycinebetaine in *Bacillus subtilis.* J Biol Chem **270**: 16701-16713

Kent C (1995) Eukaryotic phospholipid biosynthesis. Annu Rev Biochem **64**: 315-343

Kinney AJ (1993) Phospholipid head groups. *In*, Moore TS Jr, ed., Lipid metabolism in plants.

Knogge W, Weissenbock G (1984) Purification, characterization and kinetic mechanisms of *S*-adenosyl-L-methionine: vitexin 2''-*O*-rhamnoside 7-*O*-methyltransferase of *Avena sativa* L. Eur J Biochem **140**: 113-118

Kodaki T, Yamashita S (1987) Yeast phosphatidylethanolamine methylation pathway. J Biol Chem **262**: 15428-15435

Le Rudulier D, Stroma R, Dandekar M, Smith LT, Valentine RC (1984) Molecular biology of osmoregulation. Science **224**: 1064-106

Lerma C, Hanson AD, Rhodes D (1988) Oxygen-18 and deuterium labelling studies of choline oxidation by spinach and sugar beet. Plant Physiol **88**: 695-702

Lerma C, Rich PJ, Ju GC, Yang W-J, Hanson AD (1991) Betaine deficiency in maize. Complementation tests and metabolic basis. Plant Physiol **95**: 1113-1119

Lilius G, Holmberg N, Bulow L (1996) Enhanced NaCl stress tolerance in transgenic tobacco expressing bacterial choline dehydrogenase. Biotechnology **14**: 177-180

Manetas Y, Petropoulou Y, Karaabourniotis G (1986) Compatible solutes and their effects on phosphoenolpyruvate carboxylase of C_4-halophytes. Plant Cell Environ **9**: 145-151

Martin F, Tolbert NE (1983) Factors which affect the amount of inorganic phosphate, phosphorylcholine and phosphorylethanoalmine in xylem exudate of tomato plants. Plant Physiol **73**: 464-470

McCue KF, Hanson AD (1990) Drought and salt tolerance: towards understanding and application. Trends Biotech **8**: 358-362

McCue KF, Hanson AD (1992) Salt-inducible betaine aldehyde dehydrogenase from sugar beet: cDNA cloning and expression. Plant Mol Biol **18**: 1-11

McDonnell E, Wyn Jones RG (1988) Glycinebetaine biosynthesis and accumulation in unstressed and salt-stressed wheat. J Exp Bot **39**: 421-430

Mercer S (1994) Purification and characterization of ethanolamine kinase from spinach. MSc thesis, McMaster University.

Merrick WC (1983) Translation of exogenous mRNAs in reticulocyte lysates. Methods Enzymol **101**: 606-615

Moore TS Jr (1982) Phospholipid biosynthesis. Annu Rev Plant Physiol **33**: 235-259

Morgan JM (1984) Osmoregulation and water stress in higher plants. Annu Rev Plant Physiol **35**: 299-319

Mudd SH, Datko AH (1986) Phosphatidylethanolamine bases as intermediates in phosphatidylcholine synthesis in *Lemna*. Plant Physiol **82**: 126-135

Mudd SH, Datko AH (1989a) Synthesis of methylated ethanolamine moieties. Regulation by choline in *Lemna*. Plant Physiol **90**: 296-305

Mudd SH, Datko AH (1989b) Synthesis of methylated ethanolamine moieties. Regulation by choline in soybean and carrot. Plant Physiol **90**: 306-310

Mudd SH, Datko AH (1989c) Synthesis of ethanolamine and its regulation in *Lemna paucicostata*. Plant Physiol **91**: 587-597

Mudd SH, Datko AH (1990) The *S*-methylmethionine cycle in *Lemna paucicostata*. Plant Physiol **93**: 623-630

Mukherjee S, Freysz L, Kanfer JN (1995) Partial purification of a phosphoethanolamine methyltransferase from rat brain cytosol. Neurochem Res **20**: 1233-1237

Neville DM Jr (1971) Molecular weight determination of protein-dodecylsulfate complexes by gel electrophoresis in a discontinuous buffer system. J Biol Chem **246**: 6328-6334

Nikoloff DM, Henry SA (1991) Genetic analysis of yeast phospholipid biosynthesis. Annu Rev Genet **25**: 559-583

Nomura M, Ishianti M, Takabe T, Rai AK, Takabe T (1995) *Synechococcus* sp. PCC7942 transformed with *Escherichia coli* bet genes produces glycine betaine from choline and acquires resistance to salt stress. Plant Physiol **107**: 703-708

Nuccio LM, Russell BL, Nolte KD, Rathinasabapathi B, Gage DA, Hanson AD (1998) The endogenous choline supply limits glycinebetaine synthesis in transgenic tobacco expressing choline monoxygenase. Plant J. **16**: 487-496

O'Keefe BR, Beecher CW (1994) Isolation and characterization of *S*-adenosyl-L-methionine: tetrahydroberberine-*cis*-*N*-mehtyltransferase from suspension cultures of *Sanguinaria canadensis* L. Plant Physiol 105: 395-403

Papageorgiou GC, Murata N (1995) The unusually strong stabilizing effects of glycinebetaine on the structure and function of the oxygen-evolving Photosystem II complex. Photosynth Res **44**: 243-252

Pollard A, Wyn Jones RG (1979) Enzyme activities in concentrated solutions of glycinebetaine and other solutes. Planta **144**: 291-298

Popp M, Smirnoff N (1995) Polyol accumulation and metabolism during H_2O-deficit. *In*, N Smirnoff ed., Environmental and Plant Metabolism: Flexibility and Acclimation. BIOS Scientific Publishers Ltd, Oxford, UK, pp 189-198

Poulton JE (1981) Transmethylation and demethylation reactions in the metabolism of secondary plant products. *In*, DD Davis, ed., The Biochemistry of Plants Vol. 7. Academic Press, San Diego, pp 667-715

Preising CL, Matthews DE, VanEtten HD (1989) Purification and characterization of *S*-adenosyl-L-methionine:6a-hydroxymaackiain 3-*O*-methyltransferase from *Pisum sativum*. Plant Physiol 91: 559-566

Prud'homme M-P, Moore TS Jr (1992a) Phosphatidylcholine synthesis in castor bean endosperm. Free bases as intermediates. Plant Physiol **100**: 1527-1535

Prud'homme M-P, Moore TS Jr (1992b) Phosphatidylcholine synthesis in castor bean endosperm. Occurrence of an *S*-adenosyl-L-methionine: ethanolamine *N*-methyltransferase. Plant Physiol **100**: 1536-1540

Rathinasabapathi B, Burnet M, Russell BL, Gage DA, Liao P-C, Nyes GJ, Scott P, Glodbeck JH, Hanson AD (1997) Choline monoxygenase, an unusual iron-sulphur enzyme catalyzing the first step of glycinebetaine synthesis in plants: Prosthetic group characterization and cDNA cloning. Proc Natl Acad Sci USA **94**: 3454-3458

Rhodes D (1987) Metabolic responses to stress. *In* DD Davis, ed., The Biochemistry of Plants, Vol. 12. Academic Press, San Diego, pp 201-241

Rhodes D, Hanson AD (1993) Quarternary ammonium and tertiary sulfonium compounds in higher plants. Annu Rev Plant Physiol Plant Mol Biol **44**: 357-384

Ridgeway ND, Vance DE (1987) Purification of phosphatidylethanolamine *N*-methyltransferase from rat liver. J Biol Chem **262**: 17231-17239

Robinson SP, Jones GP (1986) Accumulation of glycinebetaine in chloroplasts provides osmotic adjustment during salt stress. Aust J Physiol **13**: 659-568

Rodwell VW (1985) Kinetic properties of enzymes. *In*, Martin DW Jr, Mayes PA, Rodwell VW, Granner DK, eds, Harper's Review of Biochemistry. Koon Wah Printing Pte Ltd, Singapore, pp 72-90

Rozwadaowski KL, Khachatourians GG, Selveraj G (1991) Choline oxidase, a catabolic enzyme in *Arthrobacter pascens*, facilitates adaptation to osmotic stress in *Escherichia coli.* J Bacteriol **173**: 472-478

Russell BL, Rathinasabapathi B, Hanson AD (1998) Osmotic stress induces expression of choline monoxygenase in sugar beet and amaranth. Plant Physiol **116**: 859-865

Samaras Y, Bressan RA, Csonka LN, Garcia-Rios MG, Paino D'Urzo M, Rhodes D (1995) Proline accumulation during drought and salinity. *In*, N Smirnoff, ed., Environment and Plant Metabolism: Flexibility and Acclimation. BIOS Scientific Publishers Ltd, Oxford, UK, pp 189-198

Saneoka H, Nagasaka C, Hahn DT, Yang W-J, Premachandra GS, Joly RJ, Rhodes D (1995) Salt tolerance of glycinebetaine-deficient and -containing maize lines. Plant Physiol **107**: 631-638

Schluckebier G, O'Gara M, Saenger W, Cheng X (1995) Universal catalytic domain structure of adomet-dependent methyltransferases. J Mol Biol **247**: 16-20

Segel IH (1976) Biochemical calculations 2ND edition. John Wiley & Sons Ltd, USA

Shockey JM, Rajasekharan R, Kemp JD (1995) Photoaffinity labeling of developing jojoba seed microsomal membranes with a photoreactive analog of acyl-Coenzyme A (acyl-CoA). Plant Physiol **107**: 155-160

Smirnoff N (1995) Metabolic flexibility in relation to environment. *In*, N Smirnoff, ed., Environment and Plant Metabolism: Flexibility and Acclimation. BIOS Scientific Publishers Ltd, Oxford, UK, pp 189-198

Smith DD (1995) Phosphoethanolamine *N*-methyltransferase from spinach. MSc thesis, Dept of Biology, McMaster University

Smith DD, Summers PS, Weretilnyk EA (1999) Phosphocholine synthesis in spinach: Characterization of phosphoethanolamine *N*-methyltransferase. Plant Physiol, *In press.*

Som S, Friedman S (1989) Direct photolabeling of the *Eco*RII methyltransferase with *S*-adenosyl-L-methionine. J Biol Chem **265**: 4278-4283

Som S, Friedman S (1990) Identification of a highly conserved domain in the *Eco*RII methyltransferase which can be photolabeled with *S*-adenosyl-L-[*methyl*-^{3}H]methionine. J Biol Chem **266**: 2937-2945

Somero GN (1992) Adapting to water stress: Convergence on common solutions. *In*, Somero GN, Osmond CB, Bolis CL, eds, Water and Life. Springer-Verlag, Heildelberg, pp 3-18

Storey R, Wyn Jones RG (1979) Responses of *Atriplex spongiosa* and *Suaeda monoica* to salinity. Plant Physiol **63**: 156-162

Stryer L (1988) Biochemistry, third edition. WH Freeman and Company, New York

Subbaramaiah K, Simms SA (1992) Photolabeling of CheR Methyltransferase with *S*-adenosyl-L-methionine (AdoMet). J Biol Chem **267**: 8636-8642

Summers PS, Weretilnyk EA (1993) Choline synthesis in relation to salt stress. Plant Physiol **103**: 1269-1276

Taiz L, Zeiger E (1991) Plant Physiology. The Benjamin/ Cummings Publishing Company, Inc., California, USA

Timasheff SN (1992) A physiochemical basis for the selectivity of osmolytes by nature. *In*, Somero G, Bolis CL, eds, Water and Life. Springer – Verlag, Berlin, Heidelberg, pp 70-84

Trossat C, Nolte KD, Hanson AD (1996) Evidence that the pathway of dimethylsulfoniopropionate biosynthesis begins and ends in the chloroplast. Plant Physiol **111**: 965-973

Trossat C, Rathinasabapathi B, Hanson AD (1997) Transgenically expressed betaine aldehyde dehydrogenase efficiently catalyzes oxidation of dimethylsulfoniopropionaldehyde and ω-aminoaldehydes. Plant Physiol **113**: 1457-1461

Vance DE (1990) Phosphatidylcholine metabolism: masochistic enzymology, metabolic regulation, and lipoprotein assembly. Biochem Cell Biol **68**: 1151-1165

Valenzuela-Soto EM, Munoz-Clares RA (1994) Purification and properties of betaine aldehyde dehydrogenase extracted from detached leaves of *Amaranthus hypochondriacus* L. subjected to water deficit. J Plant Physiol **143**: 145-152

Wallevick K, Jensenius JC (1982) A simple and reliable method for drying of polyacrylamide slab gels. J Biochem Biophys Methods **6**: 17-21

Warfe J, Harwood JL (1979a) Lipid metabolism in germ seeds. Purification of ethanolamine kinase from soybean. Biochim Biophys Acta **575**: 102-111

Weigel P, Weretilnyk EA, Hanson AD (1986) Betaine aldehyde oxidation by spinach chloroplasts. Plant Physiol **82**: 753-749

Wenzel C, Moulard M, Lobner-Olensen A, Guschlbauer W (1991) Cross-linking of Dam methyltransferase with *S*-adenosyl-L-methionine. FEBS **280**: 147-151

Weretilnyk EA, Hanson AD (1988) Betaine aldehyde dehydrogenase polymorphism in spinach: genetic and biochemical characterization. Biochem Genet **26**: 143-151

Weretilnyk EA, Bednarek S, McCue KF, Rhodes D and Hanson AD (1989) Comparative biochemical and immunological studies of the glycine betaine synthesis pathway in diverse families of dicotyledons Planta **178**: 342-352

Weretilnyk EA, Hanson AD (1992) Molecular cloning of a plant betaine-aldehyde dehydrogenase, an enzyme implicated in adaptation to salinity and drought. Proc Natl Acad Sci USA **87**: 2745-2749

Weretilnyk EA, Summers PS (1992) Betaine and choline metabolism in higher plants. *In*, Singh BK, Flores HE, Shannon JC, eds, Biosynthesis and Molecular Regulation of Amino Acids in Plants. American Society of Plant Physiologists, Rockville, Maryland, pp 89-97

Weretilnyk EA, Smith DD, Wilch GA, Summers PS (1995) Enzymes of choline synthesis. Response of phospho-base *N*-methyltransferase activities to light and salinity. Plant Physiol **109**: 1085-1091

Wood AJ, Saneoka H, Rhodes D, Joly RJ, Goldsbrough PB (1996) Betaine aldehyde dehydrogenase in sorghum. Molecular cloning and expression of two related genes. Plant Physiol **110**: 1301-1308

Wood WB, Wilson JH, Benbow RM, Hood LE (1981) Biochemistry: A problems approach. The Benjamin/ Cummings Publishing Company Inc., California, USA pp 126-143

Wray W, Boulikas T, Wray VP, Hancock R (1982) Silver staining of proteins in polyacrylamide gels. Anal Biochem **118**: 197-203

Wyn Jones RG, Storey R, Leigh RA, Ahmad N, Pollard A (1977) A hypothesis on cytoplasmic osmotic regulation. *In*, Marre E, Cifferri O, eds, Regulation of Cell Membrane Activities in Plants. Elsevier/ North-Holland Biomedical Press, Amsterdam.

Wyn Jones RG, Brady CJ, Speirs J (1979) Ionic and osmotic relations in plant cells. *In*, Laidman DL, Wyn Jones RG, eds, Recent Advances in the Biochemistry of Cereals. Academic Press, London, pp 63-98

Wyn Jones RG, Storey R (1981) Betaines. *In*, Paleg LG, Aspinall D, eds, The Physiology and Biochemistry of Drought Resistance in Plants. Academic Press, Australia, pp 172-204

Wyn Jones RG, Gorham J (1983) Osmoregulation. *In*, Osmond CB, Zeigler DH, eds, Encyclopedia of Plant Physiology. Springer-Verlag, Berlin, pp 35-58

Yamashita S, Oshima A, Nikawa J-i, Hosaka K (1982) Regulation of the phosphatidylethanolamine methylation pathway in *Saccharomyces cerevisiae.* Eur J Biochem **128**: 589-595

Yamshita S, Oshima A (1980) Regulation of phosphatidylethanolamine methyltransferase by *myo*-inositol in *Saccharomyces cerevisiae.* Eur J Biochem **104**: 611-616

Yancey PH, Clark ME, Hand SC, Bowlus RD Somero GN (1982) Living with water stress: evolution of osmolyte systems. Science **217**: 1214-1222

Yang W-J, Nadolska-Orczyk A, Wood KV, Hahn DT, Rich PJ, Wood AJ, Saneoka H, Premachandra GS, Bonham CC, Rhodes JC, Joly RJ, Samaras Y, Goldsbrough PB, Rhodes D (1995) Near-isogenic lines of maize differing for glycinebetaine. Plant Physiol **107**: 621-630.

Zeisel SH, Blusztan JK (1994) Choline and human nutrition. Annu Rev Nutr **14**: 269-296